Science
AAAS

# Supplementary Materials for

## Biosynthesis of the allelopathic alkaloid gramine in barley by a cryptic oxidative rearrangement

Sara Leite Dias *et al*.

Corresponding authors: John C. D'Auria, dauria@ipk-gatersleben.de; Jakob Franke, jakob.franke@botanik.uni-hannover.de

*Science* **383**, 1448 (2024)
DOI: 10.1126/science.adk6112

**The PDF file includes:**



**Other Supplementary Material for this manuscript includes the following:**

## Materials and Methods

### Plant material

*N. benthamiana* plants (4-6 weeks old) were grown in a greenhouse at 55% humidity, 22 °C, and 16-h-light/8-h-dark photoperiod.
*Arabidopsis thaliana* Col-0 plants (4-5 weeks old) were grown in Ø 5 cm pots and located in a climatized chamber at 45% humidity, 20 °C, and 14-h-light/10-h-dark photoperiod, light intensity 240 µmol $m^{-2}$ $s^{-1}$.

### Chemicals

Gramine, L-tryptophan, and glyoxylic acid monohydrate were purchased from Sigma-Aldrich (Steinheim, Germany). D-Tryptophan (99%) was purchased from Fisher Scientific (Schwerte, Germany). (3-Aminomethyl)-1*H*-indole was purchased as the free base from Fluorochem (Hadfield, United Kingdom) or as the corresponding oxalate salt from Apollo Scientific (Stockport, UK). Phenylhydrazine was purchased from Alfa Aesar (Kandel, Germany). Sodium borohydride was purchased from ICN Biomedicals (Aurora, USA). Acetonitrile, methanol and ultra-pure water were purchased from Chemsolute (Renningen, Germany), while formic acid was obtained from J. T. Baker (Gross Gerau, Germany). Silica gel 60M (40-60 µm) and TLC plates ($F_{254}$) were purchased from Macherey-Nagel.
L-tryptophan-2,3,3-$d_3$ (98 atom % D) was purchased from CDN Isotopes (Pointe-Claire, Canada). L-Tryptophan-$^{15}N_2$ tryptophan was purchased from Biotrend (Cologne, Germany). $CDCl_3$, DMSO-$d_6$ and MeOH-$d_4$ were purchased from DEUTERO (Kastellaun, Germany).
Other chemicals without specific mention were purchased from Fisher Scientific or Carl Roth.

### NMR analysis

NMR spectra were recorded at 298 K using a Bruker Ascend 400 or Ascend 600 spectrometer operating at 400 MHz or 600 MHz for $^1H$ NMR and at 101 MHz or 151 MHz for $^{13}C$ NMR respectively. All chemical shifts (δ) were calibrated to the residue solvent peaks ($CDCl_3$: $\delta_H$ = 7.26 ppm, $\delta_c$ = 77.16 ppm; MeOH-$d_4$: $\delta_H$ = 3.31 ppm, $\delta_c$ = 49.00 ppm; DMSO-$d_6$: $\delta_H$ = 2.50 ppm, $\delta_c$ = 39.52 ppm) and expressed in ppm with coupling constants reported in Hz. Analysis was conducted with TopSpin (Version 4.0.6) or MestReNova (Version 14.2).

### *Arabidopsis thaliana* transformation and analysis

Vectors for *Agrobacterium tumefaciens* mediated stable expression in *A. thaliana* were assembled using Golden Gate Modular Cloning (*40*). Primers are listed in Table S4. Gene sequences of *HvNMT* and *HvAMIS,* codon-optimized for *Arabidopsis thaliana*, were purchased from Genewiz®, Leipzig, Germany. Any instances of BsmBI, SapI, BbsI, and BsaI recognition sites were removed from synthetic sequences. Synthetic genes on a pUC-

GW-Amp vector were used for level 0 MoClo reactions with pICH41308 as an entry vector. These level 0 parts were assembled into level 1 acceptors in a one-step cloning reaction with level 0 parts encoding CaMV 35S promoter (CaMV35S) and 5' UTR from tobacco mosaic virus (TMV) for the plasmid carrying *HvAMIS* and *nos* promoter and 5' UTR from TMV for the one carrying the *HvNMT* gene. The final vectors – namely the construct for the integration of *HvAMIS* (BAR + HvAMIS pAGM4673, Fig. S19), the construct for the integration of *HvNMT* (BAR + HvNMT pAGM4673, Fig. S20), and the double construct (BAR + HvNMT + HvAMIS pAGM4673, Fig. S21) – included a transcription unit for a BASTA resistance gene (with its Nos-promoter and Nos-terminator), allowing for the selection of transformed plants. Level 2 constructs were verified by Sanger sequencing before transformation.

*A. tumefaciens* strains GV3101 or LBA4404 were transformed with a binary plasmid encoding both *HvNMT* and *HvAMIS* genes and, separately, with plasmids containing the single genes (*41*). *Arabidopsis thaliana* Col-0 plant transformation was performed based on Weigel *et al.* (*41*). Briefly, colonies were precultured in liquid LB medium containing 50 µg/mL streptomycin and 50 µg/mL kanamycin and two days later inoculated in 300 mL YEP medium containing the same antibiotics. After two days of incubation, the Agrobacterium cells were pelleted and resuspended into infiltration media. All siliques and open flowers of *A. thaliana* plants were removed, and the plants transformed by vacuum infiltration. The plants were allowed to recover and grew until they set seed. Once they were dry, seeds were collected and sown in new soil. Two weeks after germination, the seedlings were treated with BASTA spraying (200 mg/L) to select the transformed individuals. When the plants were 6 weeks old, approximately 50 mg of healthy and undamaged leaf material was harvested from each transformed plant for chemical analysis. The leaves were transferred into a tube containing steel balls and frozen in liquid nitrogen. Samples were stored at −80°C. Grinding and extraction were performed as described in Leite Dias et al. (*15*). Chromatographic analysis is described in a section below.

**Generation and analysis of barley overexpression lines**

*HvAMIS* and *HvNMT* coding sequences were introduced into barley (*Hordeum vulgare* L.) cv. "Golden Promise", which is a barley variety lacking the genes for the biosynthesis of gramine. Primers are listed in Table S4. The *HvAMIS* and *HvNMT* genes were first cloned into the intermediate vector UbiFull-AB-M containing the *Zea mays Polyubiquitin 1* promotor and the *nos* terminator, along with compatible *Sfi*I restriction sites for the cloning into the binary p6i-d35S-TE9 vector. The final vectors, named "HvAMIS p6i-d35S", for the integration of *HvAMIS*, and "HvNMT p6i-d35S", for the integration of *HvNMT*, are reported in Fig. S22 and Fig. S23, respectively. The vectors also contained a CaMV35S promoter-controlled *hpt* plant selectable marker gene. Transformation was conducted using the hypervirulent *A. tumefaciens* strain AGL1 as previously described (*42*).

Barley grains of cv. "Golden Promise" were germinated in a substrate mix (Spezialmischung Petuniensubstrat, Klasmann-Dalmann, Germany) within a growth chamber with the following conditions: 14/12 °C day/night, 12 hours light, 136 µmol $s^{-1}$ $m^{-2}$. After three weeks, the plants were transferred to the greenhouse with 16 h photoperiod and 18/16 °C day/night temperature. Three weeks after anthesis, caryopses were harvested and immature embryos were excised for Agrobacterium-mediated DNA transfer using

p6i_AMIS and p6i_NMT individually and in co-transformation, followed by regeneration of primary transgenic plants as described in Marthe *et al.* (*43*).
After the transfer of regenerated plantlets to the greenhouse, genomic DNA was extracted from a sample of leaf tissue by the phenol-chloroform-based protocol from Pallotta *et al.* (*44*). Insertion of *HvAMIS* and *HvNMT* expression cassettes was confirmed by PCR from genomic DNA using primers specific for *AMIS* and *NMT* genes with DreamTaq Green PCR MM 2x (ThermoFisher Scientific, Bremen, Germany), UbiP_FWD as the forward primer and either AMIS_REV or NMT_REV as reverse primers (Fig. S24).
The vectors "HvAMIS p6i-d35S", and "HvNMT p6i-d35S" (Fig. S22 and Fig. S23) were used as positive controls, whereas the negative control was constituted by genomic DNA of wild type "Golden Promise" barley. Primary transgenics were additionally evaluated by chemical analysis of barley leaves. The leaf underneath the flag leaf (3rd leaf) was collected and cut into four equally sized pieces. The second quarter was used for analysis. The material was immediately frozen in liquid nitrogen and stored at −80°C. Extraction was carried out as described in Leite Dias et al. (*15*); chromatographic analysis is described in a section below.

**Generation and analysis of barley knockout lines**

To generate Tafeno knockout lines, the "HvAMIS 3 gRNA + Cas9 pIK48" knockout construct was designed to contain gRNAs for three target motifs on the *HvAMIS* gene and a transcription unit for the Cas9 protein (Fig. S25). The target motifs were located at positions 26, 52 and 87 of the coding gene sequence of *HvAMIS* (Fig. S8). The construct was created based on hierarchical Golden Gate cloning using the CasCADE vector system (*19*). In brief, DNA oligos complementary to the target motifs were hybridized and cloned by specific overhangs into the BsaI restriction sites of gRNA modules pIK5 to pIK7, containing the TaU6 promoter and gRNA scaffold. These gRNA modules were assembled in pIK61 via Golden Gate cloning using Esp3I. Final assembly of the 3-gRNA expression cassette with pIK83, carrying the Cas9 coding sequence run by ZmUBI1 promotor, into pIK48 backbone was performed by BsaI-based Golden Gate cloning ("HvAMIS 3 gRNA + Cas 9 pIK48" vector, Fig. S25). *Via* SfiI, the whole expression unit was transferred into the p6i-d35s-TE9 binary vector for Agrobacterium-mediated DNA transfer into immature embryos of Tafeno as mentioned above (*43*), but adding eight weeks of vernalization at 4 °C for seedlings of donor plants and regenerated plantlets. After regeneration, genomic DNA was extracted from leaf samples as described above and the target region was PCR amplified and analyzed for mutations by Sanger sequencing.

**Chromatographic analysis of transformed *Arabidopsis* and barley plants**

Detection of AMI and gramine in transformed *A. thaliana* and barley plants was performed by RP-UPLC-FLD (Reversed Phase Ultra Performance Liquid Chromatography Fluorescence Detection). The instrument, an Acquity UPLC system (Waters Corporation, Milford, MA, USA), was coupled to a 740002848-TAP Acquity Fluorescence Detector (1PM) and equipped with a 740001685-TAP Acquity solvent manager (1PM) and a sample manager (740001698-TAP (1PM)). Injections were carried out via a PLNO (Partial-Loop with Needle-Overfill) with an injection volume of 5 µL. To achieve good chromatographic

separation, a Waters Acquity UPLC HSS T3 (2.1 × 100 mm; 1.8 µm) column coupled to Acquity UPLC HSS T3 VanGuard (2.1 × 5 mm; 1.8 µm; Waters, Germany) pre-column was used at 30 °C and a flow rate of 0.4 mL $min^{-1}$ over a total run time of 15 min/sample. The initial mobile phase consisted of 99.9% of water supplemented with 0.1% formic acid (A) and 0.1% of acetonitrile supplemented with 0.1% formic acid (B). The following gradient was used: 0-1 min, 0.1% B isocratic; 1-3 min, 0.1-5% B; 3-6 min, 5-12.6% B; 6-7 min, 12.6% B isocratic; 7-10 min, 12.6-50% B; 10-10.5 min, 50-99% B; 10.5-12.5 min, 99% B; 12.5-13 min, 99-0.1% B; 13-15 min, 0.1% B. Both data acquisition and instrument control were coordinated by Empower 3 software (Waters Corp.). Chromatograms were extracted to match excitation and emission wavelengths of 280 nm and 320 nm, respectively. Peak areas for each compound of interest were curated manually and their values quantified.

Confirmation of peak shape and quality as well as fragmentation pattern and masses of fragments was performed by liquid chromatography-tandem mass spectrometry on a Bruker Maxis II qTOF mass spectrometer run in MS1 mode with an electrospray ionization interface in positive mode using the above-mentioned column and flow rate. The detection was performed via a Bruker Elute DAD set to scan 200-500 nm wavelength with a bunch width of 1 and a data rate of 10.0 Hz. The desolvation gas was nitrogen set at a nebulizer pressure of 2.5 bar. Drying gas flow was set to 8 L/min and the drying gas temperature was maintained at 200 °C. End Plate Offset 500 V, capillary voltage was set at 4000 V, target mass at 50 – 1000 *m*/*z* with a spectra rate of 5.0 Hz. The peak area of each compound was manually curated, and the values were quantified using Compass DataAnalysis 5.3 package (Bruker Daltonik GmbH). In the case of gramine and AMI, the main fragment was not the molecular ion, rather an in-source fragment with a *m*/*z* of 130.0666. Extracted ion chromatograms for this ion were also used for quantification. Both LC-UV-MS data acquisition and instrument control were coordinated by Bruker Compass Hystar 5.1 (version: 5.1.8.1).

**Transient expression in *Nicotiana benthamiana***

Primers for the amplification of *HvAMIS* and *HvNMT* were designed based on annotated CDS sequences from the genome sequence of *H. vulgare* cv. HOR 10350 (*13*). All primer sequences for cloning and sequencing are listed in Table S5. The insert sequences were amplified with SuperFi II polymerase (Thermo Fisher Scientific) from cDNA of barley strain Lina. Amplicons were cloned into the vector pHREAC by Golden Gate cloning as described previously (*17*). Cloned sequences were confirmed by Sanger sequencing. The cloned coding sequence of *HvAMIS* was identical to the coding sequence in the *H. vulgare* cv. HOR 10350 genome (*13*) and was deposited in GenBank under accession number OR461264.

Agroinfiltration into *Nicotiana benthamiana* was performed according to the procedure described earlier by us (*17*). *Nicotiana benthamiana* LAB strain was grown from seeds in a greenhouse with 11 to 16 hours illumination per day and at a temperature between 21 °C to 23 °C. Plasmids containing gene candidates for transient expression were transformed into *Agrobacterium tumefaciens* GV3101 by electroporation. *A. tumefaciens* strains were cultured in LB medium with antibiotics (25 µg/mL gentamicin, 50 µg/mL rifampicin, 50 µg/mL kanamycin) for 2 days at 28 °C shaking at 180 rpm. *A. tumefaciens* cells were then

harvested by centrifugation and resuspended in MMA infiltration buffer (10 mM $MgCl_2$, 10 mM 2-(*N*-morpholino)ethanesulfonic acid (MES), 100 µM acetosyringone). All strains were adjusted to final OD600 0.1 prior to syringe infiltration into the abaxial side of leaves of 4-week-old *N. benthamiana* plants. After infiltration, plants were maintained in a greenhouse until further analysis.
For analytical-scale metabolite extraction and LC-MS analysis, leaves were harvested 7 days after infiltration. Five leaf disks (~10 mg dry weight in total) were collected using cork-borer no. 5 (⌀ = 10 mm) and lyophilized before extraction with 800 µL of 90/10 MeOH/$H_2O$. Samples were centrifuged and the clean supernatant was directly used for LC-MS analysis. Conditions for LC-MS analysis are described in a section below ("Chromatographic analysis of samples from *N. benthamiana*, yeast and microsome assays").

**Isolation of AMI (3) from *N. benthamiana* transiently expressing *AMIS***

Purification of aminomethylindole (AMI) (**3**) from *N. benthamiana* leaves expressing *AMIS* was achieved using a modified version of the protocol by Poocharoen *et al.* (*45*). Infiltrated leaves were harvested 7 days after infiltration and lyophilized for two days. Dry leaves (4.98 g) were ground with a mortar and pestle and extracted with 3 × 300 mL MeOH containing 5% ammonia (i.e., 173 mL ammonia solution 28-30 wt% per 1 L) for 1 hour per extraction round at room temperature. The crude extracts were pooled, concentrated *in vacuo*, suspended in 60 mL 0.1 M HCl and washed with 2 × 60 mL ethyl acetate. The ethyl acetate fraction was re-extracted with 30 mL 0.1 M HCl. The aqueous layers were combined, basified with ammonia solution 28-30 wt% to pH 9 and then extracted with 4 × 80 mL ethyl acetate. These organic layers were combined and concentrated *in vacuo* to give a crude alkaloid fraction. The residue was further purified by silica chromatography (DCM:MeOH:ammonia solution 28-30 wt% from 95:5:1 to 90:10:1 v/v) to give AMI (**3**) (16 mg, 3.2 mg/g dry weight) as green oil. NMR data see Table S2. Spectra of isolated AMI (**3**) matched the synthesized standard (see Fig. S3 and Fig. S4). Spectra of isolated AMI (**3**) are shown in Fig. S26-Fig. S27, spectra of synthetic AMI (**3**) in Fig. S28-Fig. S32. ESI-HR-MS: $[M+Na]^+$ found 169.0732 (calcd. for $C_9H_{10}N_2Na^+$ 169.0736).

**Isolation of gramine (1) from *N. benthamiana* transiently expressing *AMIS* and *NMT***

Purification of gramine (**1**) from *N. benthamiana* leaves expressing *AMIS* and *NMT* was achieved using a modified version of the protocol by Poocharoen *et al.* (*45*). Infiltrated leaves were harvested 7 days after infiltration and lyophilized for two days. Dry leaves (6.49 g) were ground with a mortar and pestle and extracted with 3 × 400 mL MeOH containing 5% ammonia (i.e., 173 mL ammonia solution 28-30 wt% per 1 L) for 1 hour per extraction round at room temperature. The crude extracts were pooled, concentrated *in vacuo*, suspended in 80 mL 0.1 M HCl and washed with 80 mL ethyl acetate. The aqueous layer was basified with ammonia solution 28-30 wt% to pH 9 and extracted with 3 × 100 mL ethyl acetate. These organic layers were combined and concentrated *in vacuo* to give a crude alkaloid fraction. The residue was further purified by silica (DCM:MeOH:ammonia solution 28-30 wt% from 95:5:2 to 90:10:2 v/v) to give gramine (**1**) (43 mg, 6.6 mg/g dry

weight) as a slightly yellow solid. NMR data see Table S3. Spectra of isolated gramine (**1**) matched the commercially available standard (see Fig. S5 and Fig. S6). Spectra of isolated gramine (**1**) are shown in Fig. S33-Fig. S37, spectra of commercially available gramine (**1**) in Fig. S38-Fig. S39. ESI-HR-MS: $[M+H]^+$ found 175.1237 (calcd. for $C_{11}H_{15}N_2^+$ 175.1230).

**Metabolic engineering of *Saccharomyces cerevisiae***

For amplification of *Catharanthus roseus* cytochrome P450 reductase (CPR) and cytochrome $b_5$ (CYB5) genes (*18*), RNA from *Catharanthus roseus* leaves was isolated using the GeneJET Plant RNA Purification Mini Kit (Thermo Scientific) and converted into cDNA using the SuperScript™ IV VILO™ Master Mix (Invitrogen).

Engineering of yeast (*Saccharomyces cerevisiae*) was achieved using the EasyClone-MarkerFree system (*46*). Gene sequences to be inserted into the yeast genome were cloned into EasyClone-MarkerFree integration vectors *via* USER cloning (*46*, *47*). To construct the mutated sequence $HvAMIS^{S211W}$, In-Fusion mutagenesis was applied with In-Fusion® HD Cloning Kit (Takara Bio, Cat# 639650), using the integration vector containing *HvAMIS* as template. Plasmids were transformed into *E. coli* DH5α competent cells (NEB) and verified by Sanger sequencing. Primers used are listed in Table S6, generated strains in Table S7 and gene sequences in Table S8.

Confirmed integration vectors were then linearized with NotI. For *HvAMIS*, HindIII was used instead, due to an internal NotI restriction site. Linearized integration fragments were transformed into yeast using the lithium acetate/single-stranded carrier DNA/PEG protocol (*48*). After transformation, the yeast cells were plated on YPD agar plates containing 200 µg/mL geneticin and 100 µg/mL nourseothricin. After growth for 48 h at 30 °C, correct insertion was confirmed by PCR. The gRNA-plasmid was removed by serial passaging without the selection marker nourseothricin and confirmed by PCR, to enable subsequent transformations.

For the analysis of metabolite profiles of yeast strains, 3 mL primary yeast cultures were inoculated in YPD medium containing 200 µg/mL geneticin. After growth for 16-18 hours at 30 °C and 210 rpm shaking speed, the primary cultures were used to inoculate 3 mL secondary cultures in YPD medium without antibiotics to OD600 0.1. Secondary culture tubes contained a sterile pipette tip to improve mixing and prevent pelleting, and a loose aluminum foil lid for improved gas exchange. The secondary cultures were grown at 30 °C for 48 hours and 210 rpm shaking speed. For the extraction of metabolites afterwards, 500 µL yeast culture was mixed with 1 mL of a 1:1 mixture (v/v) of methanol and acetone. The suspension was homogenized using a bead beating homogenizer (FastPrep-24Tm 5G) and glass beads (⌀ = 0.5 mm, shaking at 6.0 m/s for 40 s with two cycles). After centrifugation at 17,000 *g*, 500 µL of the supernatant were removed and concentrated *in vacuo*. The solid residue was dissolved in 80% (v/v) methanol/water, filtered, and analyzed by LC-MS on the Agilent Infinity II 1260 instrument with the conditions described in a section below ("Chromatographic analysis of samples from *N. benthamiana*, yeast and microsome assays"). For the quantification of AMI (**3**), gramine (**1**), MAMI (**4**) and tryptophan (**2**), calibration curves were generated from reference compounds.

**Yeast microsome purification and enzyme assays**

Yeast microsomes were used for *in vitro* enzyme assays. First, 3 mL primary yeast cultures were inoculated in YPD medium containing 200 µg/mL geneticin. After growth for 16-18 hours at 30 °C and 210 rpm shaking speed, the primary cultures were used to inoculate 50 mL secondary cultures in non-baffled shake flasks with YPD medium without antibiotics to OD600 0.1. These secondary cultures were grown under the same conditions for 48 hours. For microsome isolation, yeast cells were then harvested by centrifugation at 5,000 × *g* at RT for 5 minutes and washed with 10 mL TEK buffer (50 mM Tris, pH 7.4, 1 mM EDTA, 0.1 M KCl). The cells were centrifuged again using the same conditions. The TEK buffer supernatant was discarded and the washed cells were then lysed with glass beads (⌀ = 0.5 mm, 1/3 volume of lysate) with a bead homogenizer (FastPrep-24Tm 5G) shaking at 6.0 m/s for 40 s with two cycles in 7 mL TEB buffer (50 mM Tris, pH 7.4, 1 mM EDTA, 0.6 M sorbitol). After adjusting the volume to 20 mL with TEB buffer, the cell debris was removed by centrifugation at 10,000 × *g* at 4 °C for 10 minutes. Microsomes were then isolated from the supernatant by ultracentrifugation at 100,000 × *g* at 4 °C for 1 hour. To reduce the metabolite background of microsome preparations, an additional optional washing step was performed with 22 mL TEB buffer followed by ultracentrifugation at 100,000 × *g* at 4 °C for 1 hour. Microsomes were finally resuspended in 800 µL of TEG buffer (50 mM Tris, pH 7.4, 1 mM EDTA, 20% glycerol), aliquoted to 200 µL per tube and stored at −80 °C prior to enzyme assays.

Yeast microsome assays were performed in 200 µL total volume containing 50 µL of yeast microsomes, 250 µM of the substrates and 500 µM of NADPH in 50 mM Tris-HCl buffer, pH 7.5. Alternative substrates like isotope-labeled tryptophan, D-tryptophan, and *N*-hydroxy-DL-tryptophan were added to the reaction in the same way as non-labeled tryptophan. The enzyme reactions were conducted at 30 °C, 200 rpm for 16 hours. Alternatively, to reduce background metabolite levels and avoid interfering activities from other microsomal proteins, microsomes were optionally diluted 1:5 with TEG buffer and the reaction time was reduced to 35 minutes. All microsome reactions were stopped by removing microsomal proteins using centrifugal filters (Amicon Ultra 0.5 mL 10 kDa) and centrifugation at 14,000 × *g* at 4 °C for 15 minutes. The flow through was directly used for LC-MS analysis. The same LC-MS instrument and method described in a section below was used ("Chromatographic analysis of samples from *N. benthamiana*, yeast and microsome assays").

To test the oxygen dependency of the AMIS reaction, microsome assays were adjusted to eliminate oxygen from the reaction mixture as much as possible. Therefore, all reaction solutions and microsome suspensions were kept in sealed GC-MS vials and flushed with nitrogen gas for 10 to 12 minutes *via* a needle connected to a nitrogen line submerged in the liquid; an extra non-submerged needle was inserted into the cap to enable gas exchange (see Fig. S9B for a schematic drawing). Afterwards, the microsome solutions were mixed with substrate and NADPH solutions under a nitrogen atmosphere. The reaction vials were placed in a heat block at 30 °C. In case of oxygen-depleted samples, nitrogen gas was continuously bubbled through the reaction mixture during the assay time. Control samples to confirm that AMIS was not denatured by this procedure and that AMIS activity can be restored by addition of oxygen were carried out by flowing compressed air through the sample instead. After 35 min, the reaction was stopped by removal of microsomal proteins and analyzed by LC-MS as described above for normal microsome assays.

For iminium intermediate trapping, 40 µL of freshly prepared 20 mM $NaBH_4$ (4 mM final concentration) dissolved in assay buffer (50 mM Tris-HCl, pH 7.5) was added to yeast microsome assays (200 µL total volume). Otherwise, assays were carried out using the same setup, reaction conditions, and workup for microsomal removal as described above. The control reaction with $NaBH_4$ trapping after microsomal removal was carried out as follows: 200 µL of enzyme reaction without $NaBH_4$ were stopped using a centrifugal filter and centrifuged at 14,000 × *g* at 4 °C for 15 minutes. 50 µL of the flow through were mixed with 12.5 µL freshly prepared 20 mM $NaBH_4$ in assay buffer and incubated at 30 °C for 1 hour prior to LC-MS injection. LC-MS analysis was carried out as described in the section below ("Chromatographic analysis of samples from *N. benthamiana*, yeast and microsome assays").

**Production of tAMIS, a truncated and tagged version of AMIS**

A truncated and tagged version of *HvAMIS* (*tAMIS*) was constructed by a single round of PCR. The construct design is shown in Fig. S10A. *HvAMIS(Δ2-23)* was amplified from a plasmid containing *HvAMIS* using Q5® High-Fidelity DNA Polymerase (New England Biolabs). The forward primer AB20_HvAMIS(Δ2-23)_F was designed to remove the sequence encoding amino acids 2-23. The reverse primer AB27_tAMIS_R was designed to add sequences encoding a HA tag, StrepII tag, linkers, and a stop codon. The final sequence of *tAMIS* was verified by Sanger sequencing and is shown in Table S9. The construct was cloned into the vector pHREAC and used for transient expression as described above ("Transient expression in *Nicotiana benthamiana*"); tAMIS was still able to produce AMI (**3**) *in planta* as determined by metabolite extraction and LC-MS analysis.

**Purification of tAMIS by affinity chromatography**

For protein purification of tAMIS, *N. benthamiana* leaves were harvested three days after infiltration. Affinity chromatography was performed employing the C-terminal StrepII tag of tAMIS. For one purification, 0.75 g of *N. benthamiana* leaves were ground in 1.5 mL buffer E (100 mM Tris-HCl (pH 8.0), 5 mM EDTA, 100 mM NaCl, 0.5% Triton X-100, 15 mM DTT, 1:625 diluted BioLock (IBA Lifesciences), 1:10 diluted cOmplete™ Protease Inhibitor Cocktail (Roche)). Following centrifugation at 21,000 × *g* and 4 °C for 10 min, the supernatant was collected and 40 µL of StrepTactin Macroprep (IBA Lifesciences) were added. To improve binding of StrepII-tagged proteins to the matrix, this mixture was incubated in a rotation wheel at 4 °C for 10 min. The matrix was then collected by centrifugation at 700 × *g* for 30 s and the supernatant discarded. Afterwards, the matrix was washed three times with 0.5 mL buffer W1 (100 mM Tris-HCl (pH 8.0), 2 mM $MgCl_2$, 100 mM NaCl, 0.005% Triton X-100, first washing step: 2 mM DTT) and centrifuged at 700 × *g* for 30 s after each washing step. Finally, the StrepII-tagged protein was eluted with 75 µL buffer W2 (100 mM Tris-HCl (pH 8.0), 2 mM $MgCl_2$, 100 mM NaCl, 0.005% Triton X-100, 20 mM biotin (batches 1 & 2) / 40 mM biotin (batch 3)). The eluate was collected following centrifugation at 700 × *g* for 30 s; elution was repeated, and both fractions pooled. Typical protein concentrations obtained by this procedure were ca. 25-75 µg/mL (ca. 0.5-1.3 µM). Purified tAMIS was stored at 4 °C until further use. Leaves

infiltrated with agrobacteria harboring the empty vector pHREAC (EV) were used for mock purification and served as a negative control.
To analyze the purified fractions, 16 µL were mixed with 4 µL 5× Laemmli loading buffer and separated by SDS-PAGE on a 10% gel. Presence of tAMIS was monitored by Coomassie staining and immunoblotting. To calculate the concentration of tAMIS in the purified fractions, a serial dilution of bovine serum albumin (BSA) was included on the Coomassie-stained gels. Scanning was performed using an Odyssey Fc Imager (LI-COR Biosciences). For immunodetection, proteins were blotted onto nitrocellulose membranes in a semi-dry system. The membranes were then blocked with 20 mL of 5% (w/v) milk powder in TBS-T buffer (20 mM Tris-HCl, pH 7.6; 150 mM NaCl; 0.1% (v/v) Tween 20) for 30 min. Afterwards, murine monoclonal anti-StrepII antibody (anti-STREP-tag 7G8, antibody facility at iTUBS, Braunschweig, Germany) was added to reach a dilution of 1:4,000 and incubated at 4 °C overnight. The membranes were washed with TBS-T three times for 10 min. After washing, they were incubated with 10 mL anti-mouse IgG-alkaline phosphatase (AP) conjugate antibody produced in goat (A3562, Sigma; 1:10,000) in TBS-T for 1 h at room temperature. After washing as described above, staining was performed with nitro blue tetrazolium chloride (NBT) and 5-bromo-4-chloro-3-indolyl phosphate (BCIP).

**Heme quantification using the pyridine hemochromogen assay**

The pyridine hemochromogen assay was carried out to determine the heme concentration in the purified protein fractions as described in the literature (*49*). The spectrophotometer (V-630 UV/Vis Spectrophotometer, JASCO) was set to measure the absorbance with a spectral bandwidth of 1.5 nm and a data interval of 1 nm between 500 and 600 nm. The baseline was recorded with a mixture of 0.5 mL solution 1 (0.2 M NaOH, 40% (v/v) pyridine, 500 µM potassium ferricyanide(III)) and 0.5 mL mixture of buffer W2 (see previous section) and 100 mM Tris-HCl pH 7.5. Protein samples were diluted to 0.5 mL with 100 mM Tris-HCl pH 7.5, mixed with 0.5 mL solution 1, and the absorbance spectrum of this oxidized pyridine hemochromogen recorded. Afterwards, 10 µL of solution 3 (0.5 M sodium dithionite in 0.5 M NaOH) were added and the sample mixed well. It was scanned immediately and further times during the next minutes, until the characteristic absorbance maximum of reduced pyridine hemochromogen at 557 nm reached its maximum. In rare cases, the addition of 10 µL of solution 3 was not sufficient to reduce the heme iron; after addition of further 10 µL of solution 3, the characteristic peak at 557 nm always appeared as expected. From the obtained data, the heme *b* concentration in the protein samples was calculated using the Beer-Lambert law. The difference in absorbance between 557 and 540 nm of the difference spectrum (reduced minus oxidized sample) ($A_{red–ox,557–540}$), was used together with the dual wavelength difference extinction coefficient 23.98 $mM^{-1}$ $cm^{-1}$ (*50*). As a negative control, the assay was performed with mock purified protein obtained from leaves infiltrated with the EV strain as described above. For these controls, no absorbance peak appeared upon reduction, indicating the absence of background heme.

### Quantification of glyoxylic acid in *N. benthamiana* leaves

To quantify glyoxylic acid in *N. benthamiana* leaves after transient expression, leaves were harvested 7 days after infiltration. Seven to eight leaf disks were collected using cork borer no.5 (⌀ = 10 mm) and the fresh weights were recorded. Leaf disks were ground using a mortar and pestle in 700 µL extraction buffer (50 mM Tris-HCl, pH 7.5, 10 mM EDTA, 250 mM sucrose, 5% (v/v) glycerol, 0.5% (wt/wt) polyvinylpolypyrrolidone) on ice for 3 minutes. The extract was filtered through two layers of miracloth and centrifuged for 10 minutes at 10,000 × *g* at 4 °C to remove the solid debris. Then, 50 µL of supernatant was derivatized with phenylhydrazine and detected by LC-MS analysis as described in the following section.

### Chromatographic analysis of samples from *N. benthamiana*, yeast and microsome assays

*N. benthamiana* and samples from microsome assays were analyzed by LC-MS on an Agilent Infinity II 1260 system consisting of a G7167A autosampler, G7116A column thermostat, G7111B quaternary pump, G7110B make-up pump, G7115A diode array detector, and G6125B single quadrupole mass spectrometer equipped with an ESI source (4000 V, 12 L/min drying gas, 350 °C gas temperature). Samples were separated on a C18 column (Poroshell 120 EC-C18, 100 × 4.6 mm, 2.7 µm). The column temperature was set to 30 °C. As mobile phase, solvent A (water with 0.1% (v/v) formic acid) and solvent B (acetonitrile with 0.1% (v/v) formic acid) were used. For AMI, gramine and tryptophan detection, separation was achieved using the following gradient at a flow rate of 1.2 mL/min: 0-7 min, 5-50% B; 7-7.1 min, 50-95% B; 7.1-9 min, 95% B; 9-9.1 min, 95-5% B; 9.1-11 min, 5% B. Mass spectra were obtained in scan mode in a range of *m*/z 100-700 at a fragmentor voltage of 100 V.

For the analysis of yeast whole culture extracts, the following adjustments to the above chromatographic method were applied: The column temperature was set to 20 °C. The gradient was changed to: 0-9 min, 5% B; 9-9.1 min, 5-95% B; 9.1-11 min, 95% B; 11-11.1 min, 95-5% B; 11.1-13 min, 5% B.

For glyoxylic acid detection, 50 µL of flow through from centrifugal filters (see section above for workup of enzyme assays) was derivatized with 40 µL freshly prepared 4% (v/v) phenylhydrazine in $H_2O$ at 37 °C, 700 rpm for 15 minutes to form glyoxylic acid phenylhydrazone (**7**). An isocratic LC-MS method with 80% solvent A (water with 0.1% (v/v) formic acid) and 20% solvent B (acetonitrile with 0.1% (v/v) formic acid) was used with column temperature set to 40 °C. UV chromatograms at 324 nm were recorded with a diode array detector.

Separation and detection of trapped intermediate **8** was achieved by setting the column temperature to 10 °C with the following gradient: 0-12 min, 5% B isocratic; 12-12.5 min, 5-95% B; 12.5-14.5 min, 95% B; 14.5-15 min, 95-5% B; 15-17 min, 5% B. The flow rate was 1.0 mL/min. The mass detector was used in selected ion monitoring mode, targeting *m*/*z* 130.0, 131.0, 132.0, 133.0 with a fragmentor voltage of 100 V, and *m*/*z* 226.8, 227.8, 228.8, 229.8 with a fragmentor voltage of 10 V. The injection volume was 15 µL.

**LC-MS/MS measurements**

LC-MS/MS experiments were carried out on an Agilent Infinity II 1290 system consisting of a G7116B column thermostat, a G7167B multisampler, a G7104A quaternary pump and a 6460 triple quadrupole mass spectrometer. The sample preparation and liquid chromatography conditions for detection of GA-phenylhydrazone (**7**) and trapped intermediate **8** were the same as described in the previous section. GA-phenylhydrazone (**7**) was detected in negative mode with a scan range between *m*/*z* 50 and 170 and a scan time of 500 ms at a fragmentor voltage of 70 V. Precursor ions with *m*/*z* 163.1 (unlabeled **7**) and 164.1 (labeled **7** or isotope peak) were selected and fragmented with a collision energy of 14 eV and cell accelerator voltage of 1 V. For measuring trapped intermediate **8**, positive mode was used for data collection with a scan range from *m*/*z* 30 to 140, a scan time of 500 ms and a fragmentor voltage of 140 V. The precursor ion with *m*/*z* 130.1 was selected and fragmented with a collision energy of 30 eV and cell accelerator voltage of 1 V.

**HR-MS measurements**

HR-MS measurements were carried out on an Orbitrap Q Exactive Plus mass spectrometer (Thermo Fisher) at a resolution of 280,000 (operated in full MS mode); AGC (automatic gain control) target and maximum injection time were set to 3e6 and 200 ms, respectively. The heated ESI (electrospray-ionization) source was operated at 0 eV CID (collision-induced dissociation), sheath gas flow 45, auxiliary gas flow 10, sweep gas flow 2, spray voltage 3.5 kV, capillary temperature 250 °C, S-lens RF level 45.0 and aux gas heater 400 °C.

**Synthesis of aminomethylindole (AMI) (3)**

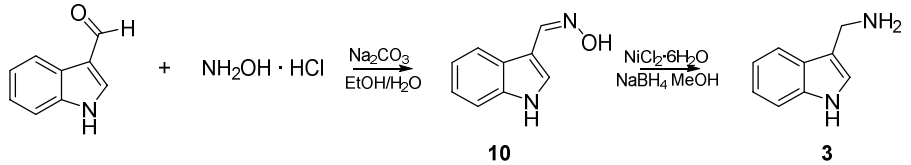


**10** **3**

The synthesis of **3** was carried out according to Guha *et al.* (*51*). Indole-3-carboxaldehyde (100 mg, 689 µmol, 1.0 eq.) was dissolved in a mixture of ethanol (5 mL) and water (1 mL), and then hydroxylamine hydrochloride (83 mg, 1.19 mmol, 1.7 eq.) and anhydrous sodium carbonate (60 mg, 566 µmol, 0.8 eq.) were added in one portion. After 3 h stirring at room temperature, the reaction mixture was concentrated under vacuum. The residue was dissolved in water (10 mL) and extracted with ethyl acetate (3 × 20 mL). The combined organic layers were dried over anhydrous $Na_2SO_4$. After evaporation of ethyl acetate, the desired oxime **10** (107 mg, 667 µmol, 97%) was obtained as a yellowish solid, which was directly used for the next step.

To a solution of this oxime **10** (107 mg, 667 µmol, 1.0 eq.) in methanol (10 mL), nickel (II) chloride hexahydrate (167 mg, 702 µmol, 1.05 eq.) and sodium borohydride (175 mg, 4.63 mmol, 6.9 eq.) were added in one portion under cooling in an ice-water bath. The reaction mixture was then allowed to stir for 3 h at room temperature, followed by concentration under vacuum. The residue was dissolved in 0.8 M ammonia solution (10 mL) and extracted with ethyl acetate (3 × 15 mL). The combined organic layers were dried over anhydrous $Na_2SO_4$. The resulting yellowish oil was purified by column chromatography (silica, DCM:MeOH:ammonia solution 28-30 wt% from 95:5:1 to 80:20:1 v/v) to give **3** (67 mg, 459 µmol, 69%) as a slight yellowish solid. $^1$H NMR (400 MHz, DMSO-$d_6$) δ 10.84 (s, 1H), 7.59 (d, $J$ = 7.8 Hz, 1H), 7.34 (d, $J$ = 8.1 Hz, 1H), 7.20 (s, 1H), 7.11 – 7.02 (m, 1H), 7.02 – 6.93 (m, 1H), 3.88 (s, 2H). $^{13}$C NMR (101 MHz, $CDCl_3$) δ 136.5, 126.5, 122.3, 120.9, 118.7, 118.2, 117.4, 111.3, 37.2. NMR spectra are shown in Fig. S28-Fig. S32. ESI-HR-MS: $[M+Na]^+$ found 169.0735 (calcd. for $C_9H_{10}N_2Na^+$ 169.0736).

**Synthesis of *N*-methylaminomethylindole (MAMI) (4)**

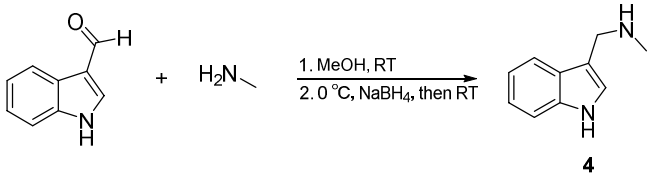


**4**

*N*-Methylaminomethylindole (MAMI) (**4**) was synthesized by a modified method of Ma *et al.* (*52*). 40% w/w methylamine in methanol (0.31 mL, 3.0 mmol, 3.0 eq.) was diluted with 2 mL methanol and added to a solution of indole-3-carboxaldehyde (145 mg, 1.0 mmol, 1.0 eq.) in methanol (10 mL) at room temperature. After the reaction mixture was stirred overnight in the dark, it was cooled to 0 °C in an ice-water bath and $NaBH_4$ (76 mg, 2.0 mmol, 2.0 eq.) was added at 0 °C in one portion. The mixture was allowed to warm to room temperature and stirred for another 3 hours; then, the solvent was removed under vacuum. The residue was suspended with 1 M NaOH (3 mL) and extracted with ethyl acetate (3 ×

10 mL). The combined organic layers were dried over anhydrous $Na_2SO_4$. Removal of volatiles gave a yellowish oil. Further purification by column chromatography (silica, DCM:MeOH:triethylamine 80:20:2 v/v) gave **4** (153 mg, 0.95 mmol, 95%) as a yellowish oil, which started to crystallize under fine vacuum. $^1$H NMR (400 MHz, DMSO-$d_6$) δ 10.88 (s, 1H), 7.60 (d, *J* = 7.9 Hz, 1H), 7.34 (dt, *J* = 8.1, 0.9 Hz, 1H), 7.22 (d, *J* = 2.2 Hz, 1H), 7.09 – 7.03 (m, 1H), 6.99 – 6.94 (m, 1H), 3.81 (d, *J* = 0.4 Hz, 2H), 2.32 (s, 3H). $^{13}$C NMR (101 MHz, $CDCl_3$) δ 136.3, 127.0, 123.6, 120.9, 118.7, 118.2, 113.1, 111.3, 46.2, 35.5. NMR spectra are shown in Fig. S40-Fig. S44. ESI-HR-MS: $[M+H]^+$ found 161.1069 (calcd. For $C_{10}H_{13}N_2^+$ 161.1073).

**Synthesis of *N*-hydroxy-DL-tryptophan (9)**

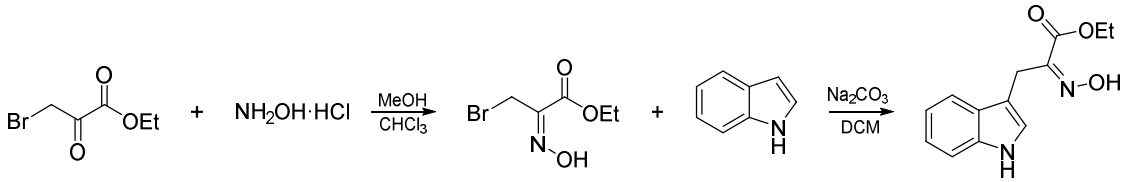


**12** **11**

**Ethyl 2-hydroxyimino-3-(indol-3-yl)propionate (11).** Ethyl 2-hydroxyimino-3-(indol-3-yl)propionate (**11**) was synthesized according to a procedure by Ottenheijm *et al.* (*53*). To a solution of ethyl bromopyruvate (tech. 90%, 519 mg, 2.40 mmol, 1.0 eq.) in a mixture of methanol (5 mL) and chloroform (7.5 mL), hydroxylamine hydrochloride (185 mg, 2.66 mmol, 1.1 eq.) was added in one portion. The mixture was stirred for 16 h at room temperature. Afterwards, the solvent was removed *in vacuo* and the residue was dissolved in dichloromethane (20 mL). The solution was then washed with 0.1 N HCl (aq.) and brine, and afterwards dried over $Na_2SO_4$. The organic phase was concentrated *in vacuo* to give a light brown solid. Recrystallization from dichloromethane and petroleum ether afforded the desired oxime **12** (424 mg, 2.02 mmol, 84%) as an off-white solid, which was directly used for the next synthesis step.

Oxime **12** (211 mg, 1.0 mmol, 1.0 eq.) and indole (353 mg, 3.0 mmol, 3.0 eq.) were dissolved in dichloromethane (25 mL), and $Na_2CO_3$ (583 mg, 5.5 mmol, 5.5 eq.) was added in one portion under vigorous stirring. The resulting suspension was stirred rapidly for one day, then, the resulting solid was filtered off. The filtrate was concentrated to dryness and purified by column chromatography (silica, DCM:MeOH from 100:0 to 50:1) to give **11** (218 mg, 0.89 mmol, 89%) as an off-white solid. $^1$H NMR (400 MHz, $CDCl_3$) δ 9.39 (brs, 1H), 8.01 (s, 1H), 7.79 (d, *J* = 7.9 Hz, 1H), 7.33 (d, *J* = 8.0 Hz, 1H), 7.22 – 7.16 (m, 1H), 7.15 – 7.09 (m, 2H), 4.27 (q, *J* = 7.1 Hz, 2H), 4.11 (s, 2H), 1.31 (t, *J* = 7.1 Hz, 3H). $^{13}$C NMR (101 MHz, $CDCl_3$) δ 163.6, 151.7, 136.0, 127.4, 123.7, 122.2, 119.7, 119.4, 111.1, 109.7, 62.0, 20.3, 14.2. NMR spectra are shown in Fig. S45 and Fig. S46. ESI-HR-MS: $[M+Na]^+$ found 269.0903 (calcd. for $C_{13}H_{14}N_2O_3Na^+$ 269.0897).

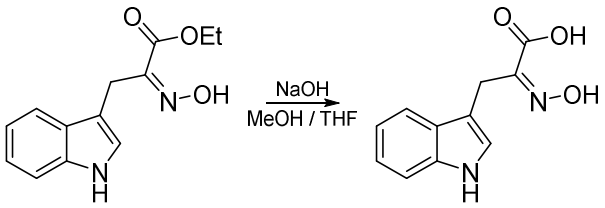


**11** **13**

**Hydroxyimino tryptophan (13).** Saponification of **11** was carried out based on a procedure by Plate *et al.* (*54*). To a solution of ester **11** (48 mg, 195 µmol, 1.0 eq.) in a mixture of MeOH and THF (v/v 1:1, 800 µL) was added 1 N NaOH aqueous solution (490 µL, 490 µmol, 2.5 eq.). The mixture was stirred for 3 days at room temperature until it reached completion as judged by TLC. The solution was neutralized with 2 N HCl. The reaction mixture was partially concentrated *in vacuo* to remove organic solvents, diluted with water and extracted with ethyl acetate. The organic layer was dried over $Na_2SO_4$ and concentrated *in vacuo* to give hydroxyimino tryptophan (**13**) (40 mg, 183 µmol, 94%) as a yellowish oil. $^1$H NMR (400 MHz, methanol-$d_4$) δ 7.67 (dt, *J* = 7.9, 1.0 Hz, 1H), 7.29 (dt, *J* = 8.1, 0.9 Hz, 1H), 7.07 (s, 1H), 7.06 (ddd, *J* = 8.2, 7.0, 1.1 Hz, 1H), 6.97 (ddd, *J* = 8.0, 7.1, 1.0 Hz, 1H), 4.02 (d, *J* = 0.6 Hz, 2H). $^{13}$C NMR (101 MHz, methanol-$d_4$) δ 167.2, 152.9, 137.8, 128.6, 124.7, 122.2, 119.9, 119.5, 112.0, 110.2, 20.8. NMR spectra are shown in Fig. S47 and Fig. S48. ESI-HR-MS: $[M+H]^+$ found 219.0771 (calcd. for $C_{11}H_{11}N_2O_3^+$ 219.0764).

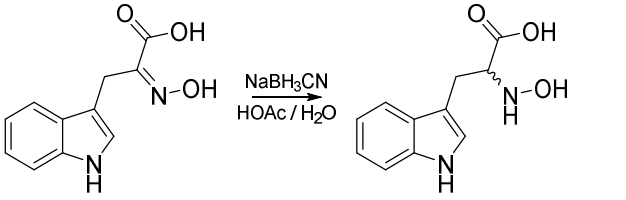


**13** *N*-hydroxy-DL-tryptophan (**9**)

***N*-hydroxy-DL-tryptophan (9).** The reduction of **13** was carried out according to Matsui *et al.* (*55*). A solution of oxime **13** (40 mg, 183 µmol, 1.0 eq.) in 50% acetic acid (4.6 mL) was added to a 20 mL glass vial charged with sodium cyanoborohydride (58 mg, 923 µmol, 5.0 eq.). The reaction mixture was stirred for 18 h at room temperature. The reaction was then quenched with 6 N HCl (1 mL). After gas formation ceased, the solution was neutralized with 6 N NaOH (aqueous solution). The aqueous layer was washed with dichloromethane and then purified by flash chromatography (Biotage, Sfär C18D, $H_2O$/MeCN 19:1 to 1:9 gradient) yielding desired *N*-hydroxy-DL-tryptophan (**9**) (25 mg, 114 µmol, 62%) as a white powder. $^1$H NMR (600 MHz, DMSO-$d_6$) δ 10.81 (s, 1H), 7.52 (d, *J* = 7.9 Hz, 1H), 7.32 (d, *J* = 8.1 Hz, 1H), 7.13 (d, *J* = 2.2 Hz, 1H), 7.08 – 7.02 (m, 1H), 7.00 – 6.94 (m, 1H), 3.63 (t, *J* = 6.9 Hz, 1H), 2.94 (dd, *J* = 14.6, 6.8 Hz, 1H), 2.87 (dd, *J* = 14.6, 6.9 Hz, 1H). $^{13}$C NMR (151 MHz, DMSO-$d_6$) δ 174.9, 136.1, 127.3, 123.6, 120.8, 118.3, 118.3, 111.3, 110.1, 66.2, 24.9. NMR spectra are shown in Fig. S49-Fig. S53. ESI-HR-MS: $[M+H]^+$ found 221.0926 (calcd. for $C_{11}H_{13}N_2O_3^+$ 221.0921).

**Synthesis of 2-(2-phenylhydrazinylidene)acetic acid (GA-phenylhydrazone) (7)**

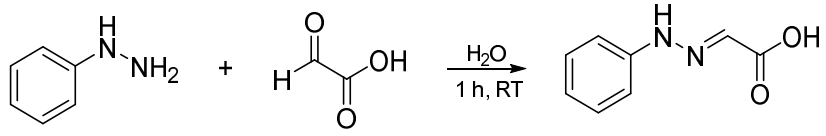


**7**

GA-phenylhydrazone (**7**) was synthesized according to ref. (*56*). To a solution of glyoxylic acid monohydrate (111 mg, 1.21 mmol, 1.0 eq.) in water (2 mL), phenylhydrazine (148 µL, 1.51 mmol, 1.2 eq.) was added dropwise. The reaction mixture was stirred for a further hour. The desired hydrazone **7** (198 mg, 1.21 mmol, quant.) was obtained by filtration and washing with water as a yellow solid. $^{1}$H NMR (400 MHz, DMSO-$d_6$) δ 11.15 (s, 1H), 7.27 (t, *J* = 7.9 Hz, 2H), 7.12 (s, 1H), 7.11 (d, *J* = 8.7 Hz, 2H), 6.89 (t, *J* = 7.3 Hz, 1H). $^{13}$C NMR (101 MHz, DMSO-$d_6$) δ 165.50, 143.64, 129.44, 126.03, 121.27, 113.30. NMR spectra are shown in Fig. S54 and Fig. S55. ESI-HR-MS: $[M-H]^-$ found 163.0497 (calcd. for $C_8H_7N_2O_2^-$ 163.0513).

**Synthesis of *N*-[(indol-3-yl) methyl]glycine (8)**

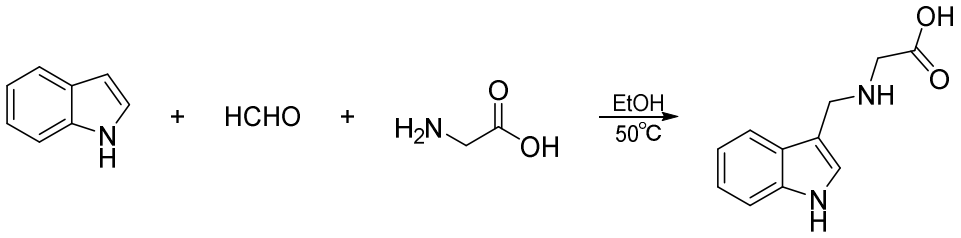


**8**

Compound **8** was synthesized following a procedure by Wiedemann *et al.* (*57*). In a round bottom flask, glycine (80 mg, 1.05 mmol, 1.05 eq.) and formalin (37% solution, 75 µL, 1.00 mmol, 1.0 eq.) were mixed with water (4 mL) and heated at 50 °C. After the reaction mixture became clear (ca. 10 mins), a solution of indole (123 mg, 1.05 mmol, 1.05 eq.) in EtOH (4 mL) was added. The mixture was stirred for 3 h at 50 °C, followed by concentration *in vacuo*. Final purification by flash chromatography (Biotage, Sfär C18D, $H_2O$/MeCN 19:1 to 0:1 gradient) gave the desired product **8** (73 mg, 357 µmol, 36%) as an off-white solid. $^{1}$H NMR (400 MHz, DMSO-$d_6$) δ 11.26 (s, 1H), 7.73 (d, *J* = 7.9 Hz, 1H), 7.46 (d, *J* = 2.5 Hz, 1H), 7.40 (d, *J* = 8.1 Hz, 1H), 7.16 – 7.10 (m, 1H), 7.05 (td, *J* = 7.5, 1.0 Hz, 1H), 4.19 (s, 2H), 3.08 (s, 2H). $^{13}$C NMR (101 MHz, DMSO-$d_6$) δ 166.6, 136.0, 2x 126.8*, 121.5, 119.1, 118.6, 111.7, 105.9, 48.6, 41.3. NMR spectra are shown in Fig. S56-Fig. S60. ESI-HR-MS: $[M+Na]^+$ found 227.0805 (calcd. for $C_{11}H_{12}N_2O_2Na^+$ 227.0791).

*Two carbon signals overlapped

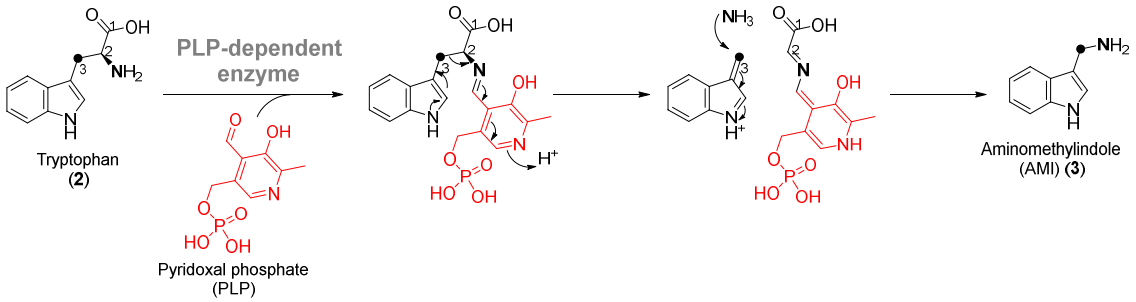


**Fig. S1. Previous biosynthetic proposal based on a pyridoxal phosphate (PLP)-dependent enzyme by Wenkert (1962) and Leete (1963).**

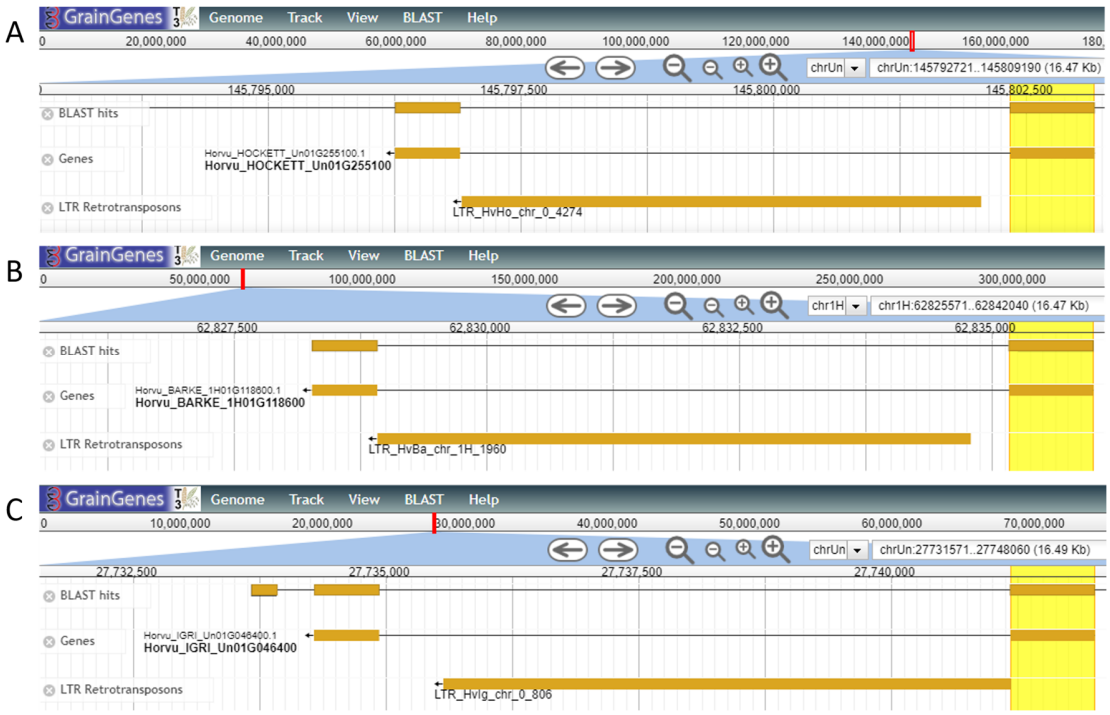


**Fig. S2. The *HvAMIS* gene in the genome annotations of the accessions Barke, Hockett and Igri is predicted to include an intron which contains an LTR retrotransposon where other cultivars do not.**

**The sequence of *HvAMIS* was visualized using the GrainGenes BLAST service (https://wheat.pw.usda.gov) based on the published pan-genome data (*13*). Thick orange lines represent exons and thin black lines represent introns.**

**(A) Genome of cultivar Hockett.**

**(B) Genome of cultivar Barke.**

**(C) Genome of cultivar Igri.**

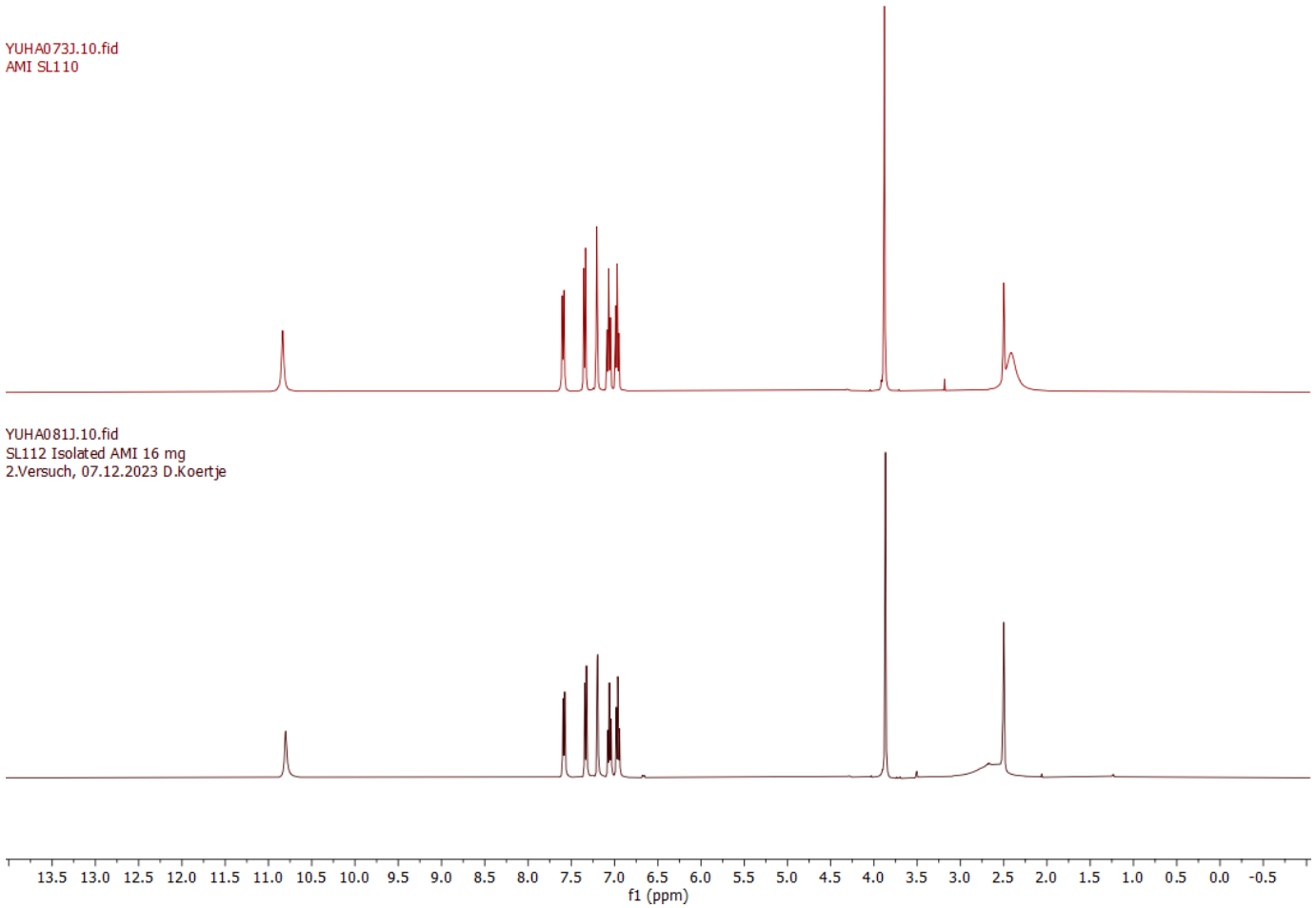


**Fig. S3. Comparison of $^{1}$H spectra of synthesized AMI (upper) and isolated AMI from *Nicotiana benthamiana* transiently expressing *AMIS* (bottom) (298 K, DMSO-d$_6$, 400 MHz).**

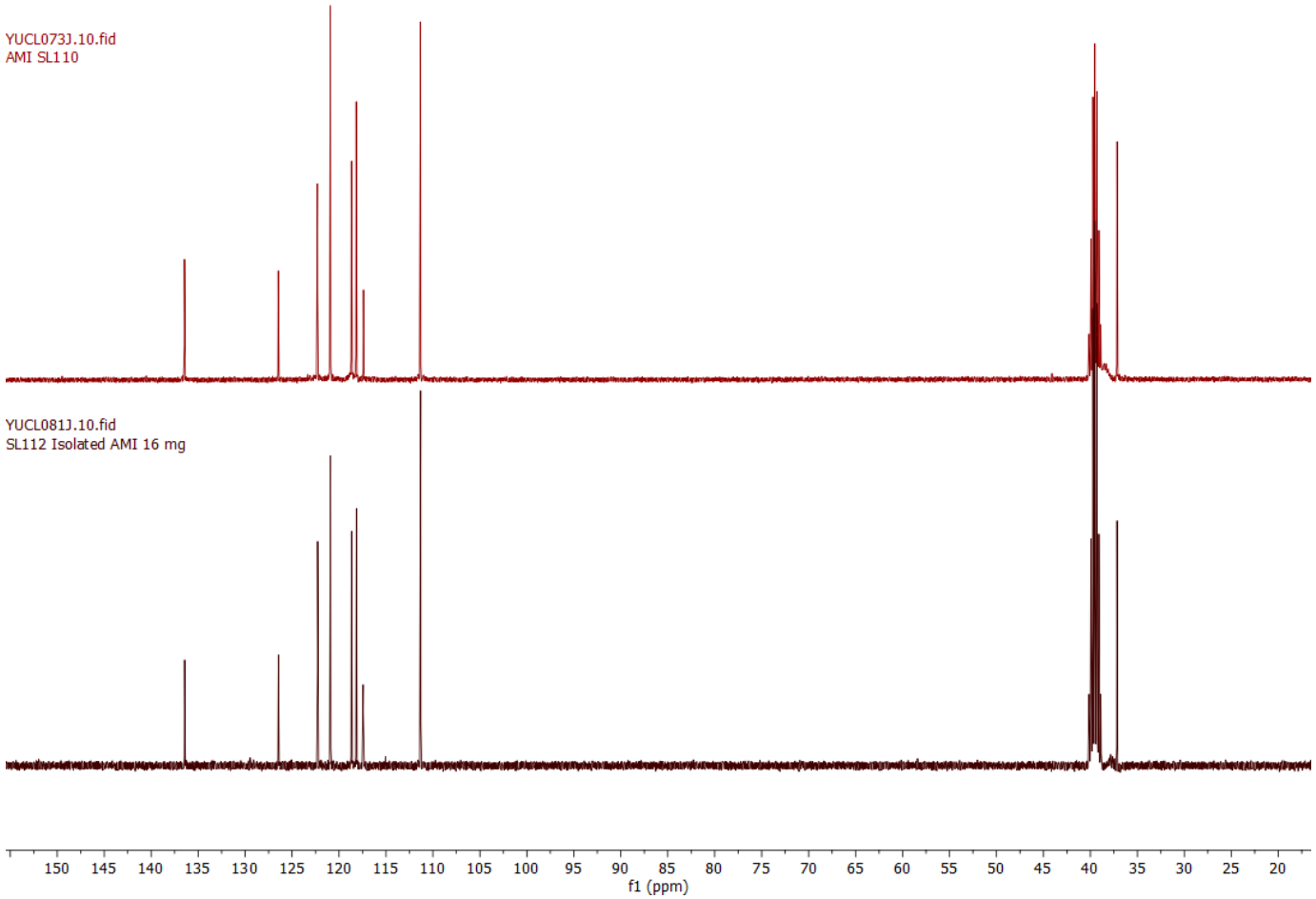


**Fig. S4. Comparison of $^{13}C$ spectra of synthesized AMI (upper) and isolated AMI from *Nicotiana benthamiana* transiently expressing *AMIS* (bottom) (298 K, DMSO-$d_6$, 101 MHz).**

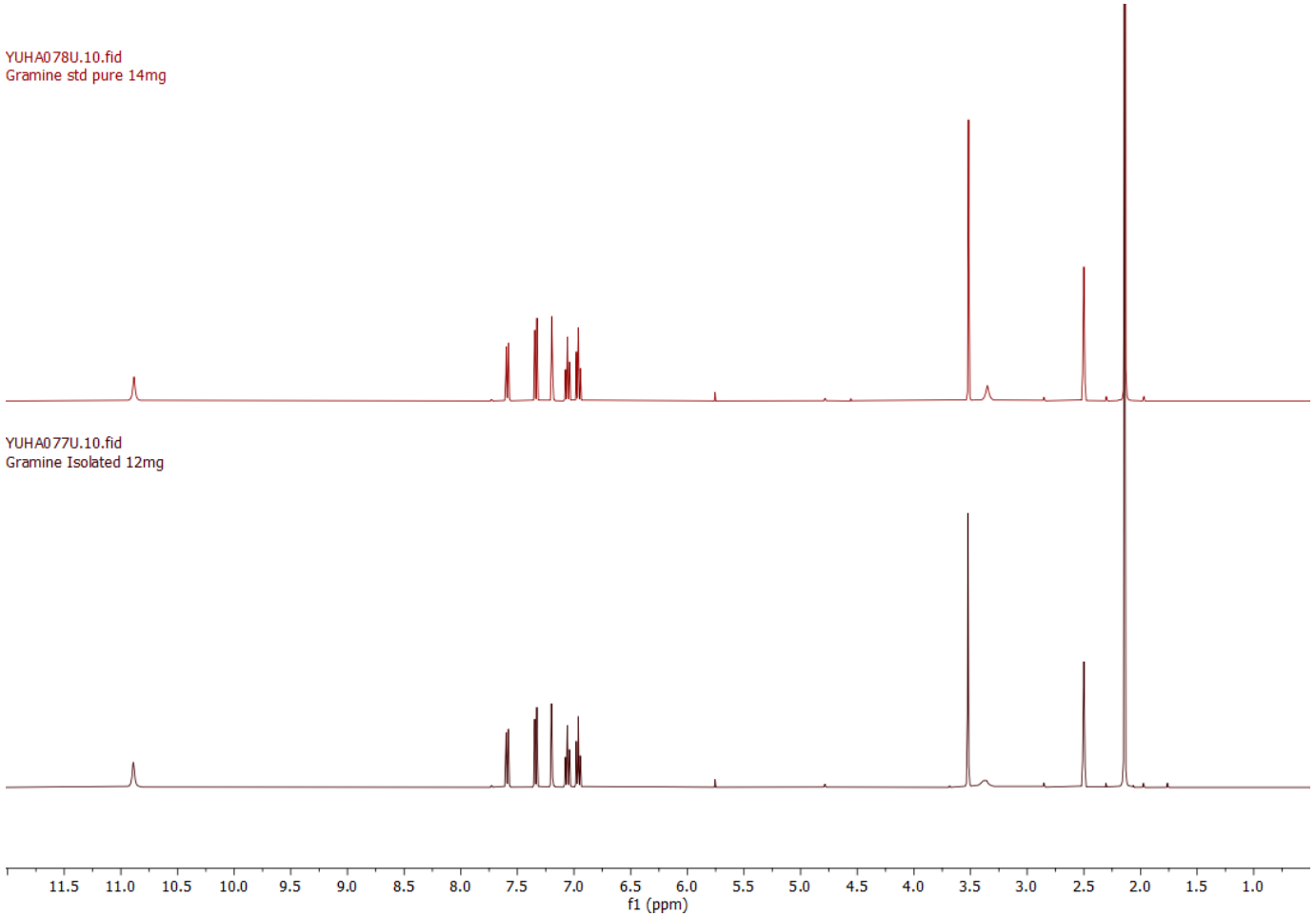


**Fig. S5. Comparison of $^{1}$H spectra of commercially available gramine (upper) and isolated gramine from *Nicotiana benthamiana* transiently expressing *AMIS* and *NMT* (bottom) (298 K, DMSO-d$_6$, 400 MHz).**

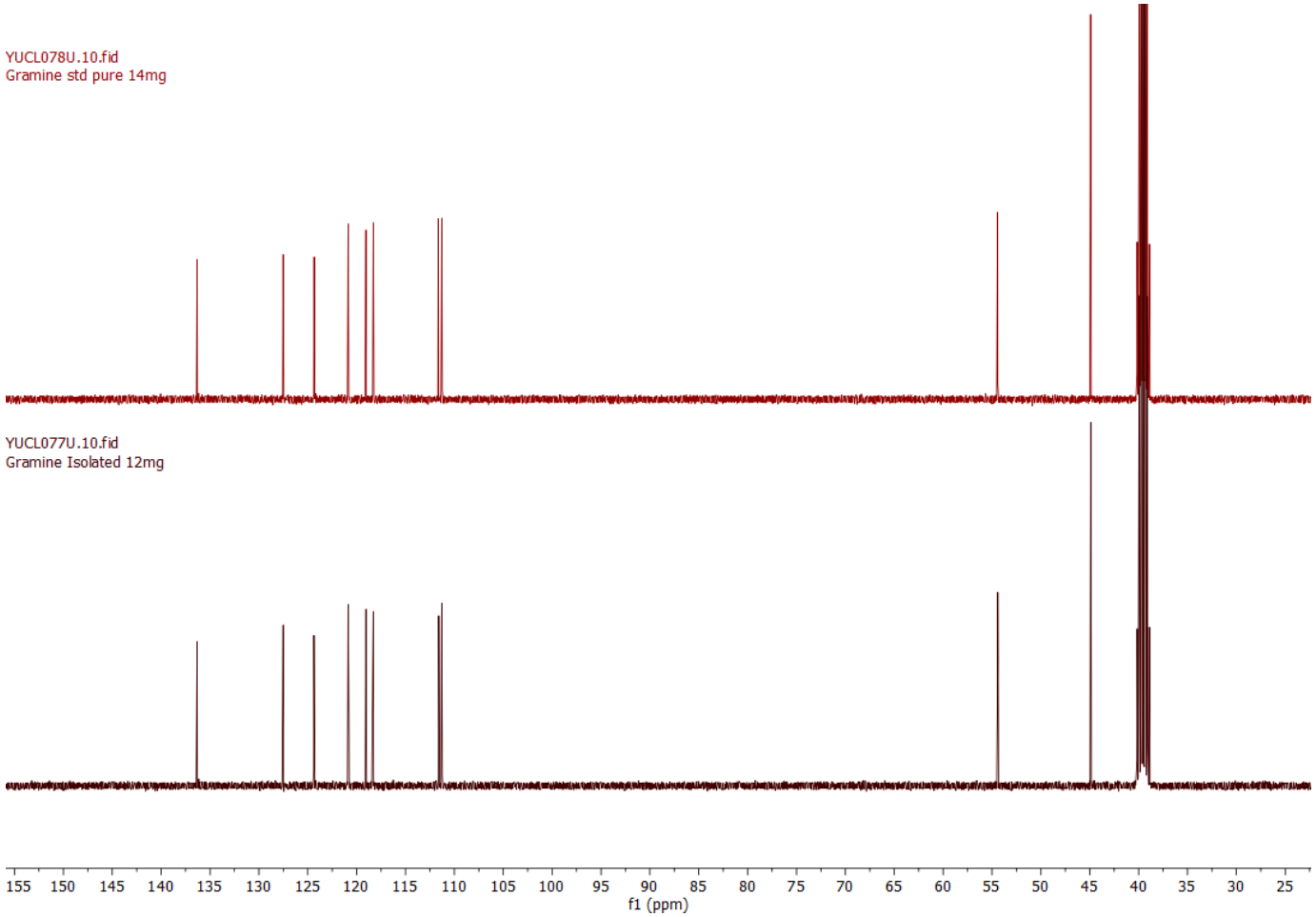


**Fig. S6. Comparison of $^{13}C$ spectra of commercially available gramine (upper) and isolated gramine from *Nicotiana benthamiana* transiently expressing *AMIS* and *NMT* (bottom) (298 K, DMSO-$d_6$, 101 MHz).**

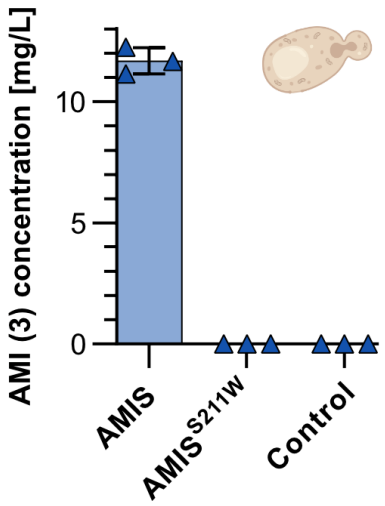


**Fig. S7. AMIS mutation S211W occurring in *H. vulgare* cv. ZDM_01467 leads to complete loss of AMIS activity in yeast whole cell cultures.**

**Genes encoding AMIS or AMIS$^{S211W}$ were integrated into yeast strain BSY1 containing *CPR* and *CYB5* genes (control). The correct genomic integration and mutation of *AMIS$^{S211W}$* was verified by PCR and sequencing.**

**The bar plot shows the means of three biological replicates. Error bars are standard deviations. Data points for each replicate are shown.**

A


B

| Target motif no. | Target motif incl. PAM | No. of regenerated plants ($T_0$) | Primary mutant plants* ($T_0$ = $M_1$) |
|---|---|---|---|
| 1 | CCGCCGGGCCCCCGTCCATGGCC | 7 | 2 |
| 2 | CCTCCTCGACCTCCGCGGGGG | | 5 |
| 3 | GGAAGAGGTGCCATGCGGTGG | | 6 |

*each mutant plant can be mutated at several target motifs

C

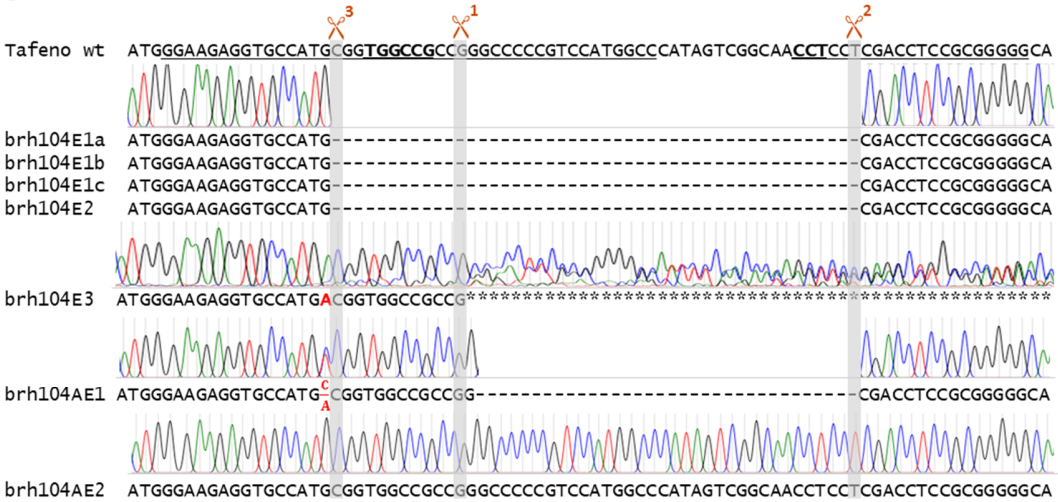


D


**Fig. S8. Knockout of the *HvAMIS* gene in winter barley cv. Tafeno.**

**(A) Localization of the target motifs for Cas9-induced mutagenesis (scissors) within the coding region of the *HvAMIS* gene (grey box).**

**(B) Summary of target motif sequences, number of generated plants and number of primary mutants thereof.**

**(C) Alignment of the *HvAMIS* target region between the wild-type (wt) sequence of Tafeno and primary mutants. Clear single peaks in the chromatogram of Sanger sequencing indicate homozygosity of the induced deletions or insertions in 5 plants (brh104E1a-c, brh104E2 and brh104AE1). These plants resulted from 3 independent mutation events as plants brh104E1a-c are clones derived from the same callus. The**

**double peaks in the chromatogram of plant brh104E3 indicate the presence of more than one allele. Plant brh104AE2 is not mutated.**

**(D) The first 57 residues of the resulting protein sequence from 47 bp deletion (brh104E1a-c, brh104E2) and 1 bp insertion + 34 bp deletion (brh104AE1) aligned to the HvAMIS wild-type protein.**

**Target motifs are underlined, and PAM double-underlined and bold; grey boxes and scissors indicate Cas9 cleavage sites, dashes indicate deleted nucleotides, red and bold letters indicate insertions or altered amino acid residues, asterisks indicate double peaks in chromatogram, wt: wild-type.**

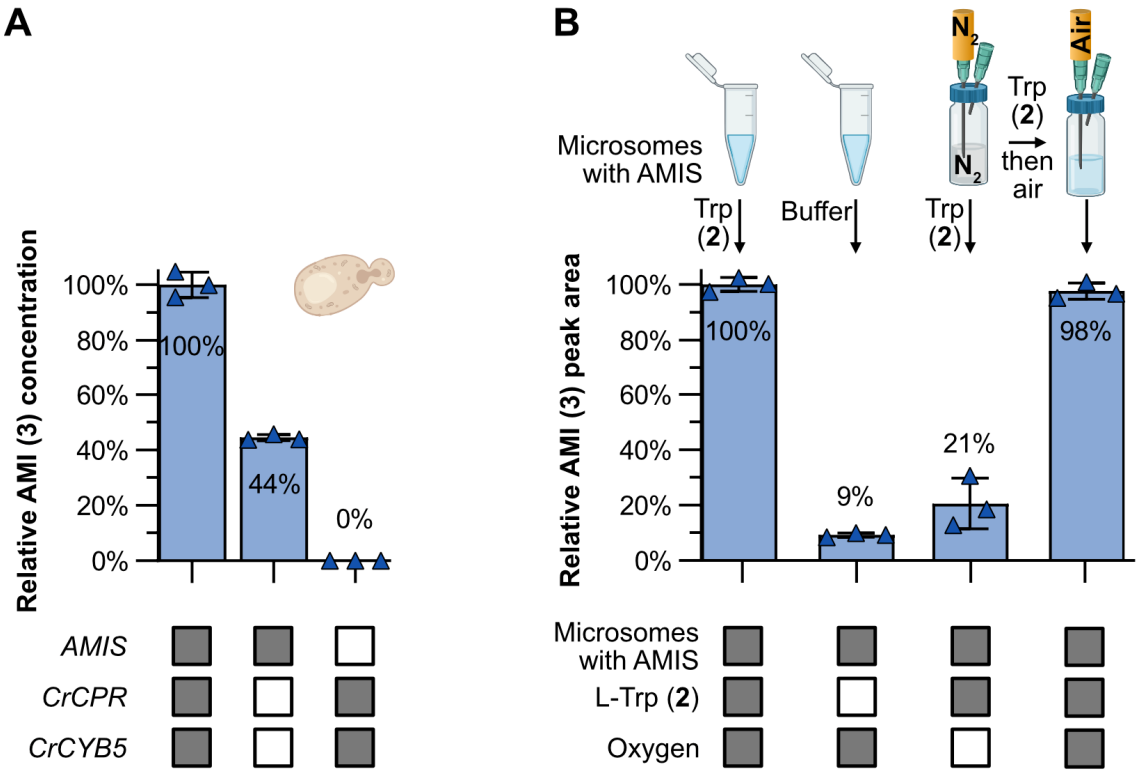


**Fig. S9. AMIS activity depends on redox partners and oxygen.**

**(A) Activity of AMIS in yeast is decreased when *C. roseus* cytochrome P450 reductase and cytochrome $b_5$ genes *CrCPR* and *CrCYB5* are absent. The residual activity is putatively enabled by presence of *S. cerevisiae* cytochrome P450 reductase NCP1. The AMI (3) concentration in yeast strain BSY23 containing *AMIS*, *CPR* and *CYB5* genes was set to 100%. The bar plot shows the means of three biological replicates. Error bars are standard deviations. Data points for each replicate are shown.**

**(B) AMIS microsome assays flushed with nitrogen to remove oxygen show a severe decrease of AMIS activity, which can be restored by flushing with pressurized air after the assay start. These assays were started by mixing nitrogen-flushed microsomes with nitrogen-flushed reaction buffer containing the substrate L-Trp (2) and NADPH. The bar plot shows the means of three replicates. Error bars are standard deviations. Data points for each replicate are shown.**

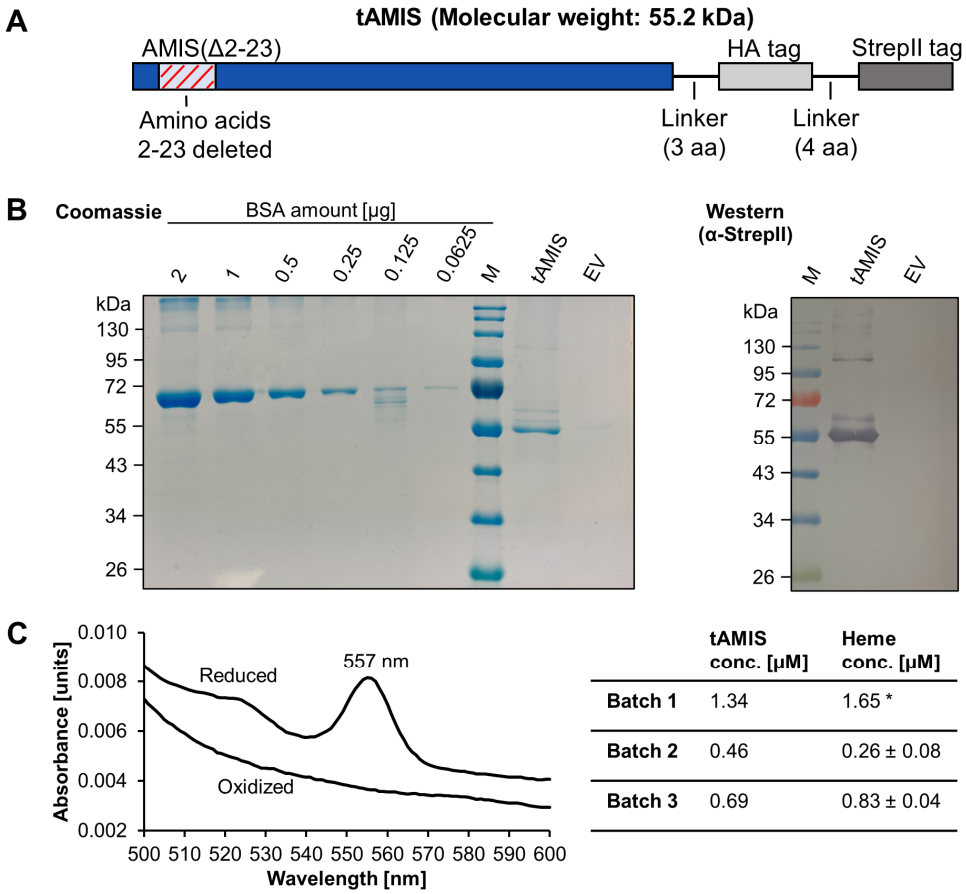


| | tAMIS conc. [µM] | Heme conc. [µM] |
|---|---|---|
| **Batch 1** | 1.34 | 1.65 * |
| **Batch 2** | 0.46 | 0.26 ± 0.08 |
| **Batch 3** | 0.69 | 0.83 ± 0.04 |

**Fig. S10. Purification of soluble truncated and tagged AMIS (tAMIS) and heme quantification.**

**(A) Schematic overview of tAMIS design. Amino acids 2-23 of AMIS were removed to eliminate the membrane anchor. Additionally, a HA tag and a StrepII tag for affinity chromatography were fused to the C-terminus, separated by short linker sequences. Predicted molecular weight of tAMIS: 55.2 kDa. The full coding sequence is shown in Table S9. Primers are shown in Table S5.**

**(B) Affinity purification of tAMIS from transient expression in *N. benthamiana* leaves *via* its C-terminal StrepII tag. The presence of tAMIS was monitored by Coomassie staining and immunoblotting. Quantification was achieved using a BSA serial dilution. As a negative control, leaves were infiltrated with *A. tumefaciens* harboring the empty vector pHREAC (EV) followed by mock affinity purification. Marker (M): Color Prestained Protein Standard, Broad Range (10-250 kDa) (New England Biolabs).**

**(C) Heme quantification using the pyridine hemochromogen assay (*49*) confirms that tAMIS is a hemoprotein. Example UV-Vis spectra of reduced and oxidized pyridine hemochromogen are shown. Approximately equimolar concentrations of protein and heme were measured for three independent protein batches (* batch 1: no replicates due to limited material). Mock protein fractions from the negative control (EV) did not show any absorbance change upon reduction.**

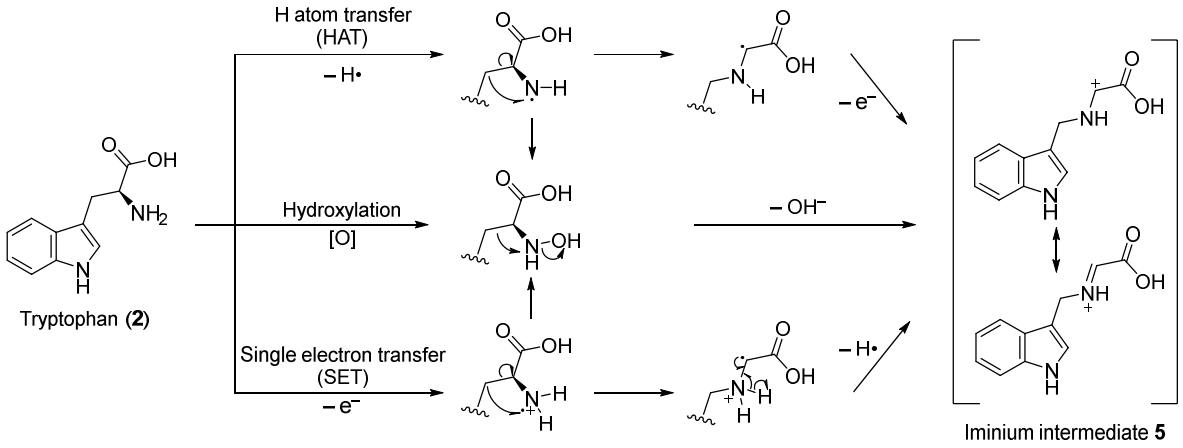


**Fig. S11. Possible mechanisms for the oxidative rearrangement of tryptophan (2) to the iminium intermediate 5 catalyzed by AMIS.**

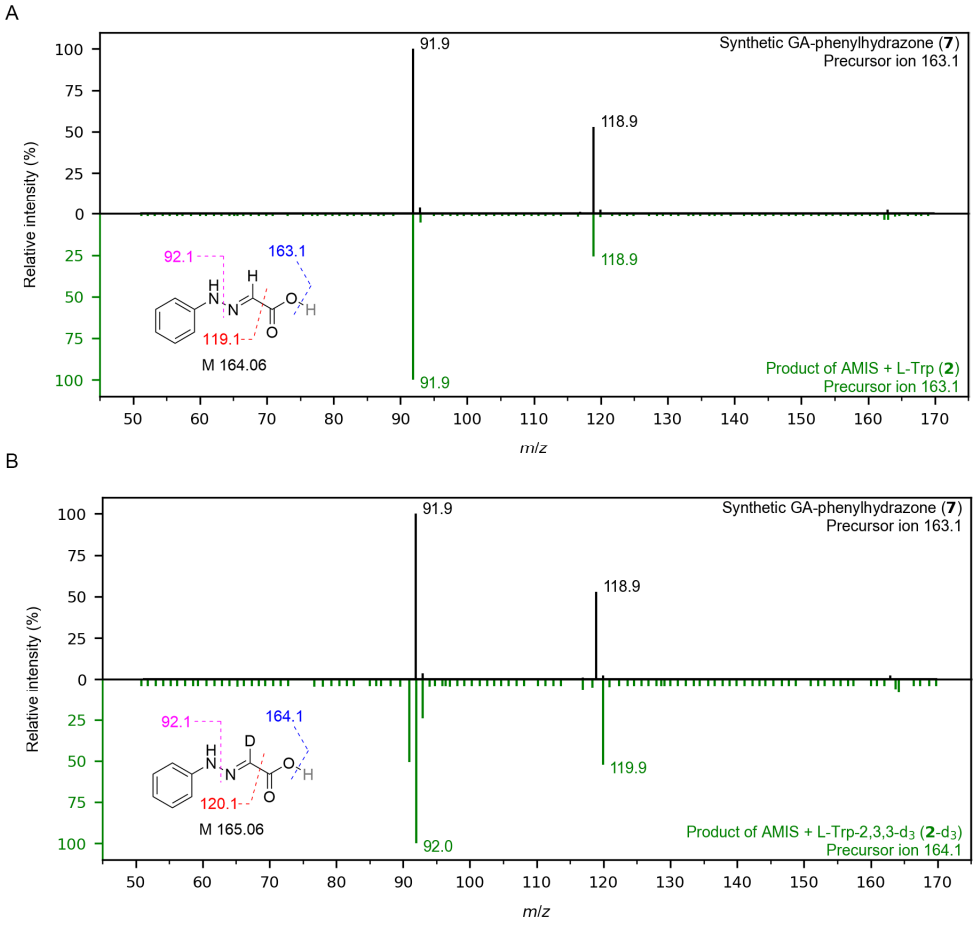


**Fig. S12. MS/MS-based verification of GA-phenylhydrazone (7).**

**(A) MS/MS spectrum of synthetic GA-phenylhydrazone (7) (black) in comparison to enzymatically produced 7 from the reaction of AMIS with L-Trp (2) (green). The structure and proposed fragments of 7 are shown.**

**(B) MS/MS spectrum of synthetic GA-phenylhydrazone (7) (black) in comparison to enzymatically produced labeled 7 from the reaction of AMIS with L-Trp-2,3,3-$d_3$ (2-$d_3$) (green). The detection of labeled fragment ion 119.9 (118.9 +1) further supports the identity of this compound. The structure and proposed fragments of labeled 7 are shown.**

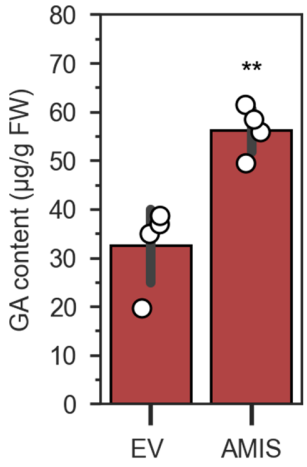


**Fig. S13. Glyoxylic acid (GA, 6) content increases in *Nicotiana benthamiana* leaves transiently expressing *AMIS* compared to an empty vector (EV) control.**

**GA was quantified after phenylhydrazine derivatization. The bar plot shows means ± standard deviation and data points of four biological replicates. ** p-value of Student t-test (two-tailed, equal variance) less than 0.01.**

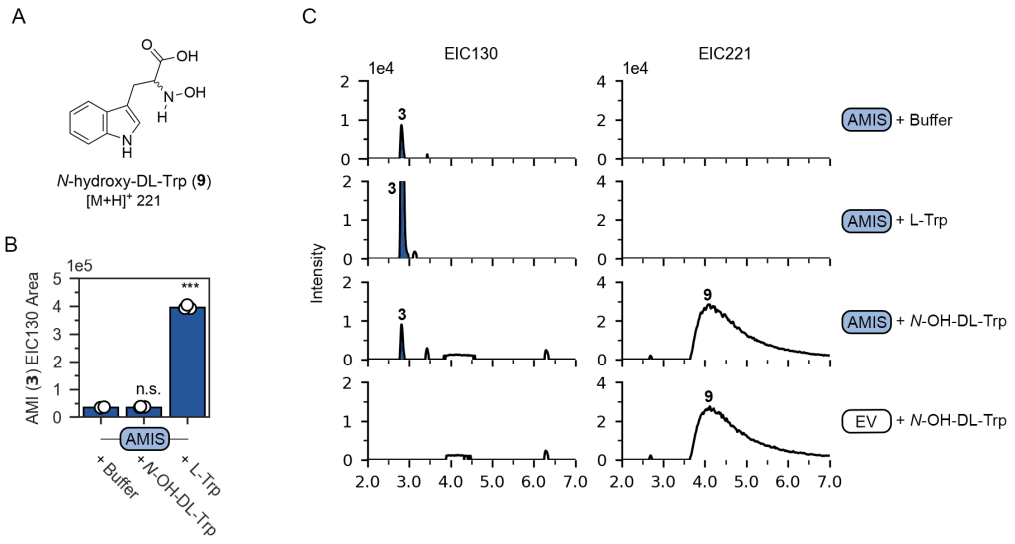


**Fig. S14. *N*-Hydroxy-tryptophan (9) is not accepted as a substrate by AMIS and is not detectable during *in vitro* assays of AMIS with Trp (2).**

**(A) Structure of *N*-hydroxy-DL-Trp (9), synthesized as a racemic mixture.**

**(B) Production of AMI (3) by AMIS using buffer (negative control), *N*-hydroxy-DL-Trp (9) and Trp (2) (positive control) as a substrate. Bars are the means of three replicates. Error bars are standard deviations. *** p-value of Student t-test less than 0.001. n.s. not significant. Data points for each replicate are shown.**

**(C) LC-MS chromatograms showing EIC130 (in-source fragment of AMI (3)) and EIC221 ($[M+H]^+$ for 9) of AMIS reactions. No *N*-hydroxy-Trp (9) is detected when the native substrate Trp (2) is used.**

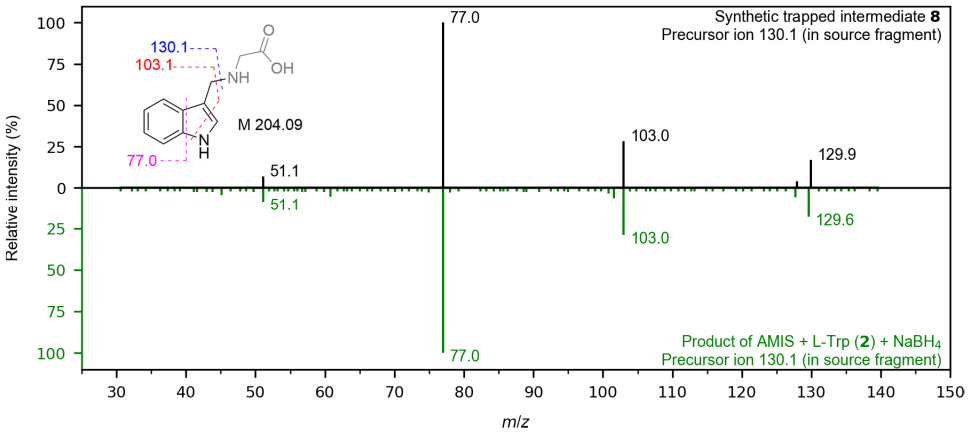


**Fig. S15. MS/MS-based verification of trapped intermediate 8.**

**MS/MS spectrum of in-source fragment *m*/*z* 130 of a synthetic standard of trapped intermediate 8 (black) in comparison to 8 observed from yeast microsome assays with AMIS and L-Trp (2) after trapping with $NaBH_4$. The structure and proposed fragments of 8 are shown.**

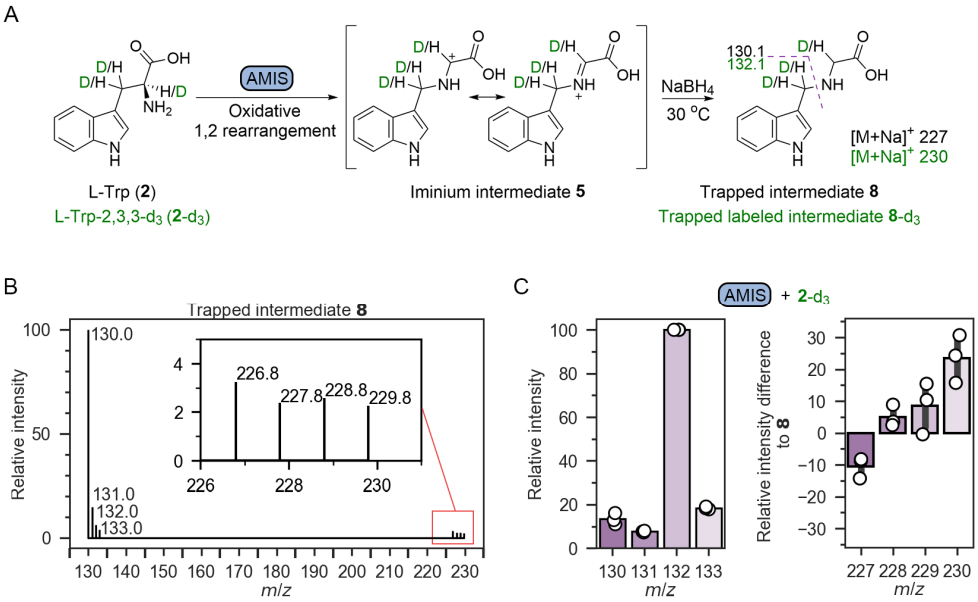


**Fig. S16. Isotope labelling experiments with L-tryptophan-2,3,3-d$_3$ (2-d$_3$) support that AMIS carries out no oxidation at C-2 and C-3 of tryptophan.**

**(A) Labeled atoms during the AMIS reaction with 2,3,3-d$_3$ labeled Trp (2-d$_3$) (green) compared to non-labeled Trp (2).**

**(B) Mass spectrum of trapped intermediate 8 obtained from non-labeled L-Trp (2). Despite strong in-source fragmentation, traces of $[M+Na]^+$ can be detected at *m*/*z* 227. Measurement was performed in single-ion monitoring mode combining *m*/*z* 130-133 and 227-230.**

**(C) Isotope pattern of trapped intermediate 8 from *in vitro* reactions of AMIS with 2-d$_3$. The increase of *m*/*z* 132 and 230 suggests that no stoichiometric loss of D and thereby no oxidation occurs at C-2 and C-3. The bars show the means of the three replicates. Error bars are standard deviations. Data points for each replicate are shown.**

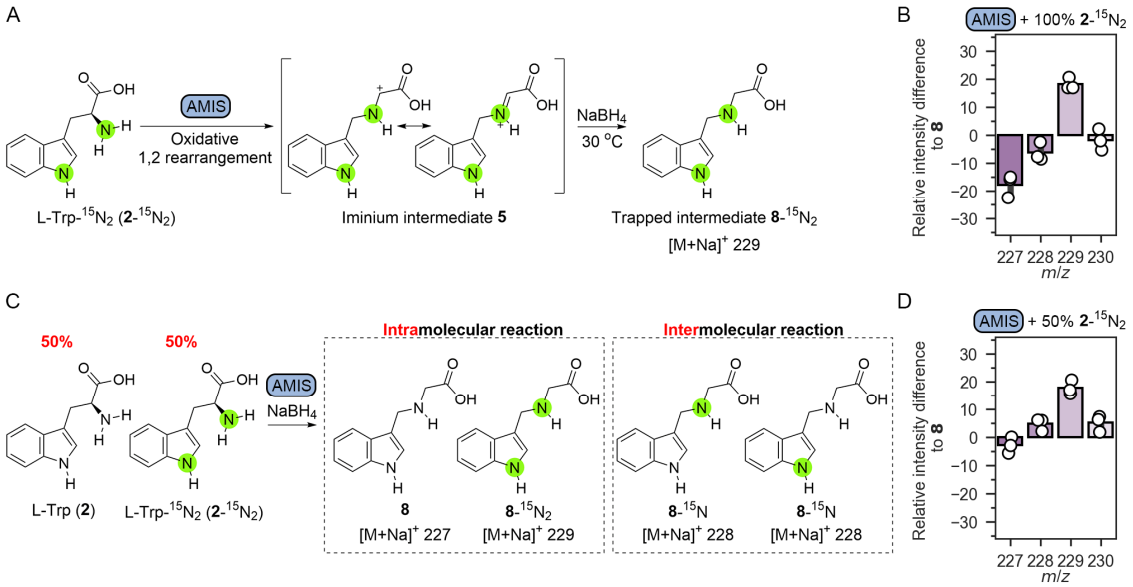


**Fig. S17. Isotope labeling experiments with L-tryptophan-$^{15}N_2$ (2-$^{15}N_2$) support that AMIS carries out an intramolecular reaction.**

**(A) Labeled atoms during the AMIS reaction with $^{15}N_2$-labeled Trp (2-$^{15}N_2$).**

**(B) Isotope pattern of trapped intermediate 8 from *in vitro* reactions of AMIS with 100% 2-$^{15}N_2$. The relative intensity difference to unlabeled 8 is shown as a bar plot.**

**(C) Labeled atoms during the AMIS reaction with a 50:50 mixture of $^{15}N_2$-labeled Trp (2-$^{15}N_2$) and unlabeled 2. Release of intermediates after bond cleavage between C-2 and C-3 could lead to an intermolecular reaction with partial loss of nitrogen label.**

**(D) Isotope pattern of trapped intermediate 8 from *in vitro* reactions of AMIS with 50% 2-$^{15}N_2$ and 50% unlabeled 2. The relative intensity difference to unlabeled 8 is shown as a bar plot. The lacking increase of *m*/*z* 228 suggests that no intermediates are released after bond cleavage between C-2 and C-3.**

**All bar plots show the means of three replicates. Error bars are standard deviations. Data points for each replicate are shown.**

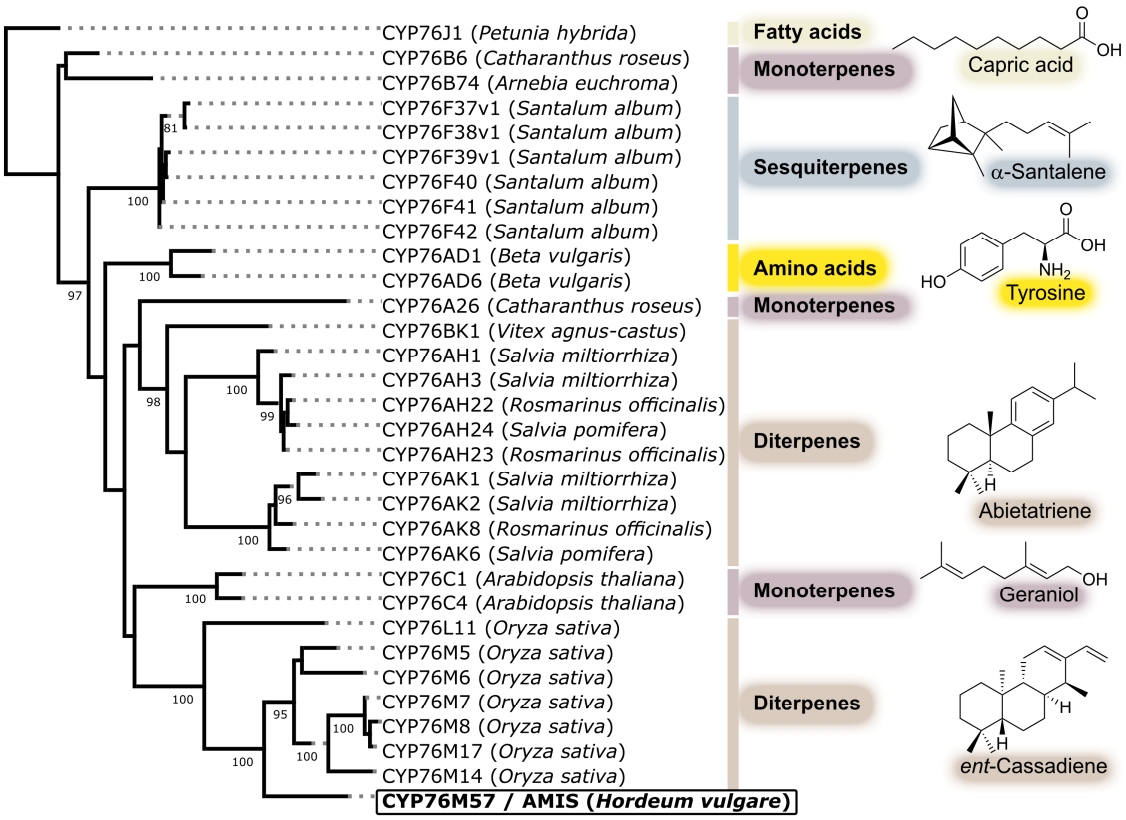


**Fig. S18. Phylogenetic tree and substrate classes of characterized CYP76s, including AMIS (CYP76M57).**

**Maximum likelihood tree using the JTT matrix in PhyML 3.2 (*58*), based on a MUSCLE alignment (*59*) of CYP protein sequences in Geneious 9.1.8 with default settings. Bootstrap values larger than 80 out of 100 bootstrap tests are shown on the tree. A list of accession numbers is provided in Table S10.**

**Structures of representative substrates are shown.**

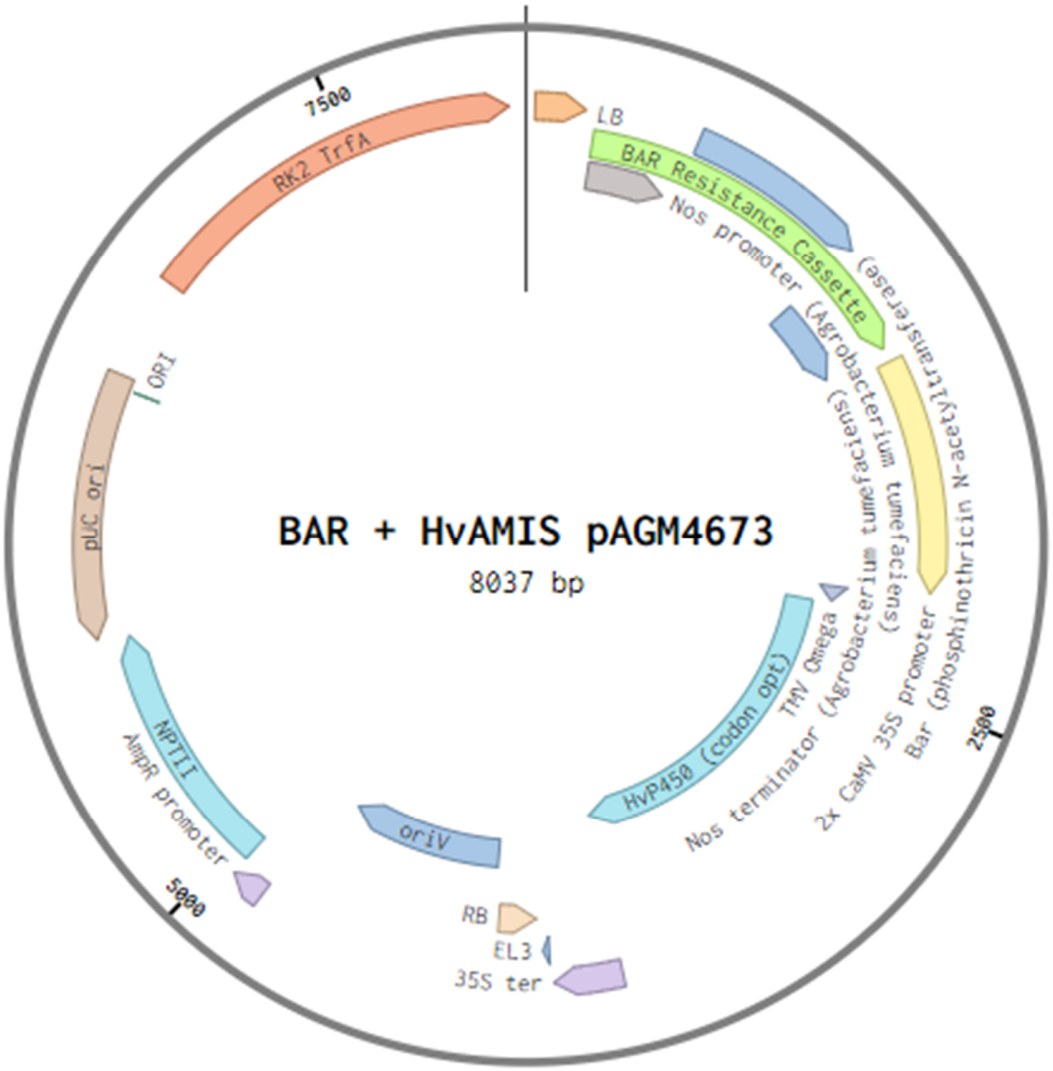


**Fig. S19. Level 2 MoClo construct for integrating *HvAMIS* into *Arabidopsis*.**

**Construct contains transcription unit for BASTA resistance gene (green segment), *HvAMIS* (HvP450) (light blue segment) and backbone pAGM4673 with kanamycin resistance (light blue segment).**

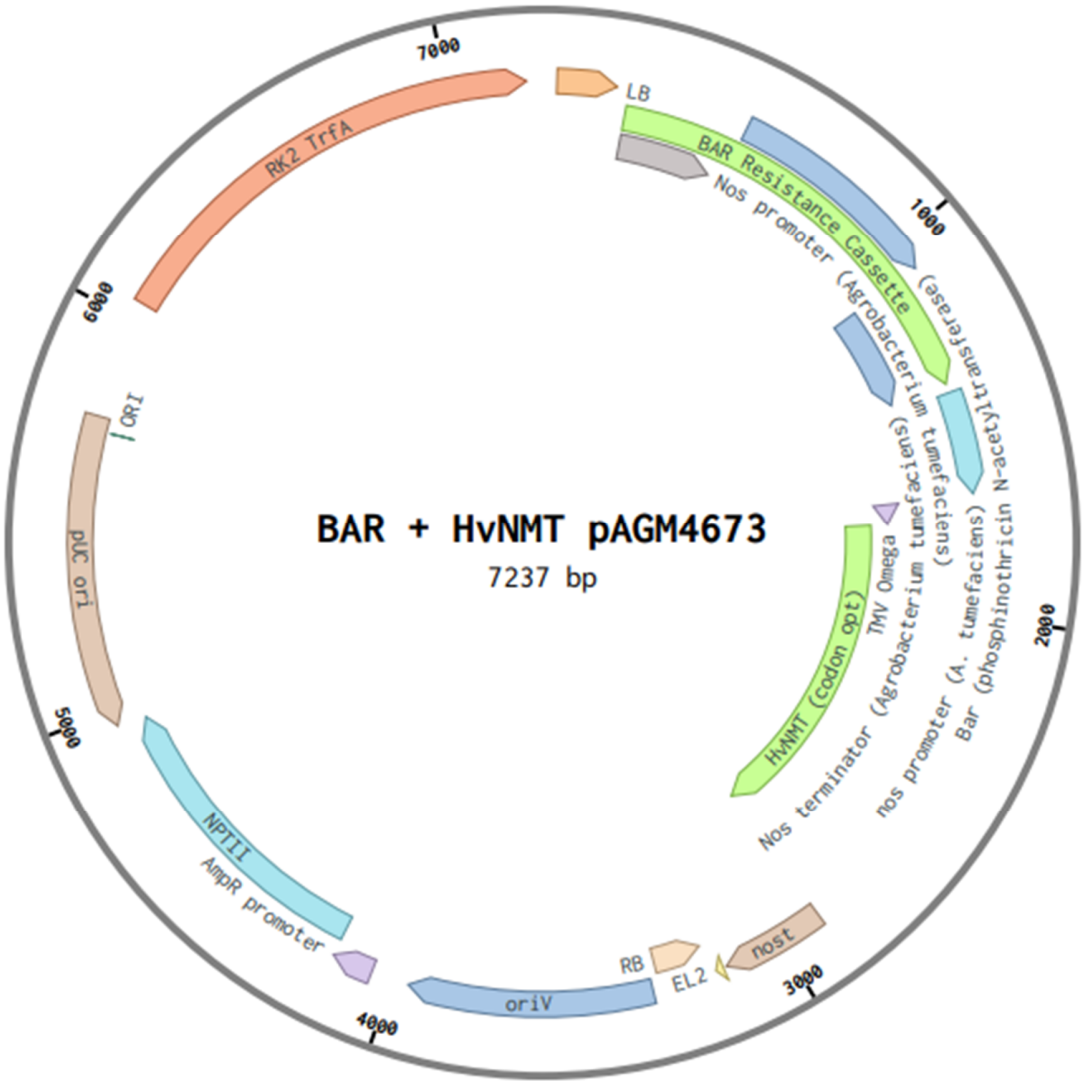


**Fig. S20. Level 2 MoClo construct for integrating *HvNMT* into *Arabidopsis*.**

**Construct contains transcription unit for BASTA resistance gene (green segment), *HvNMT* (green segment) and backbone pAGM4673 with kanamycin resistance (light blue segment).**

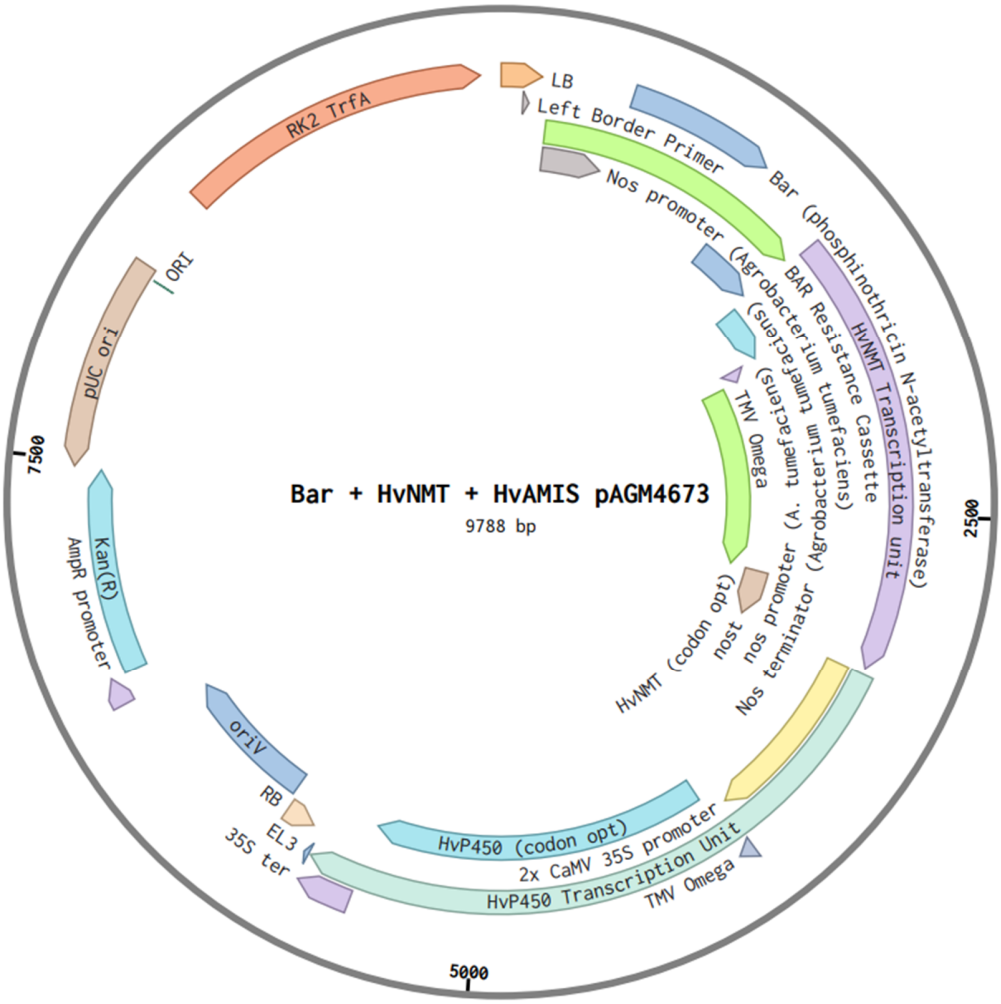


**Fig. S21. Level 2 MoClo construct for integrating both *HvNMT and HvAMIS* into *Arabidopsis*.**

**Construct contains transcription unit for BASTA resistance gene (green segment), *HvAMIS* (*HvP450*) (aquamarine segment), *HvNMT* (violet segment) and backbone pAGM4673 with kanamycin resistance (light blue segment).**

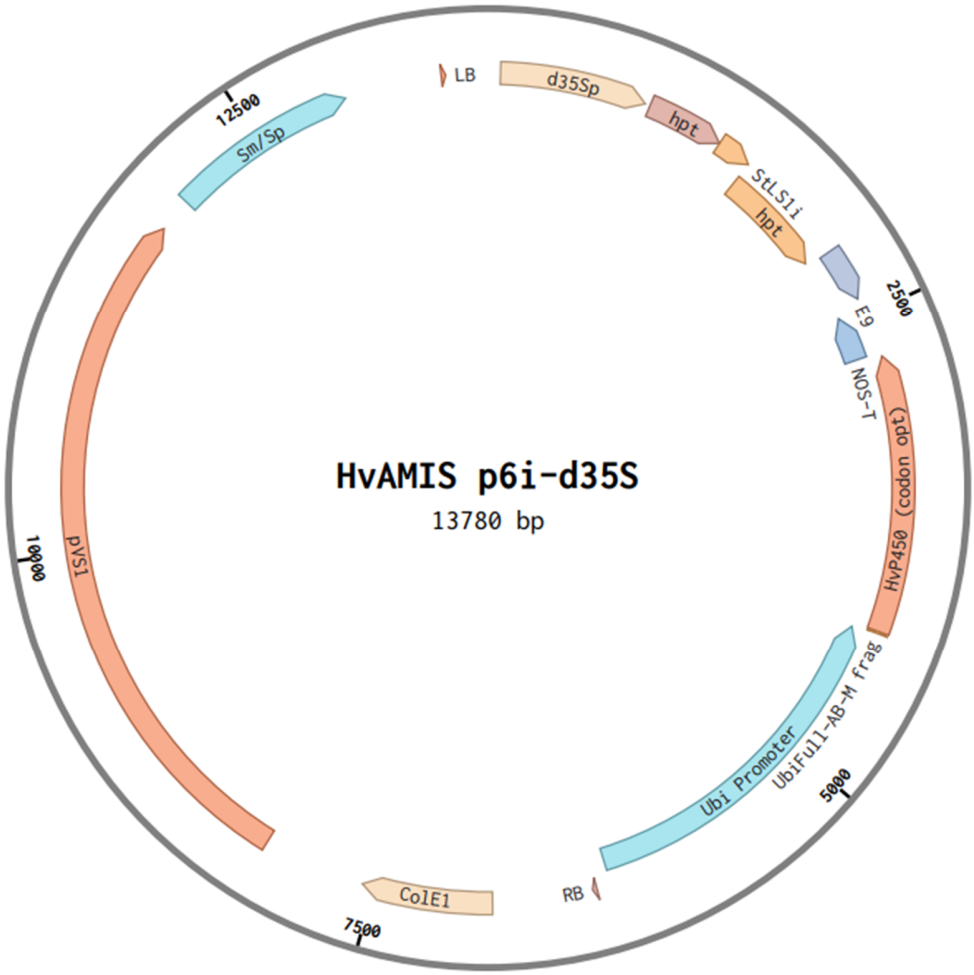


**Fig. S22. Binary vector p6i-d35S for barley transformation containing transcription unit of *HvAMIS* with Ubi-promotor and Nos-terminator.**

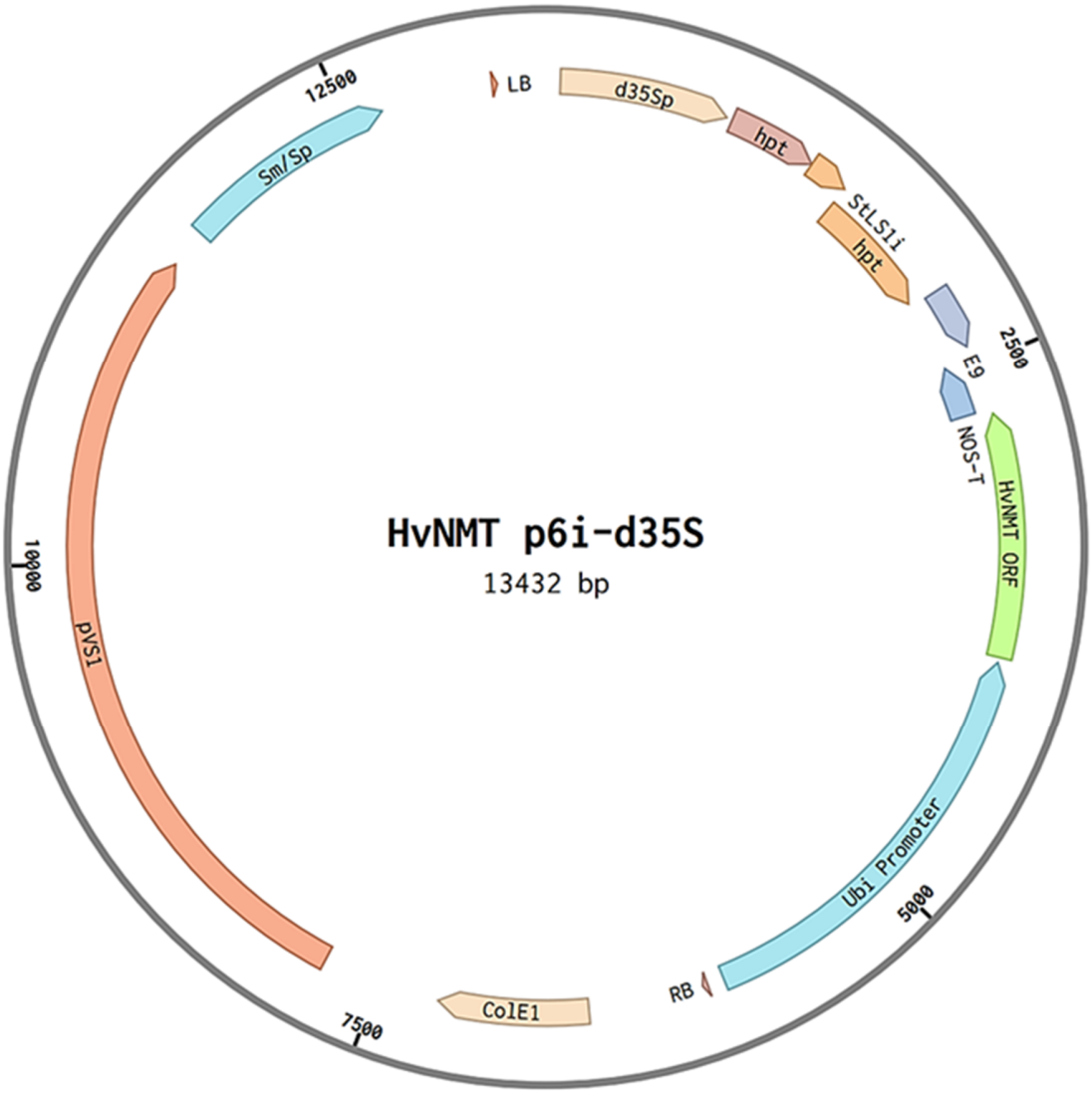


**Fig. S23. Binary vector p6i-d35S for barley transformation containing transcription unit of *HvNMT* with Ubi-promotor and Nos-terminator.**

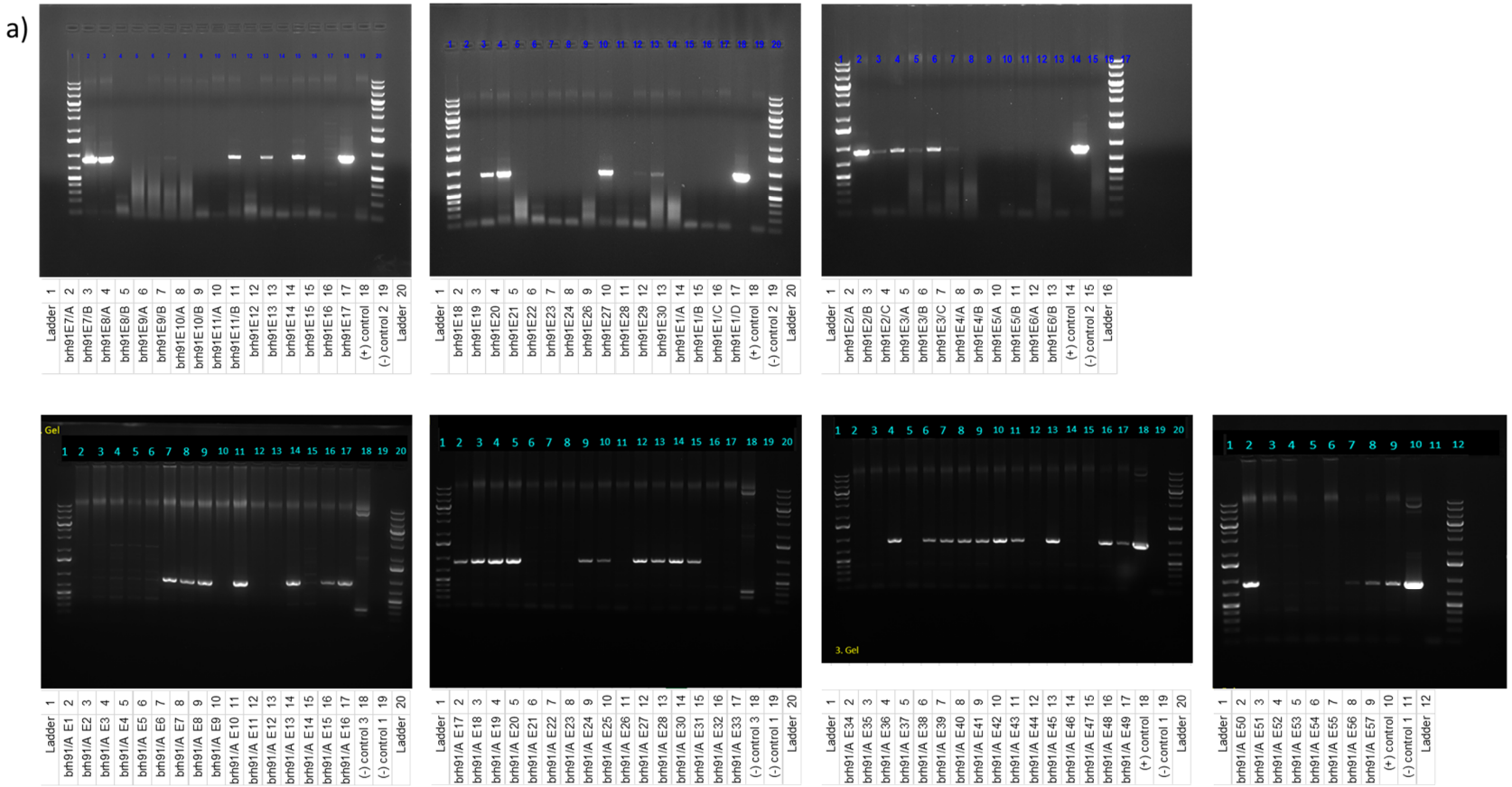


**Fig. S24. Verification of transgene insertion into *H. vulgare* cv. Golden Promise by PCR.**

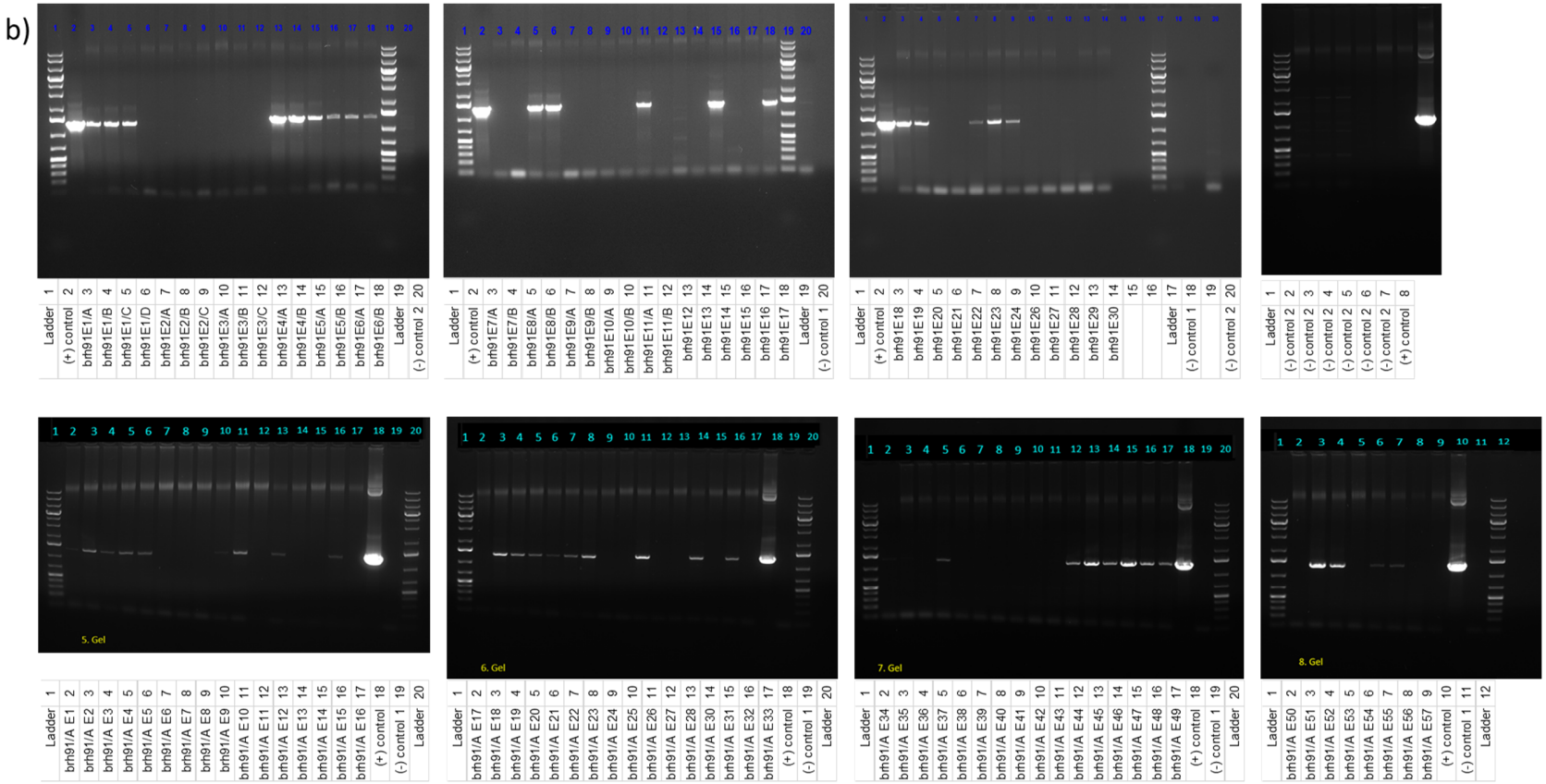


**Fig. S24 (continued). Verification of transgene insertion into *H. vulgare* cv. Golden Promise by PCR.**

**(A) PCR test for *HvNMT* presence with *HvNMT*-specific primer.**

**(B) PCR test for *HvAMIS* presence with *HvAMIS*-specific primer.**

**(+) control = positive control constituted by the barley transformation vectors for gramine overexpression, namely the *HvAMIS* gene (p6i_AMIS) or the *HvNMT* gene (p6i_NMT); (−) control 1 = negative control constituted by PCR reagents in addition to water; (−) control 2 = negative control constituted by PCR reagents (*HvNMT* or *HvAMIS*-specific primers) in addition to DNA of WT Golden promise plants; (−) control 3 = negative control constituted by PCR reagents (*HvNMT* specific primers) in addition to p6i_AMIS vector; Ladder = 1 kb Plus DNA ladder (Thermo).**

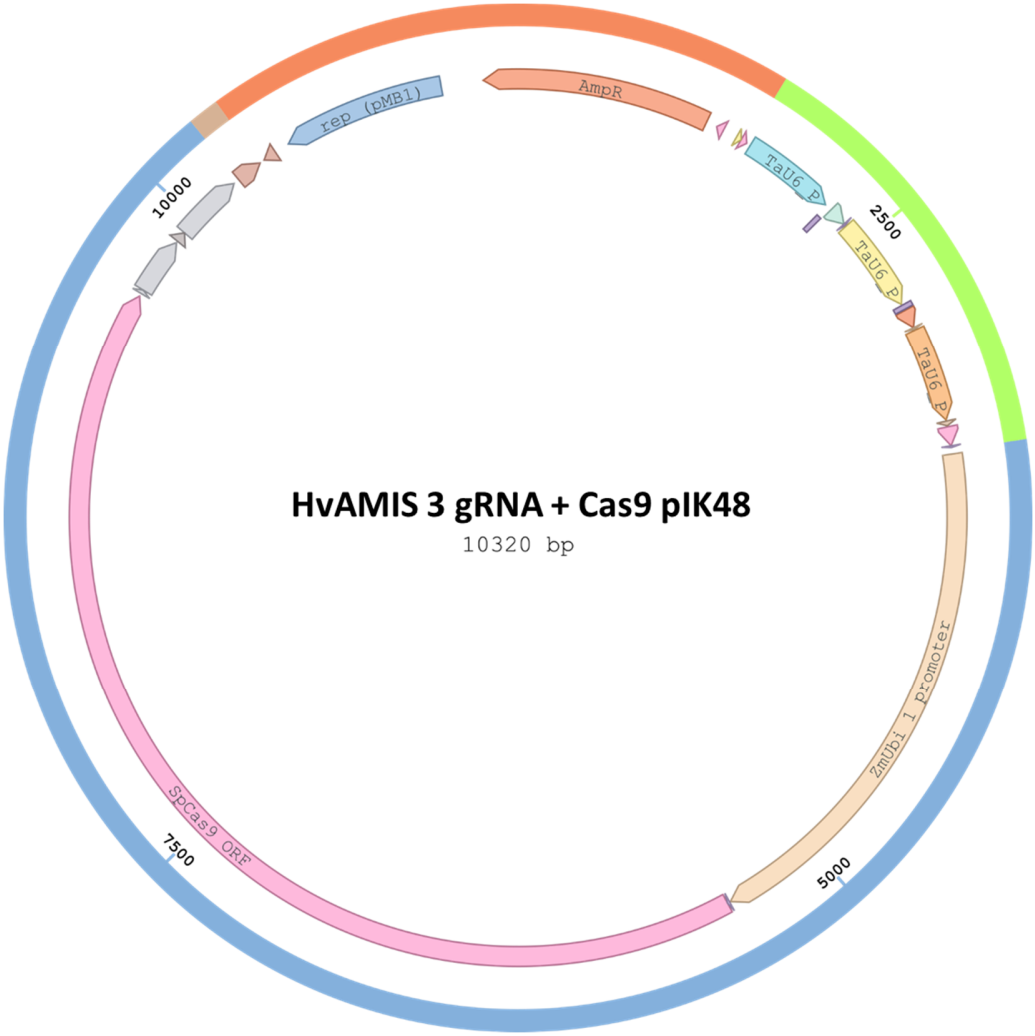


**Fig. S25. Cas9-mediated mutagenesis construct for barley transformation.**

**Construct contains three gRNAs under control of TaU6 promotors (green segment) and the coding sequence of an SpCas9 protein under control of the maize Polyubiquitin 1 promotor plus intron 1 (blue segment). Backbone pIK48 with Amp/Carb resistance (orange segment).**

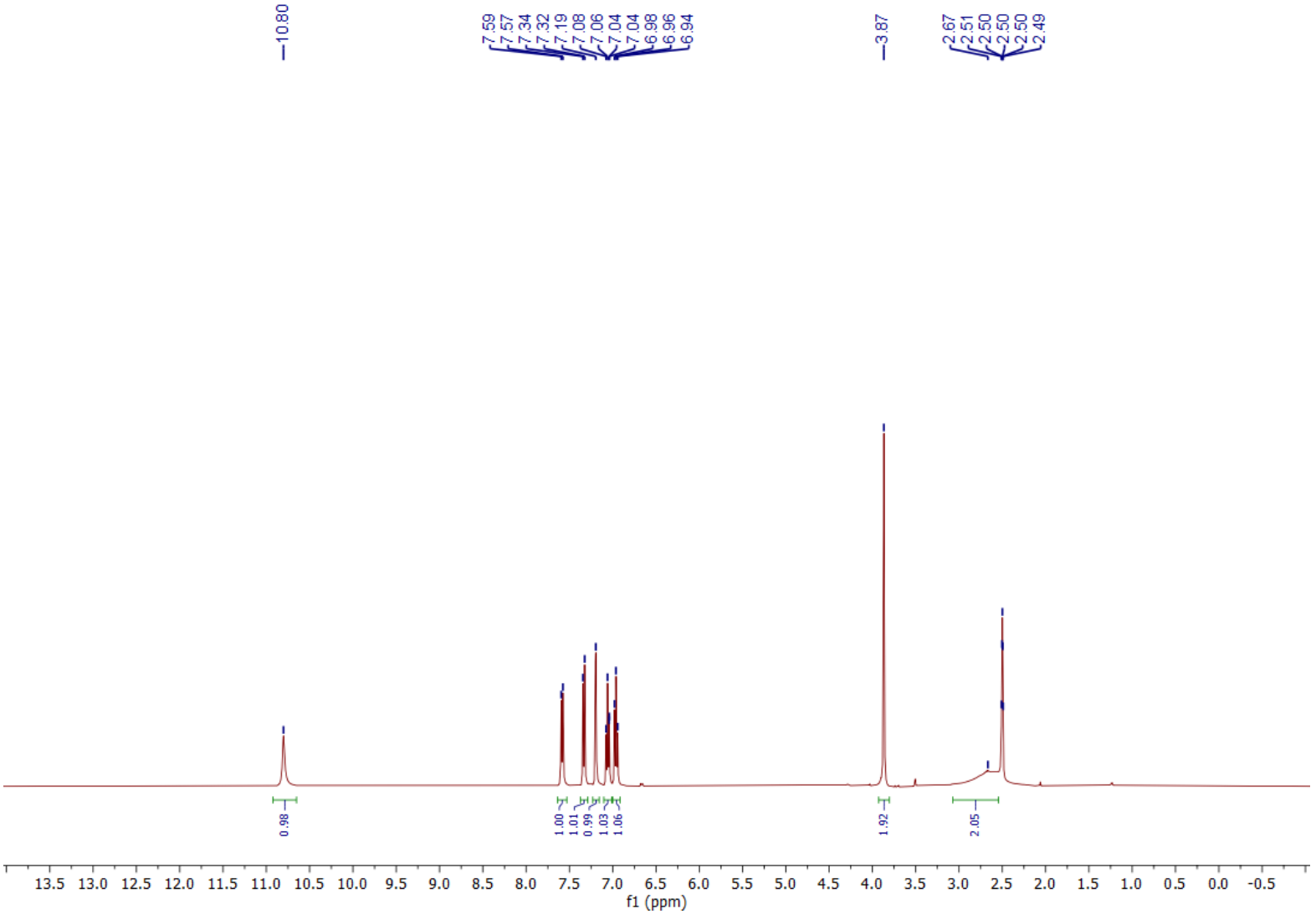


**Fig. S26. $^{1}$H spectrum of isolated AMI (3) from *Nicotiana benthamiana* transiently expressing *AMIS* (298 K, DMSO-d$_6$, 400 MHz).**

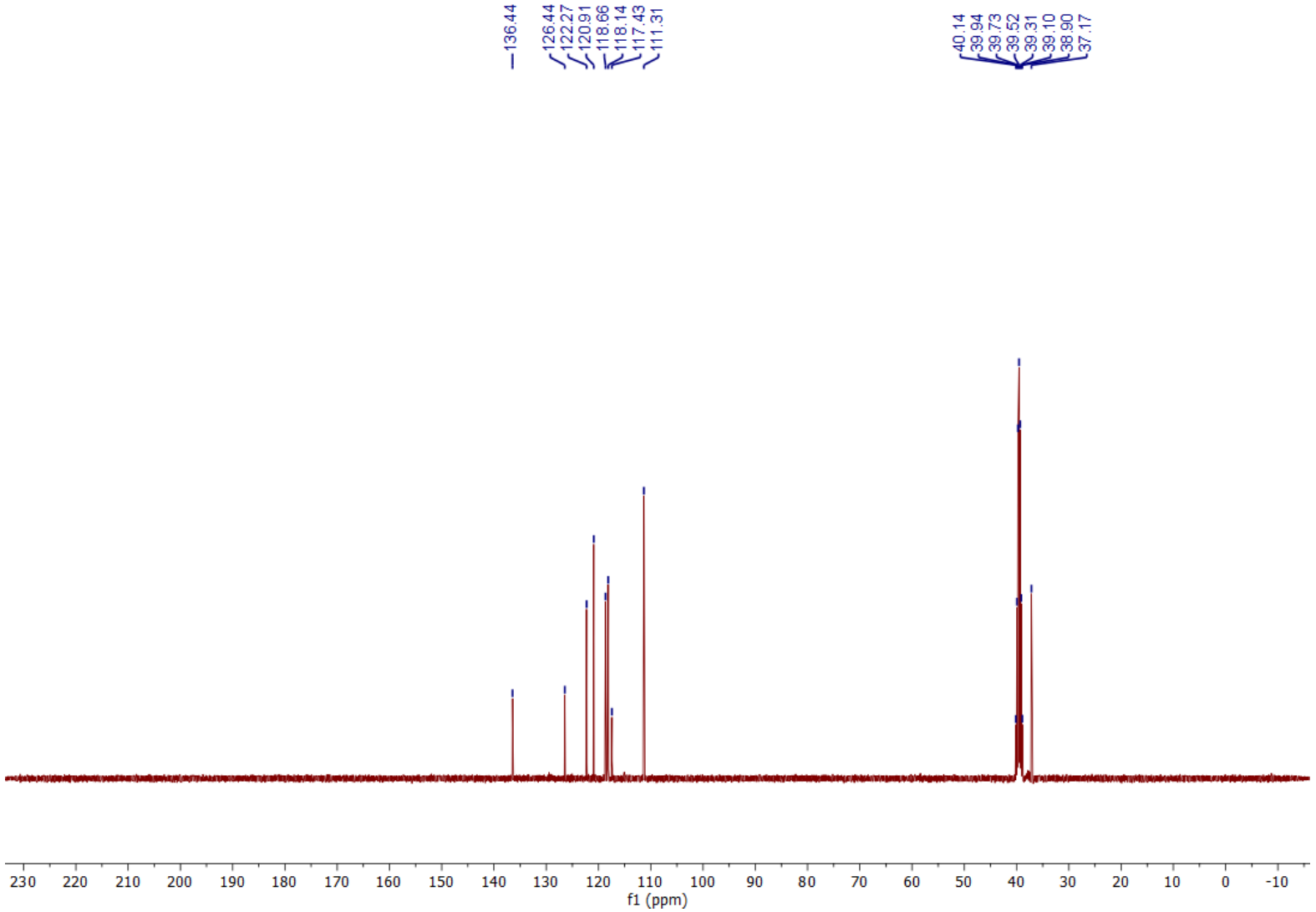


**Fig. S27. $^{13}$C spectrum of isolated AMI (3) from *Nicotiana benthamiana* transiently expressing *AMIS* (298 K, DMSO-d$_6$, 101 MHz).**

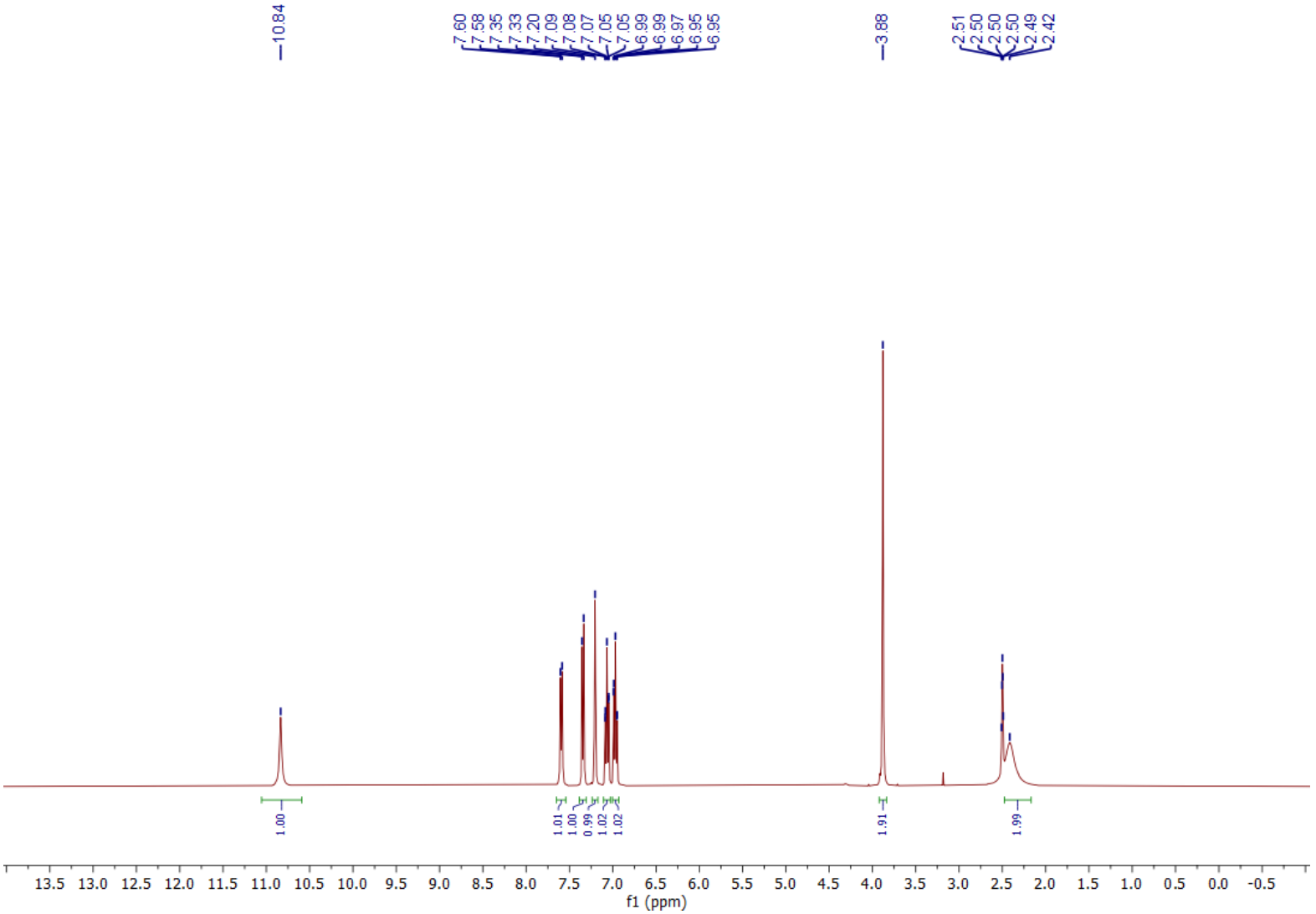


**Fig. S28. $^{1}$H spectrum of synthesized AMI (3) (298 K, DMSO-d$_6$, 400 MHz).**

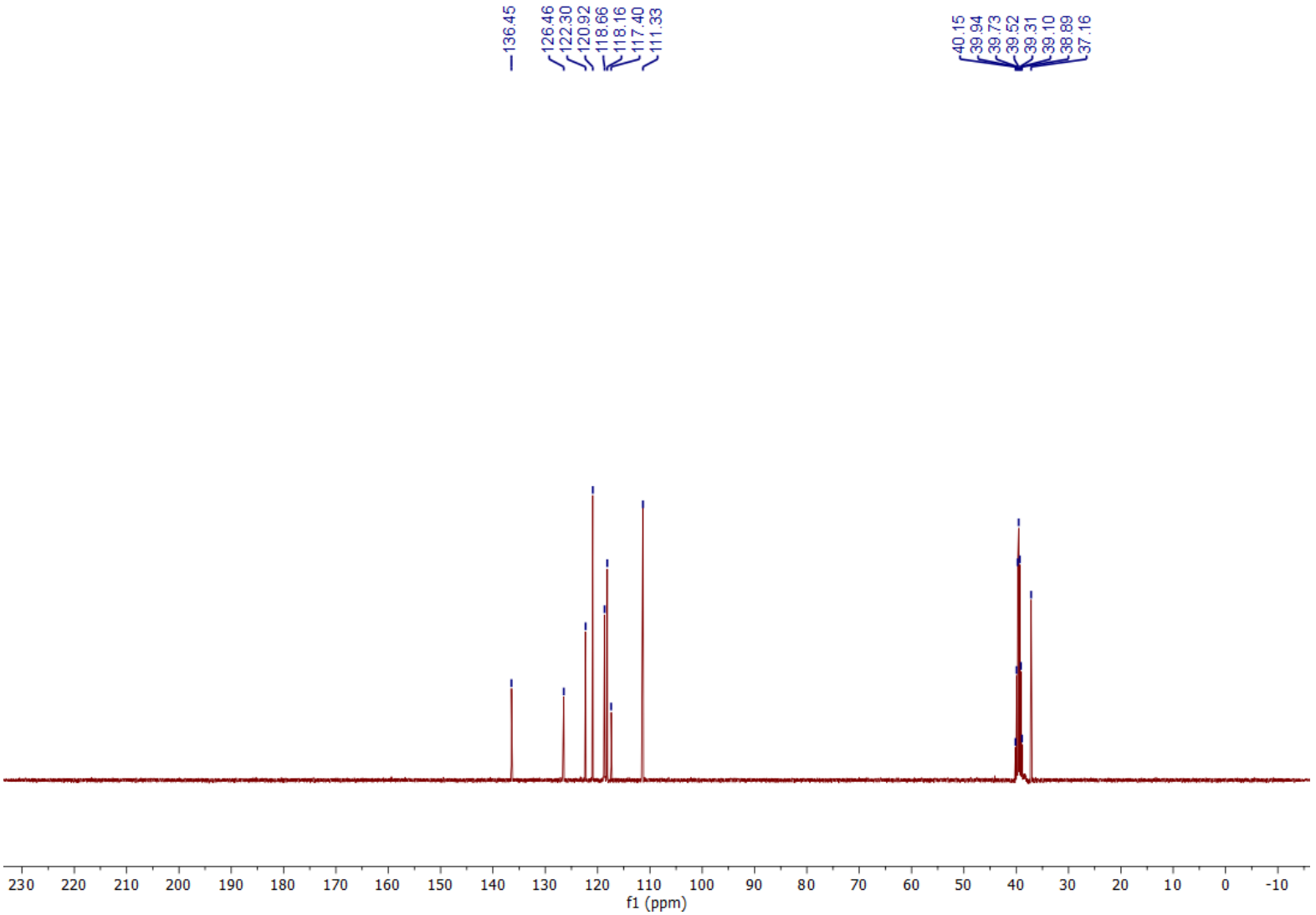


**Fig. S29. $^{13}C$ spectrum of synthesized AMI (3) (298 K, DMSO-$d_6$, 101 MHz).**

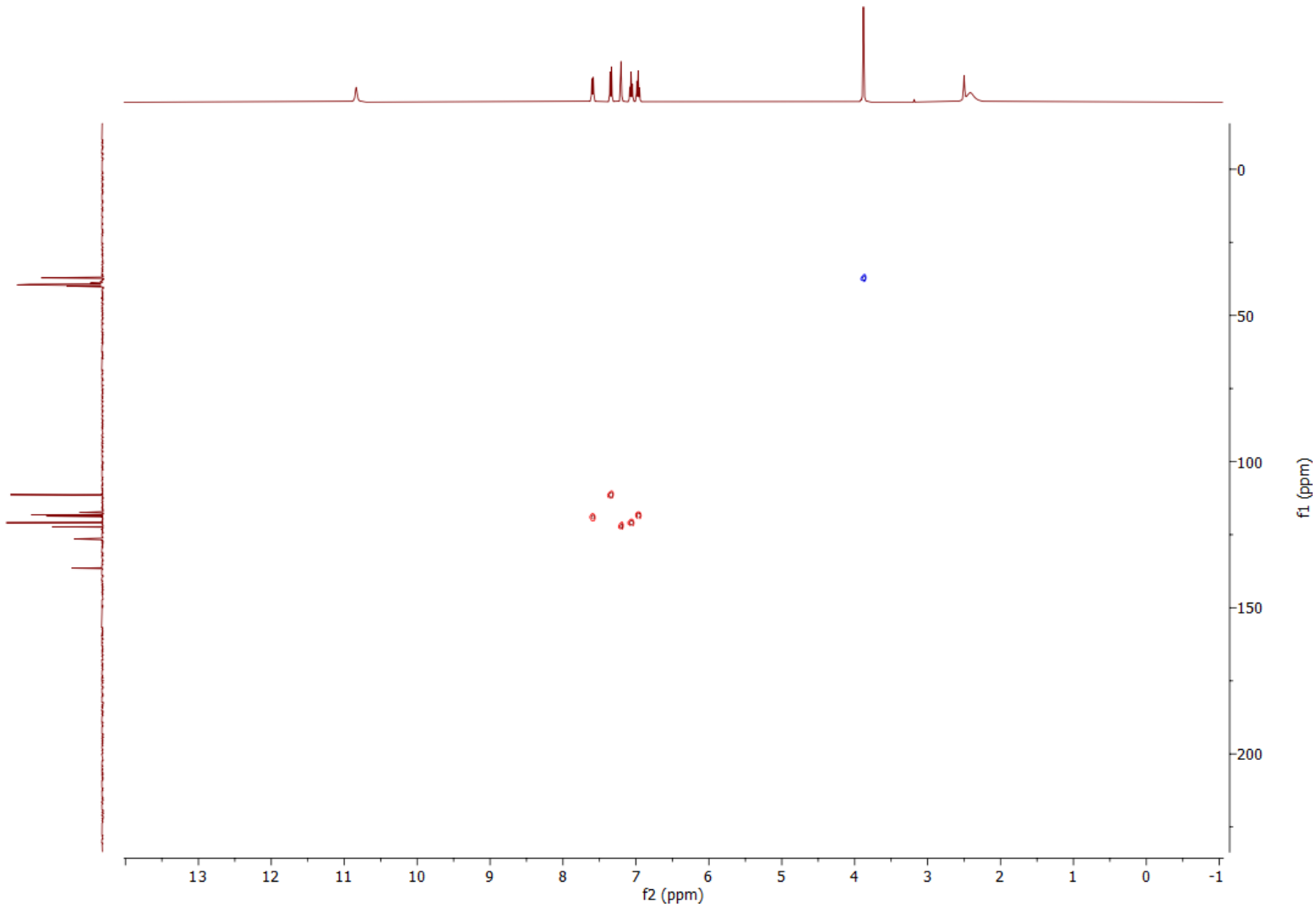


**Fig. S30. HSQC spectrum of synthesized AMI (3) (298 K, DMSO-$d_6$, 400 MHz).**

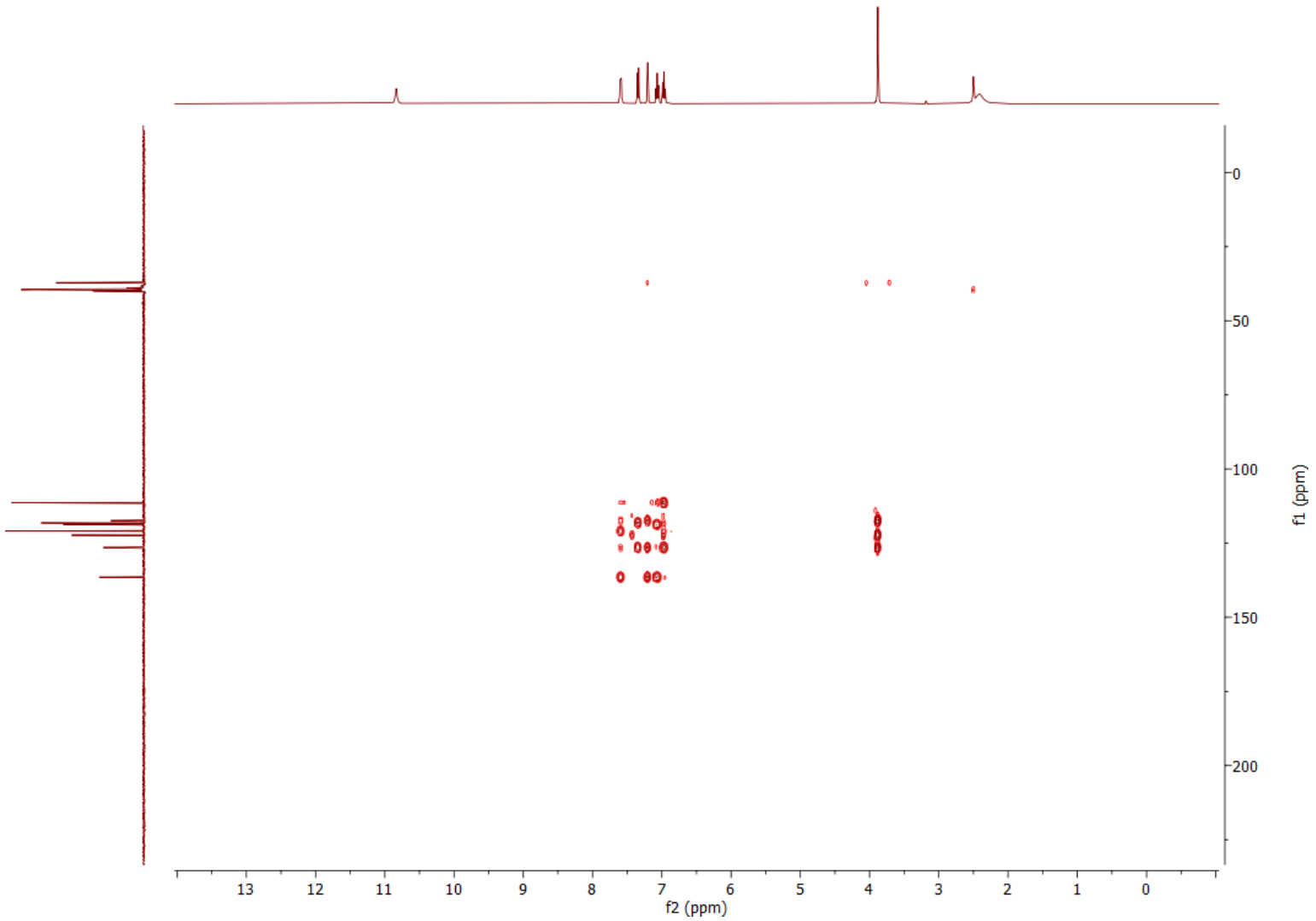


**Fig. S31. HMBC spectrum of synthesized AMI (3) (298 K, DMSO-$d_6$, 400 MHz).**

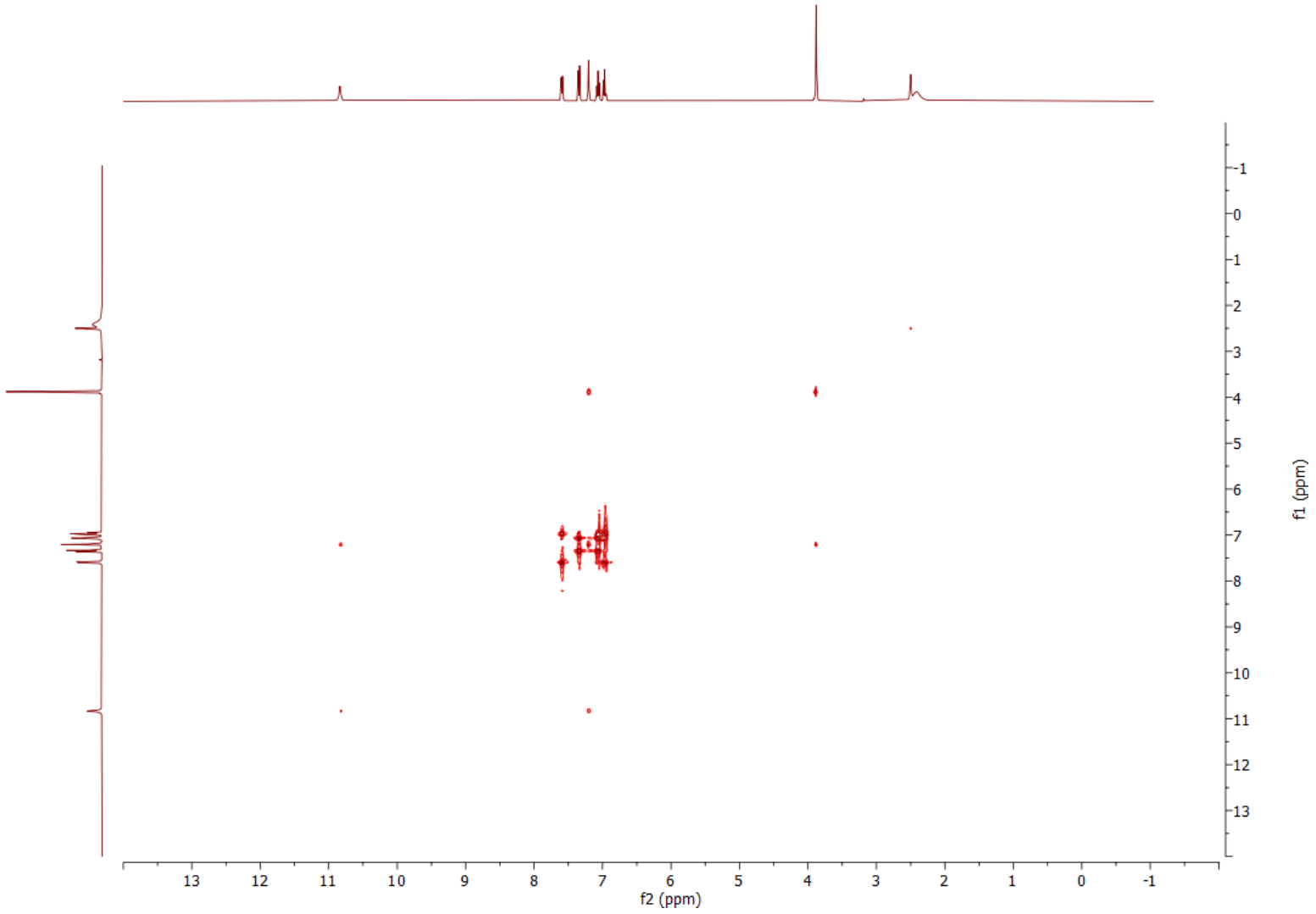


**Fig. S32. COSY spectrum of synthesized AMI (3) (298 K, DMSO-$d_6$, 400 MHz).**

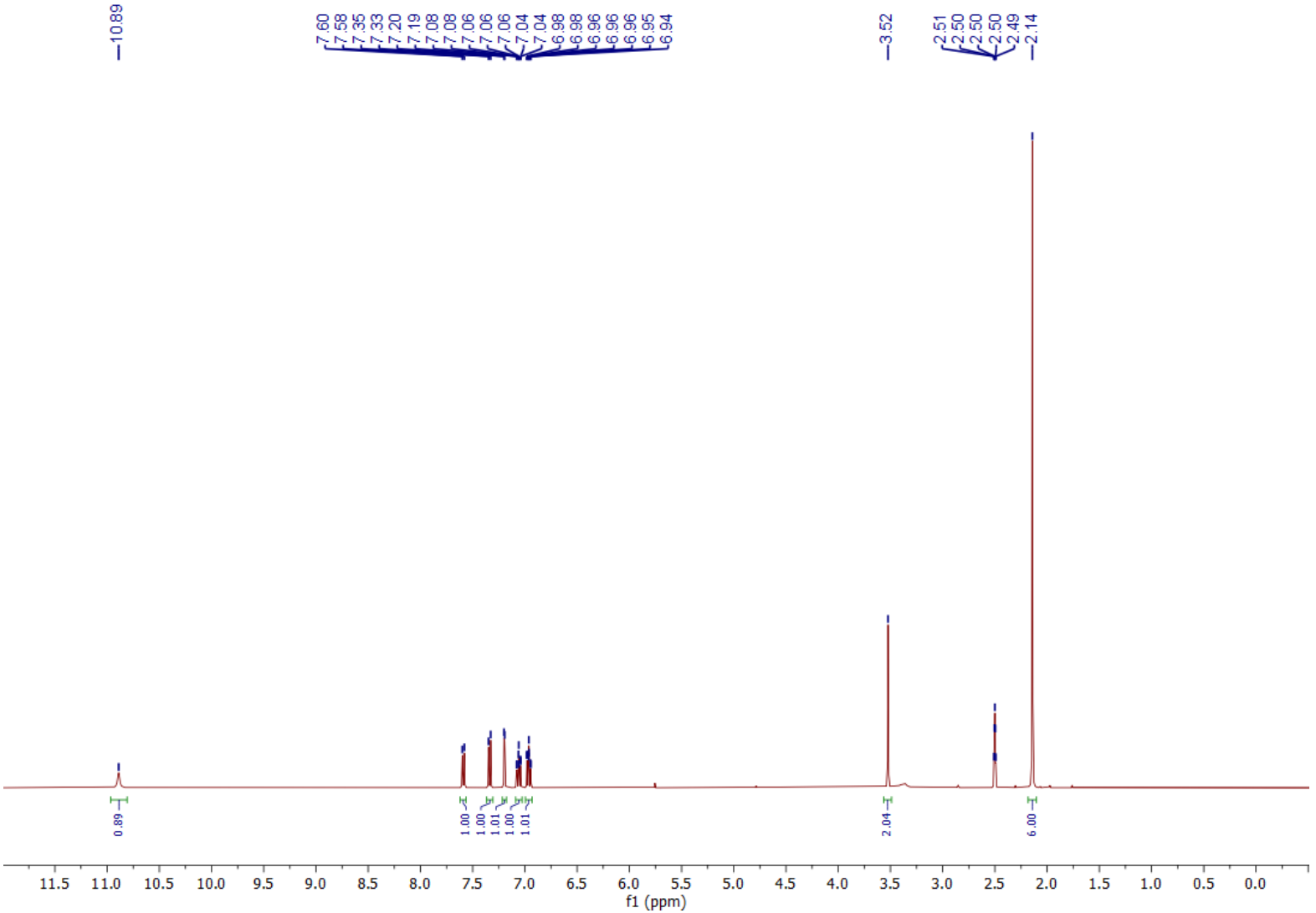


**Fig. S33. $^{1}$H spectrum of isolated gramine (1) from *Nicotiana benthamiana* transiently expressing *AMIS* and *NMT* (298 K, DMSO-d$_6$, 400 MHz).**

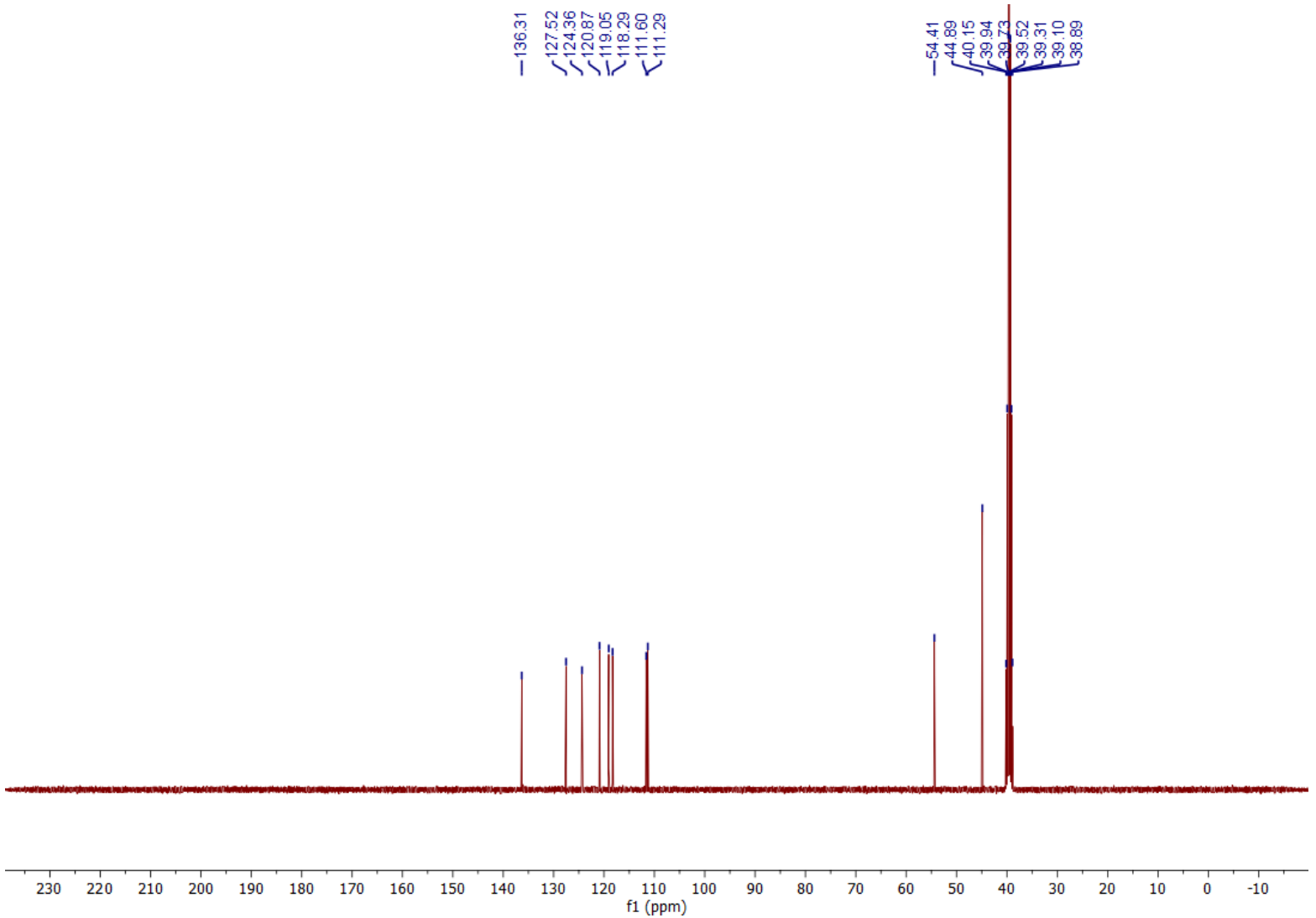


**Fig. S34. $^{13}$C spectrum of isolated gramine (1) from *Nicotiana benthamiana* transiently expressing *AMIS* and *NMT* (298 K, DMSO-d6, 101 MHz).**

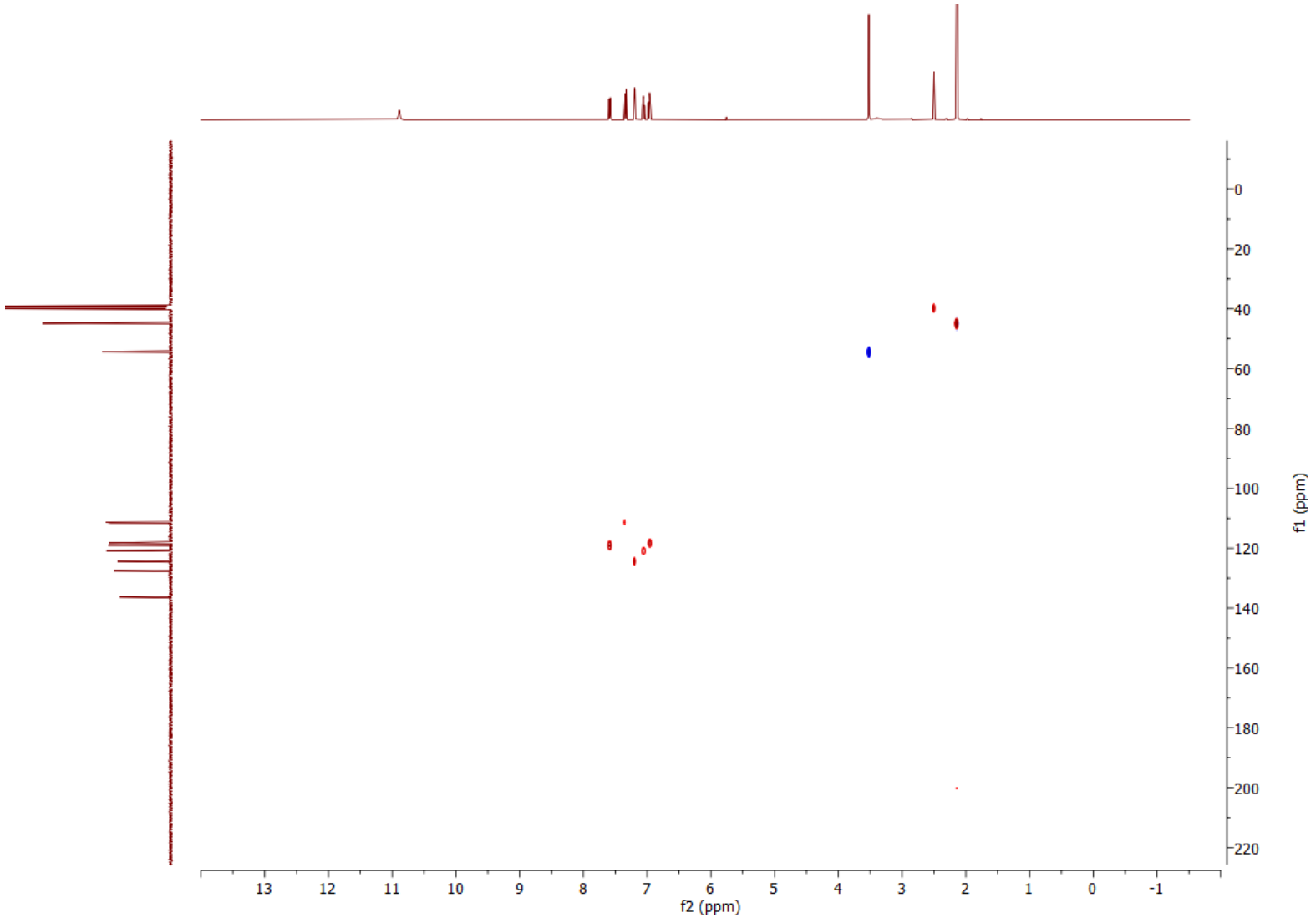


**Fig. S35. HSQC spectrum of isolated gramine (1) from *Nicotiana benthamiana* transiently expressing *AMIS* and *NMT* (298 K, DMSO-$d_6$, 400 MHz).**

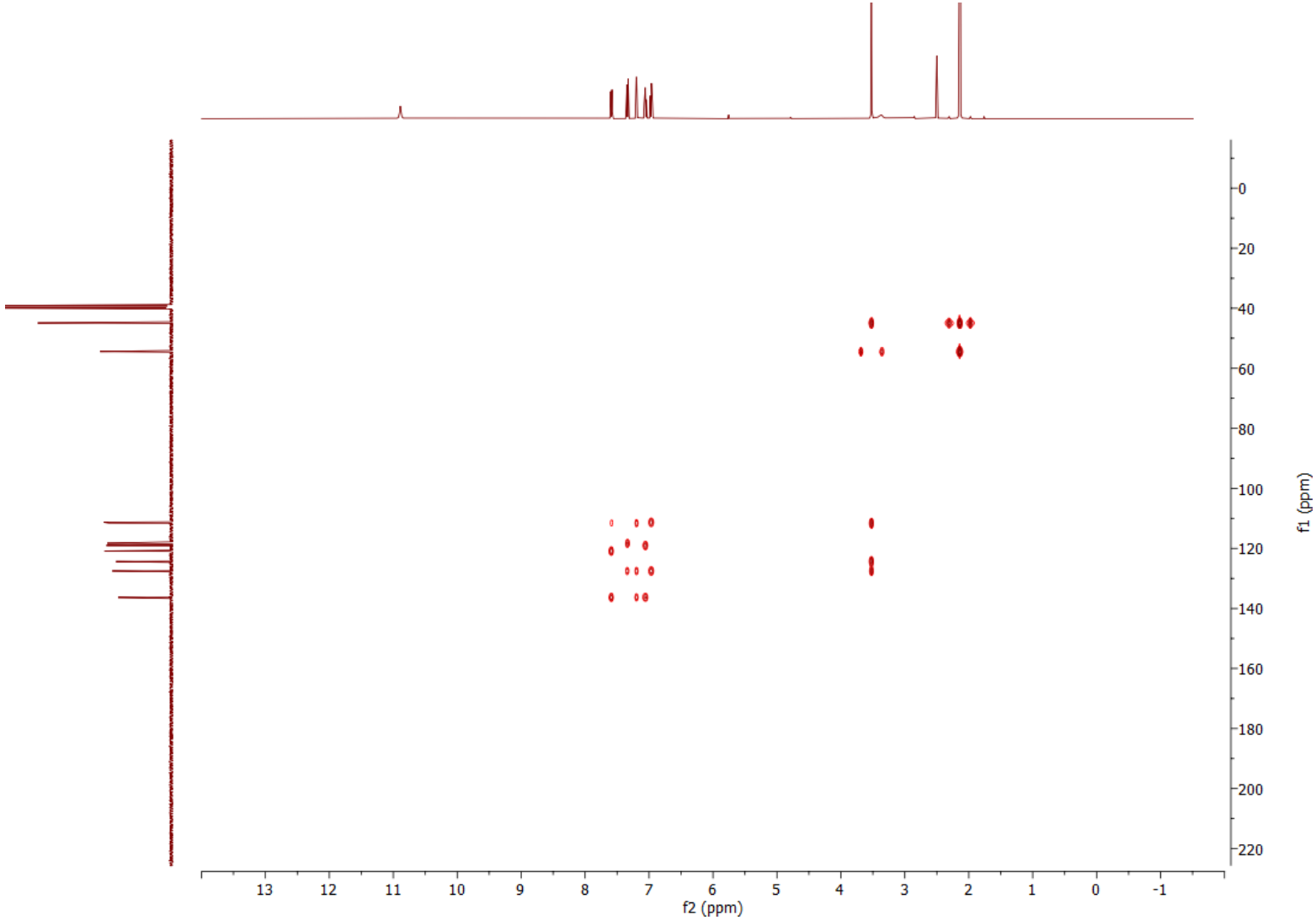


**Fig. S36. HMBC spectrum of isolated gramine (1) from *Nicotiana benthamiana* transiently expressing *AMIS* and *NMT* (298 K, DMSO-$d_6$, 400 MHz).**

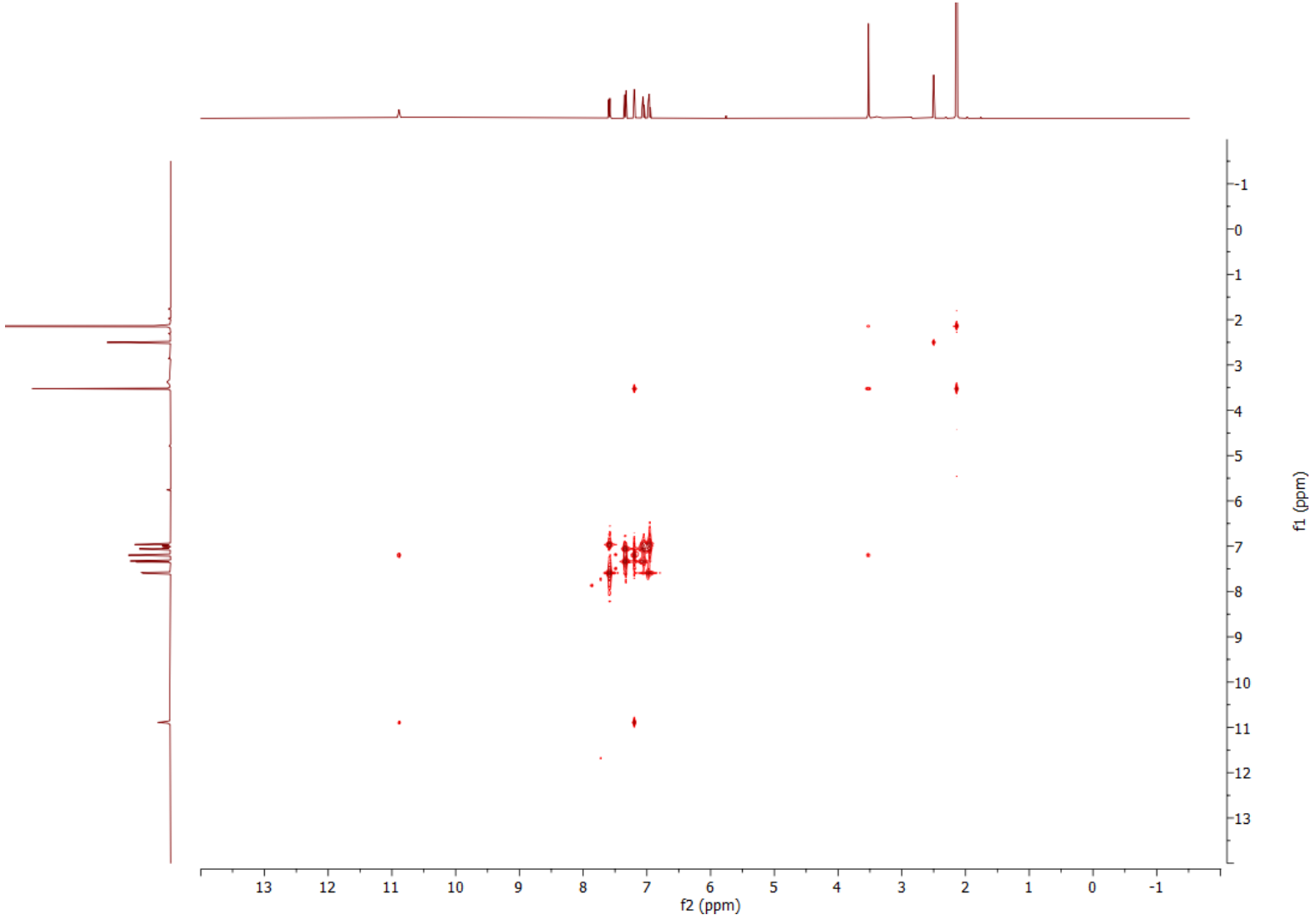


**Fig. S37. COSY spectrum of isolated gramine (1) from *Nicotiana benthamiana* transiently expressing *AMIS* and *NMT* (298 K, DMSO-$d_6$, 400 MHz).**

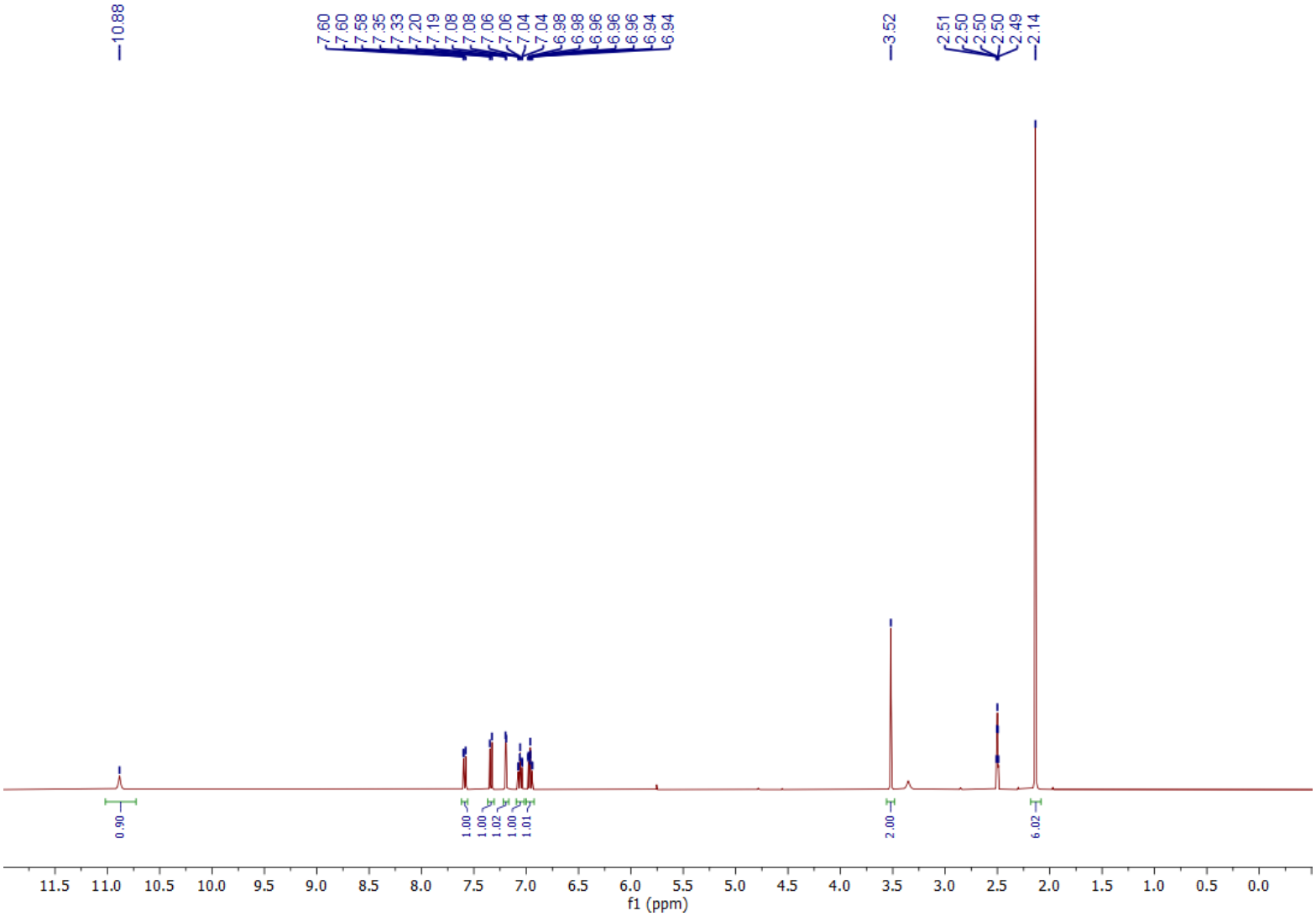


**Fig. S38. $^{1}$H spectrum of gramine (1) commercially available standard (298 K, DMSO-d$_6$, 400 MHz).**

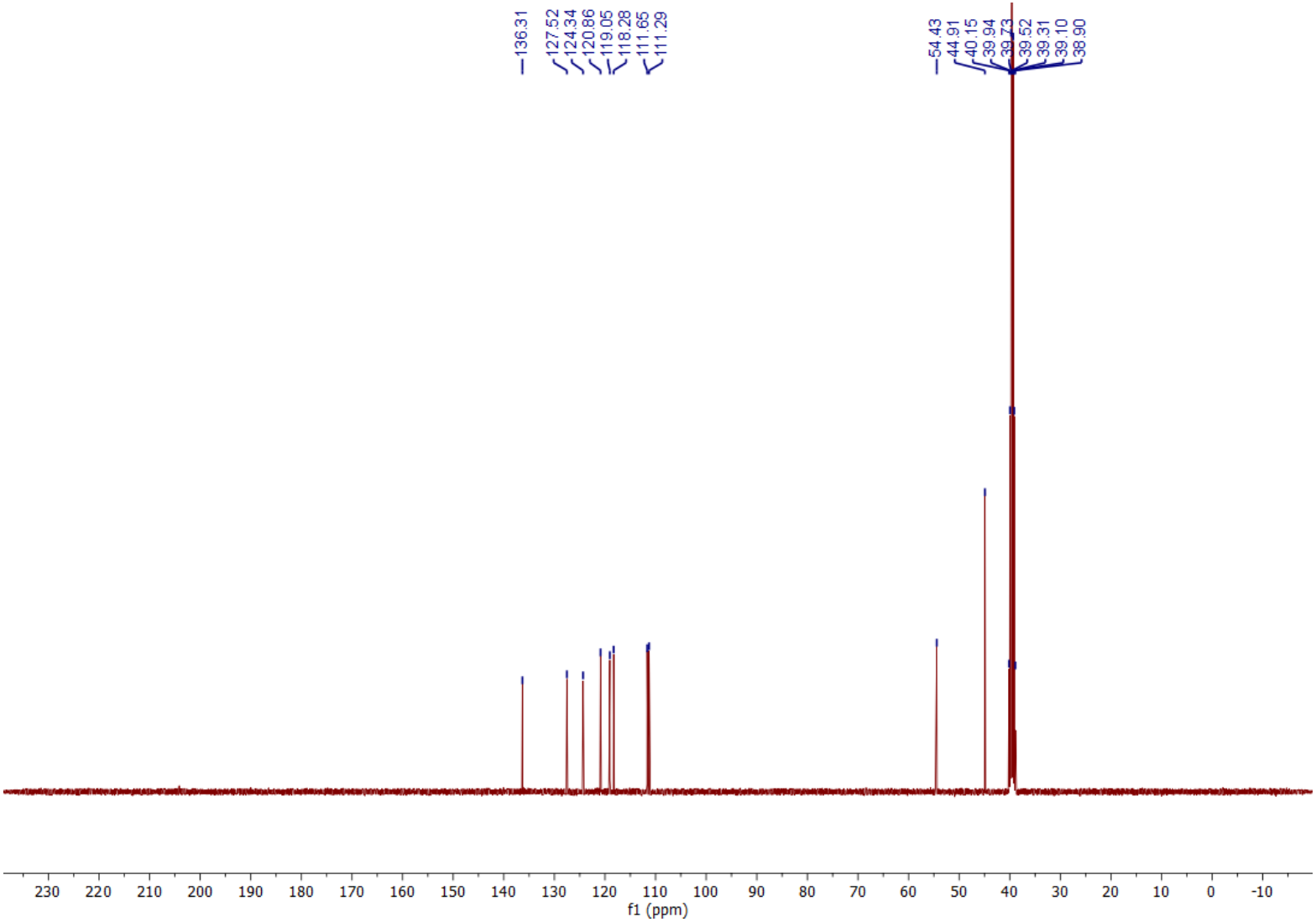


**Fig. S39. $^{13}$C spectrum of gramine (1) commercially available standard (298 K, DMSO-d$_6$, 101 MHz).**

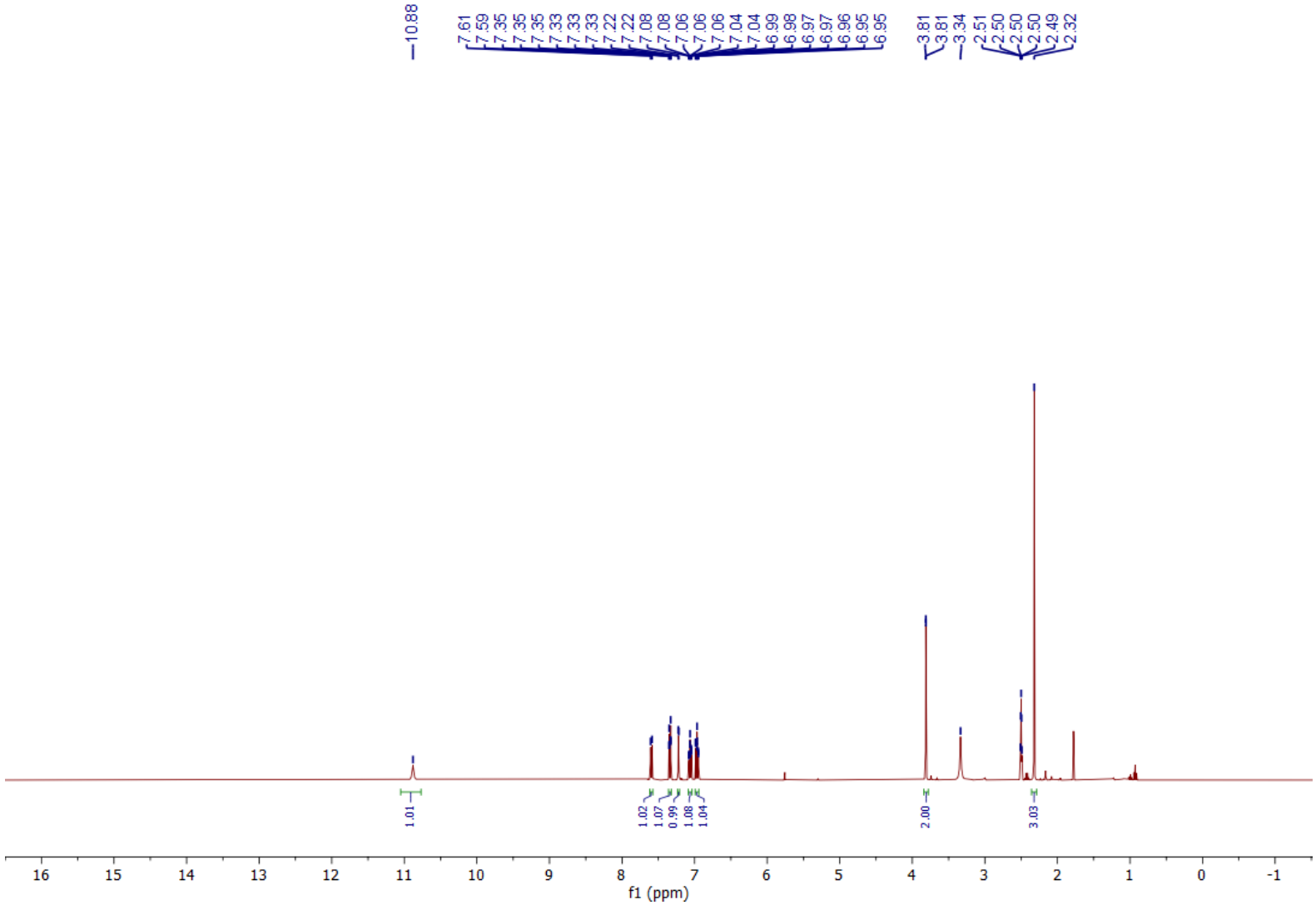


**Fig. S40. $^{1}$H spectrum of synthesized MAMI (4) (298 K, DMSO-d$_6$, 400 MHz).**

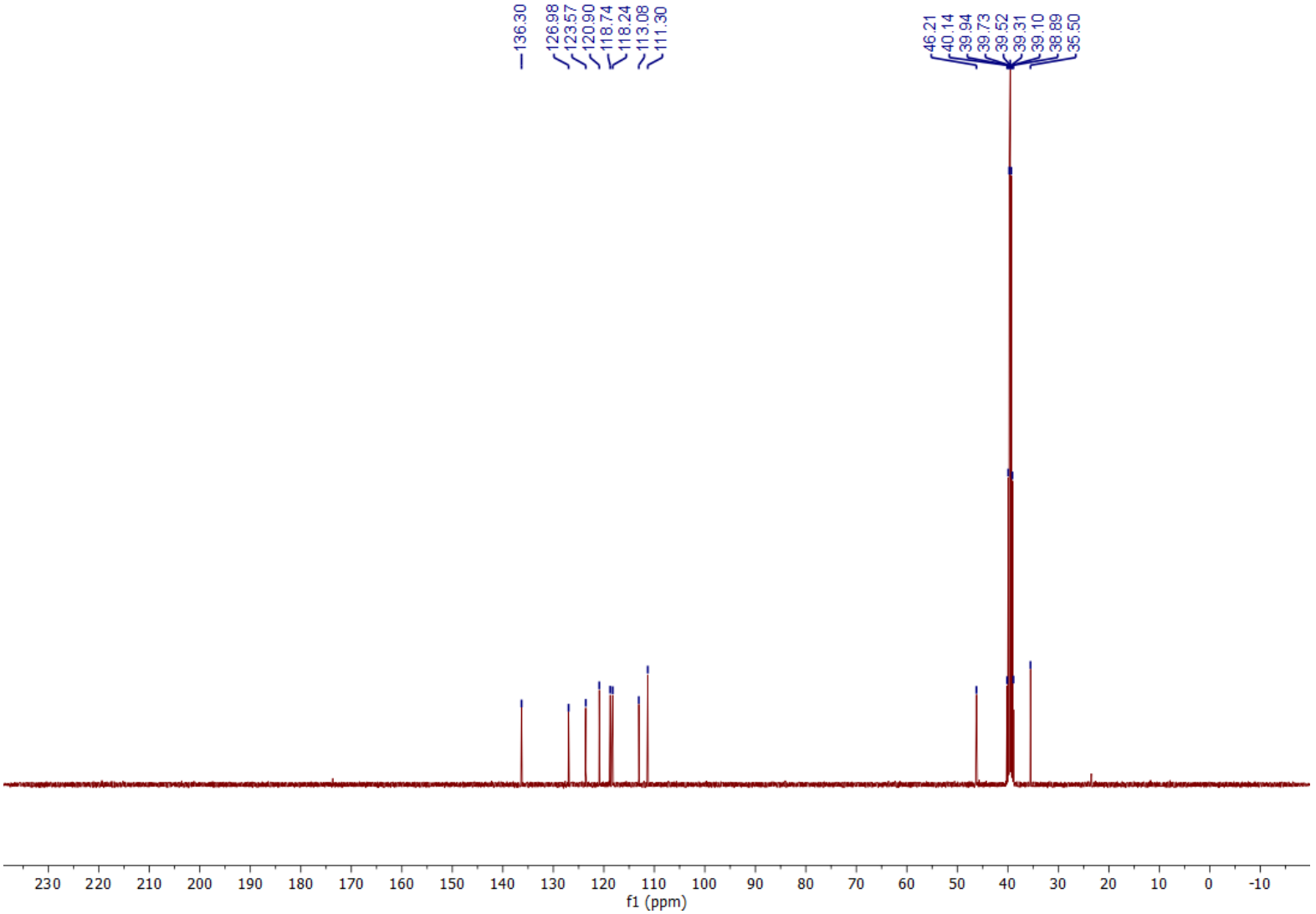


**Fig. S41. $^{13}$C spectrum of synthesized MAMI (4) (298 K, DMSO-d$_6$, 101 MHz).**

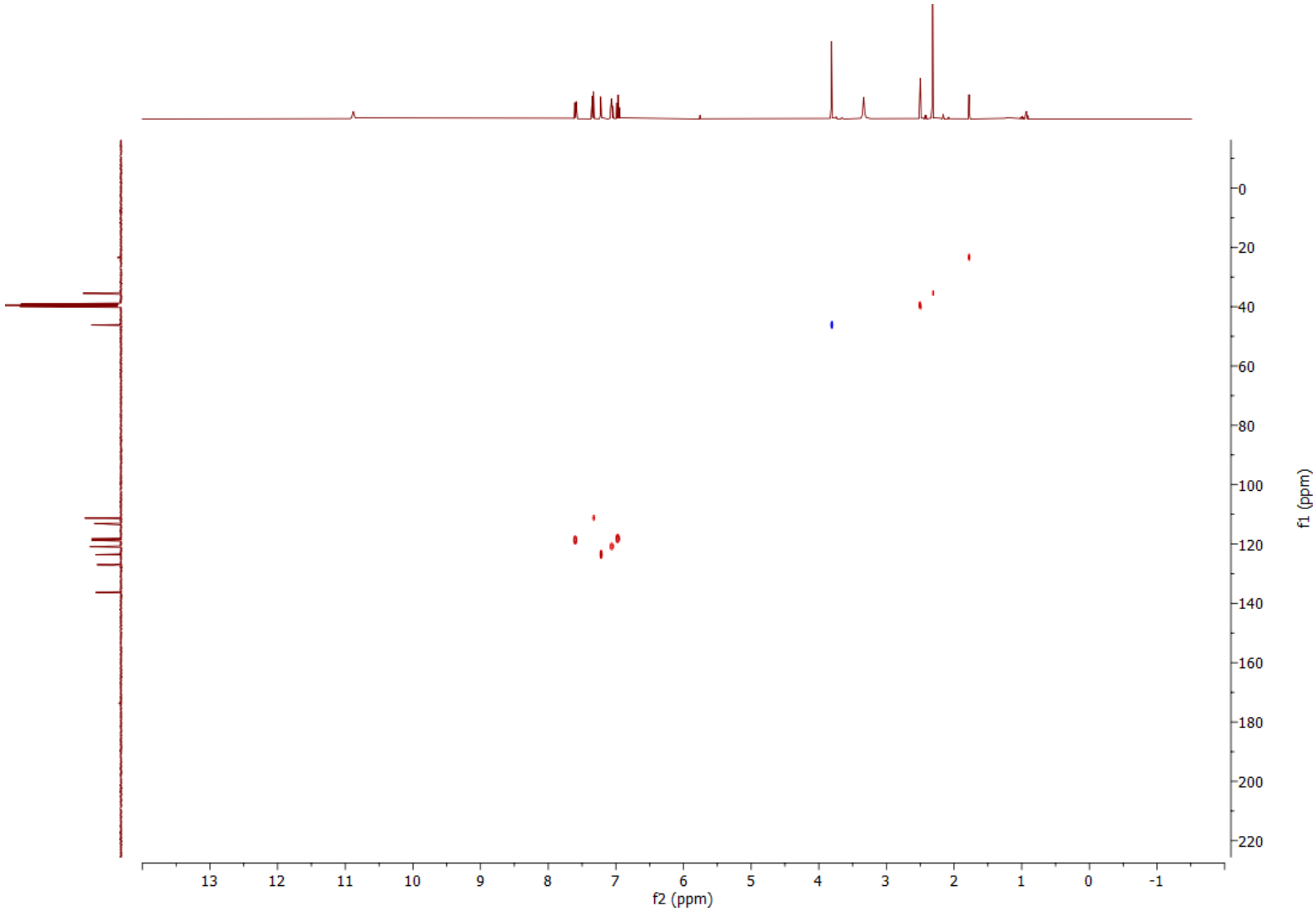


**Fig. S42. HSQC spectrum of synthesized MAMI (4) (298 K, DMSO-$d_6$, 400 MHz).**

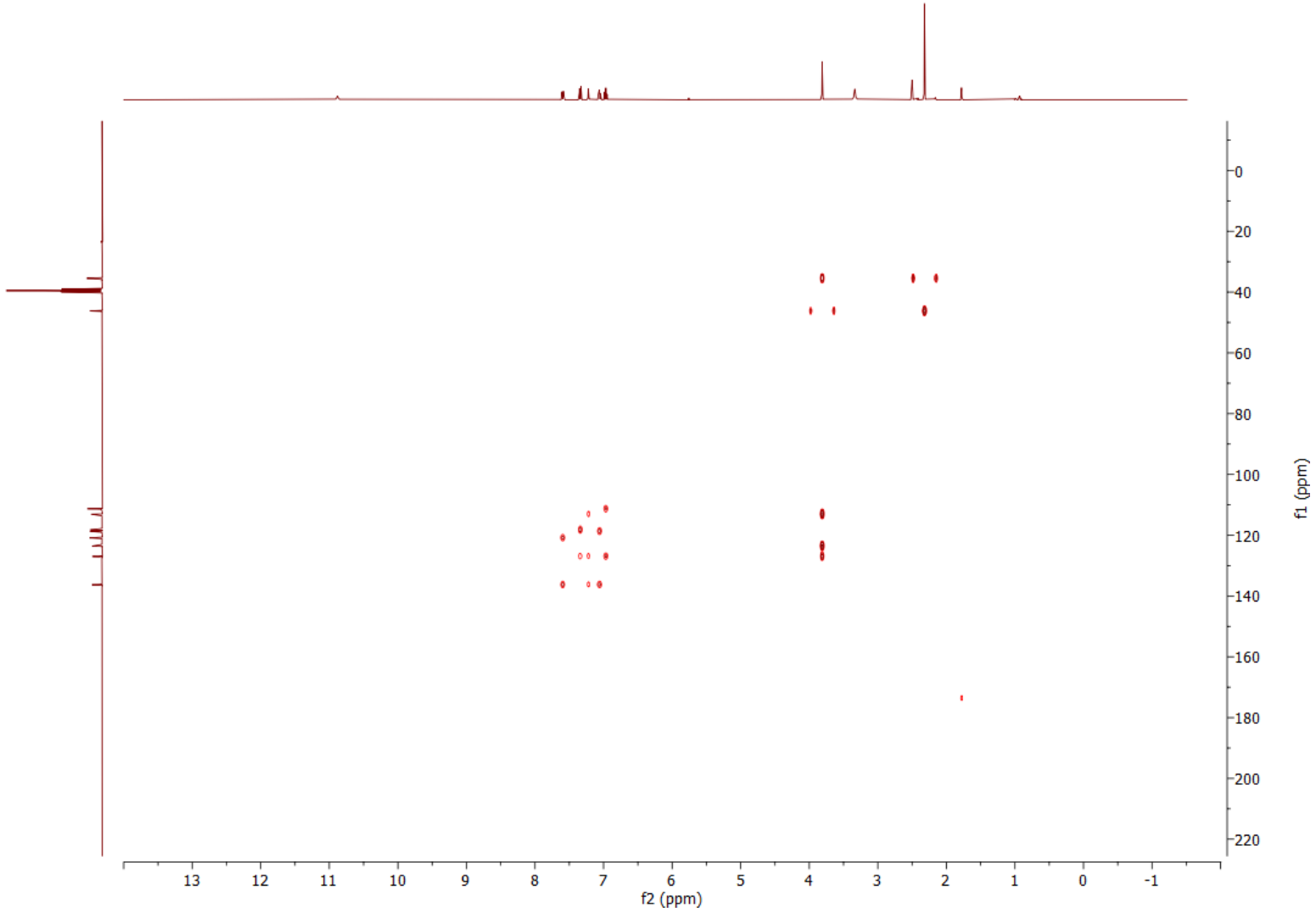


**Fig. S43. HMBC spectrum of synthesized MAMI (4) (298 K, DMSO-$d_6$, 400 MHz).**

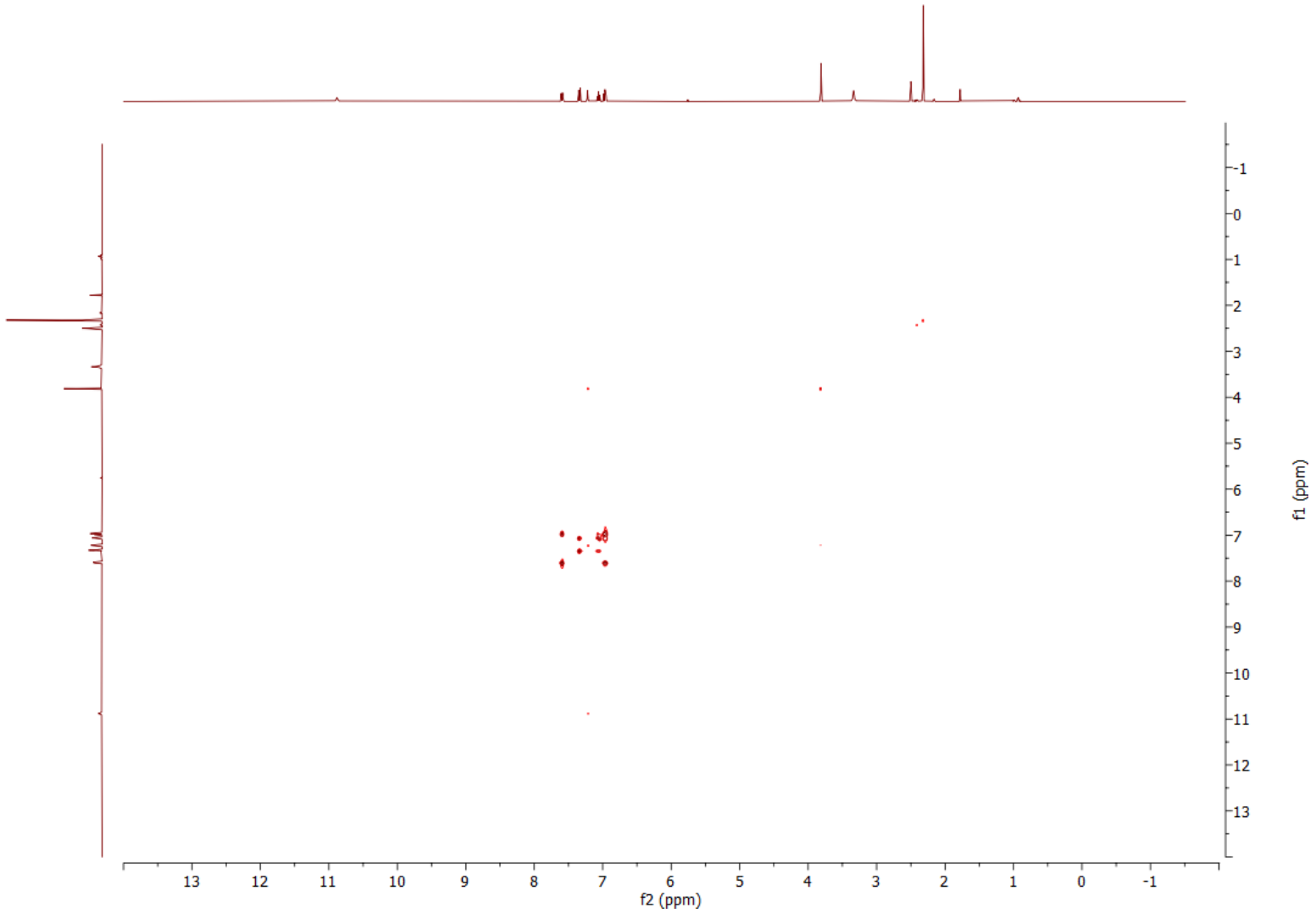


**Fig. S44. COSY spectrum of synthesized MAMI (4) (298 K, DMSO-$d_6$, 400 MHz).**

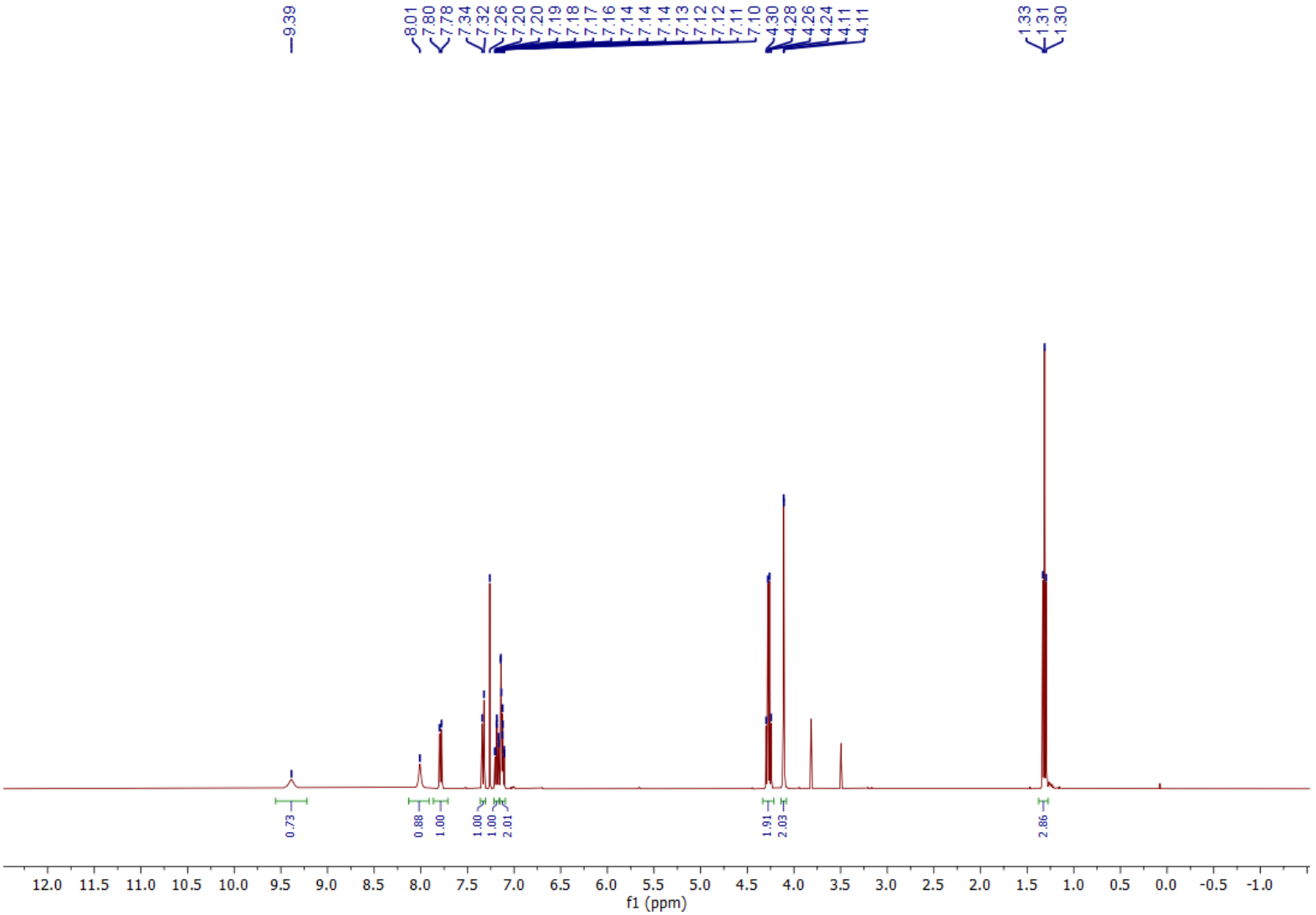


**Fig. S45. $^{1}$H spectrum of ethyl 2-hydroxyimino-3-(indol-3-yl)propionate (11) (298 K, $CDCl_3$, 400 MHz).**

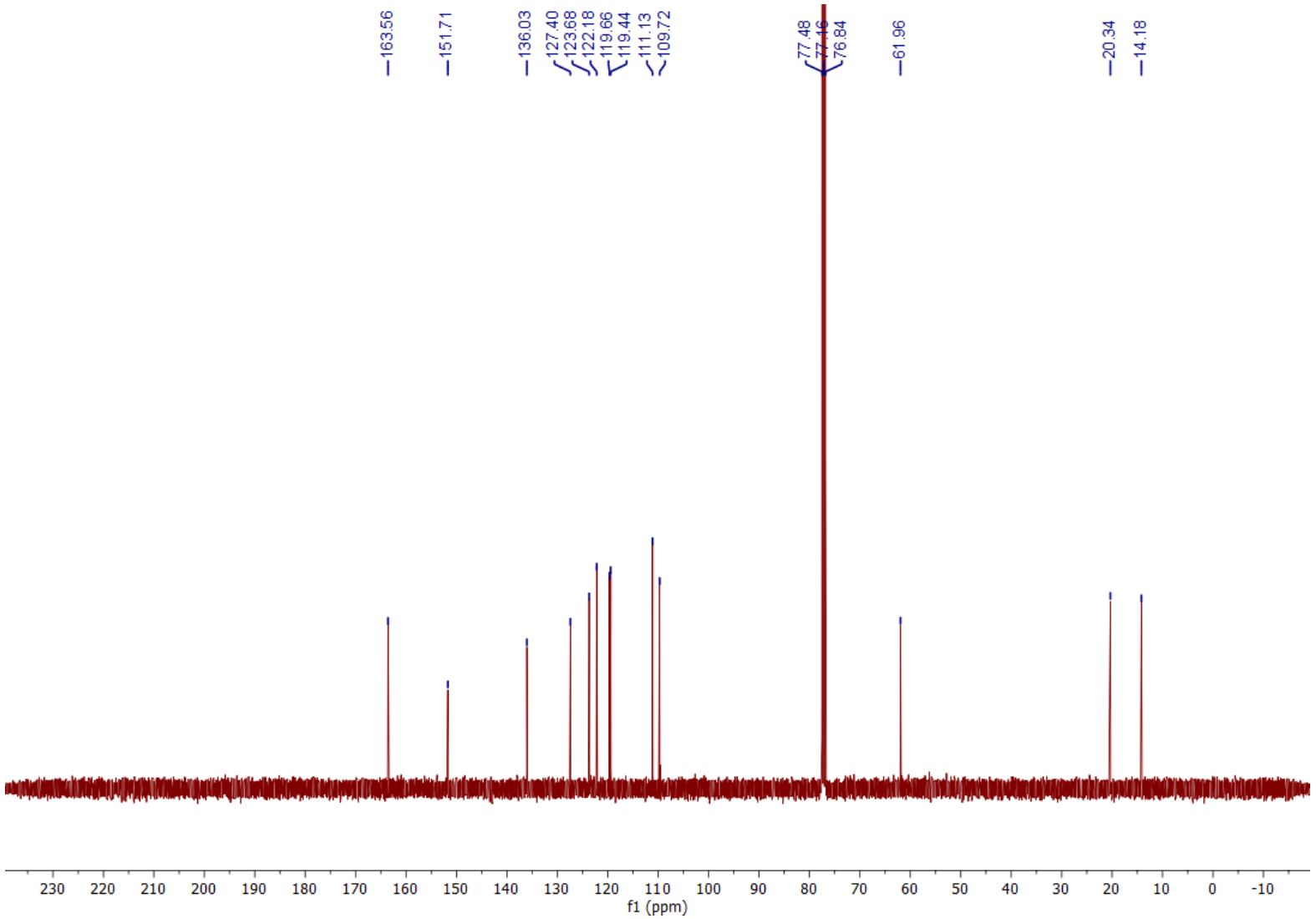


**Fig. S46. $^{13}C$ spectrum of ethyl 2-hydroxyimino-3-(indol-3-yl)propionate (11) (298 K, $CDCl_3$, 101 MHz).**

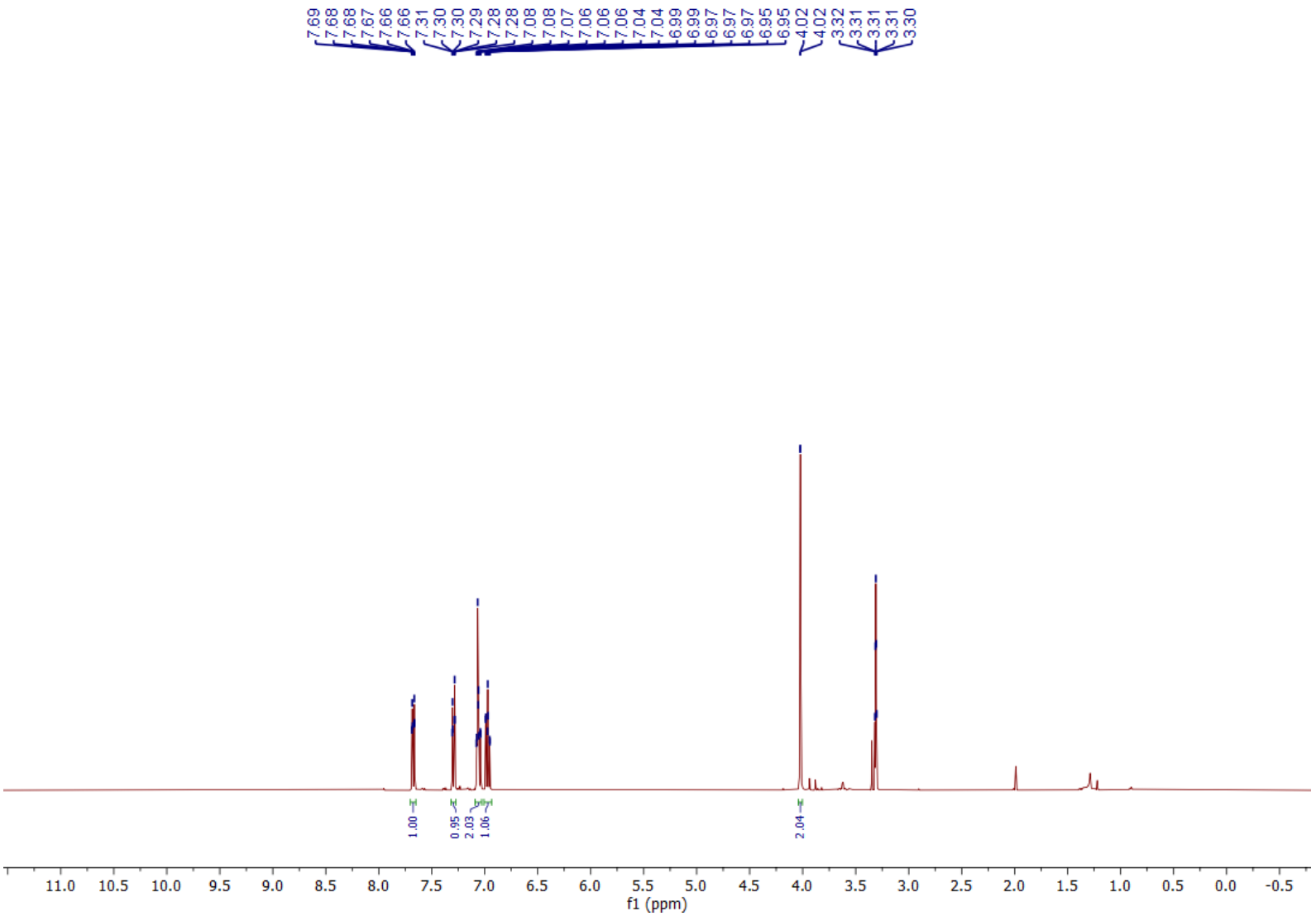


**Fig. S47. $^{1}$H spectrum of hydroxyimino tryptophan (13) (298 K, MeOH-d$_4$, 400 MHz).**

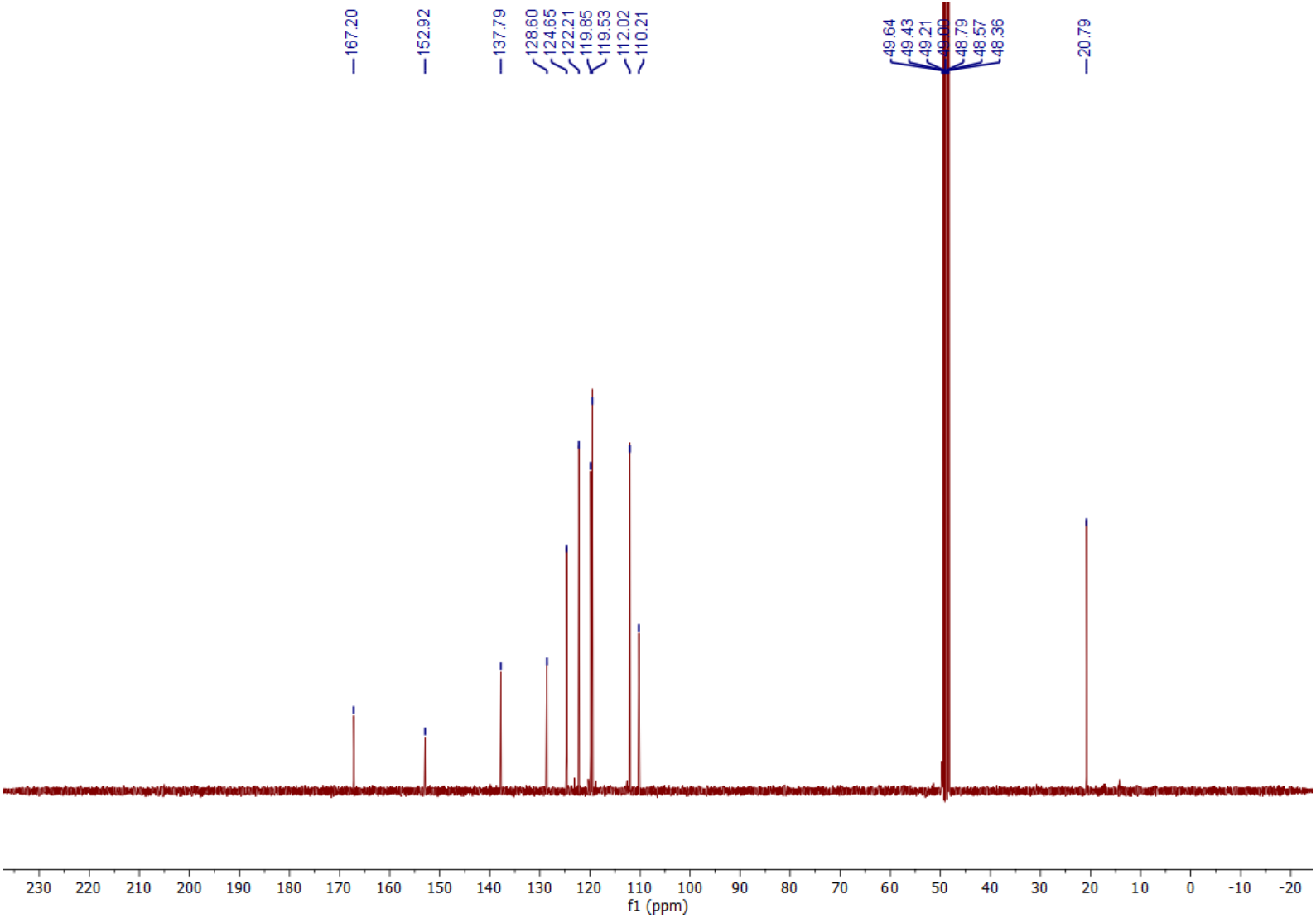


**Fig. S48. $^{13}C$ spectrum of hydroxyimino tryptophan (13) (298 K, MeOH-$d_4$, 101 MHz).**

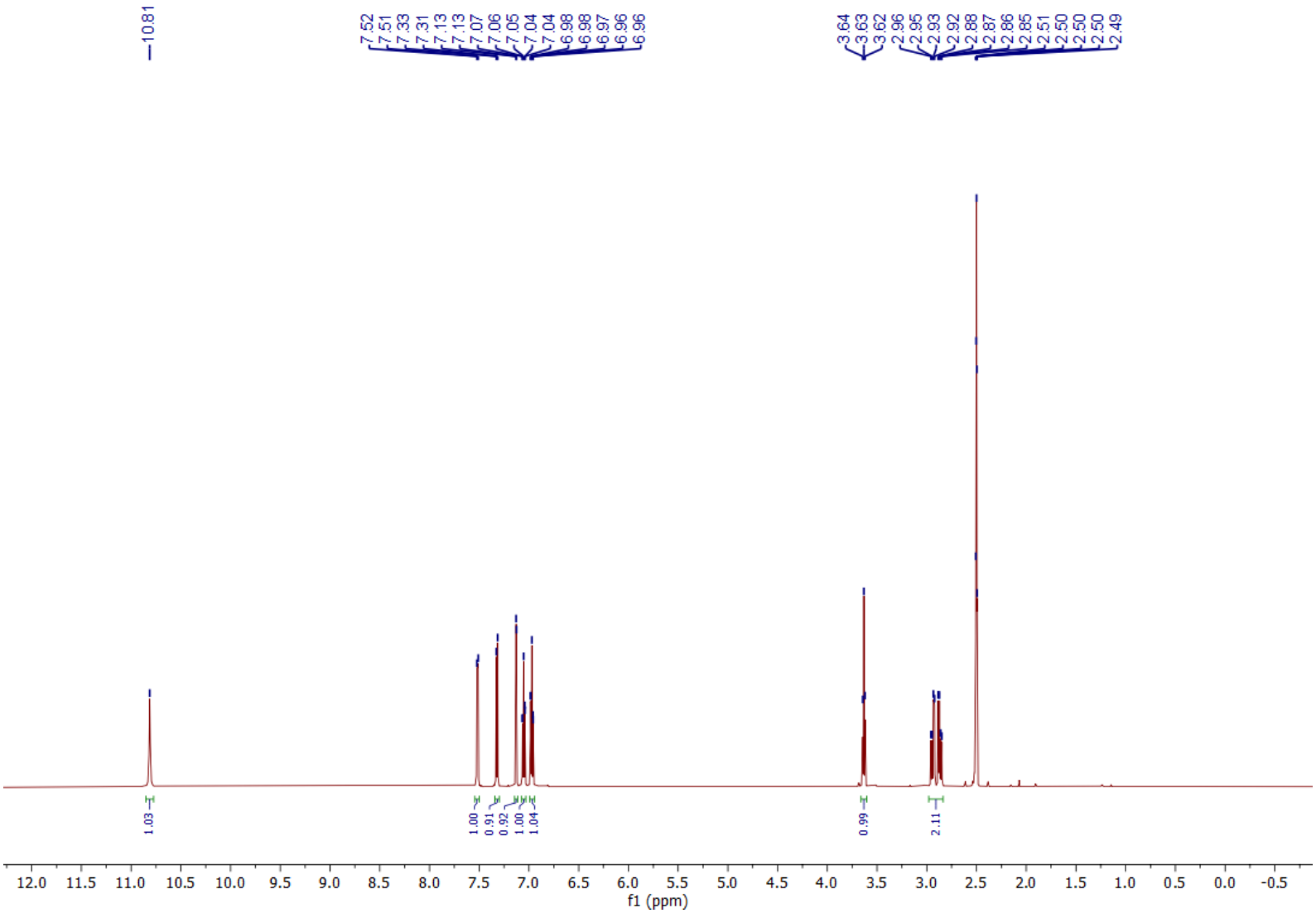


**Fig. S49. $^{1}$H spectrum of *N*-hydroxy-DL-tryptophan (9) (298 K, DMSO-d$_6$, 600 MHz).**

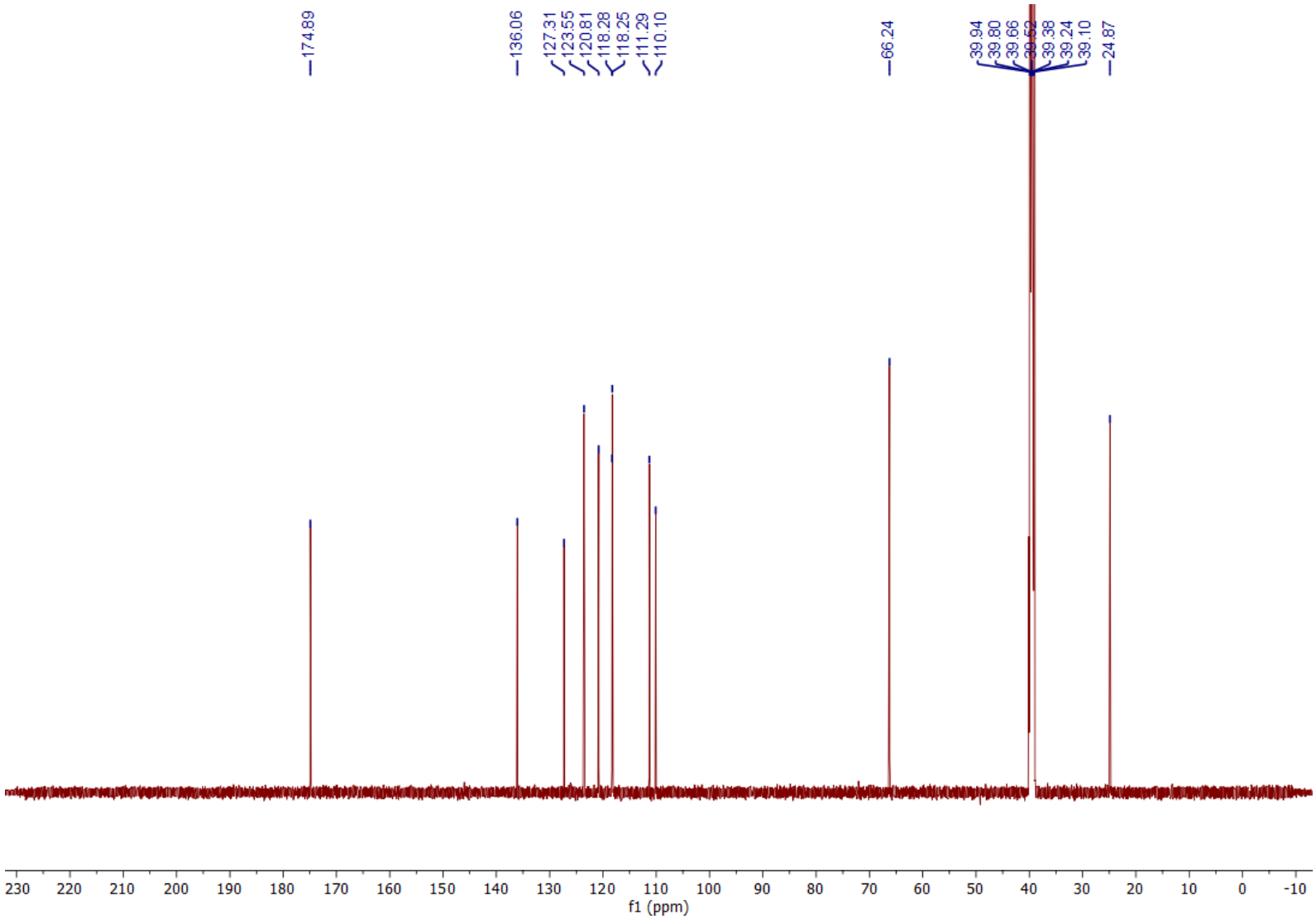


**Fig. S50. $^{13}$C spectrum of *N*-hydroxy-DL-tryptophan (9) (298 K, DMSO-d$_6$, 151 MHz).**

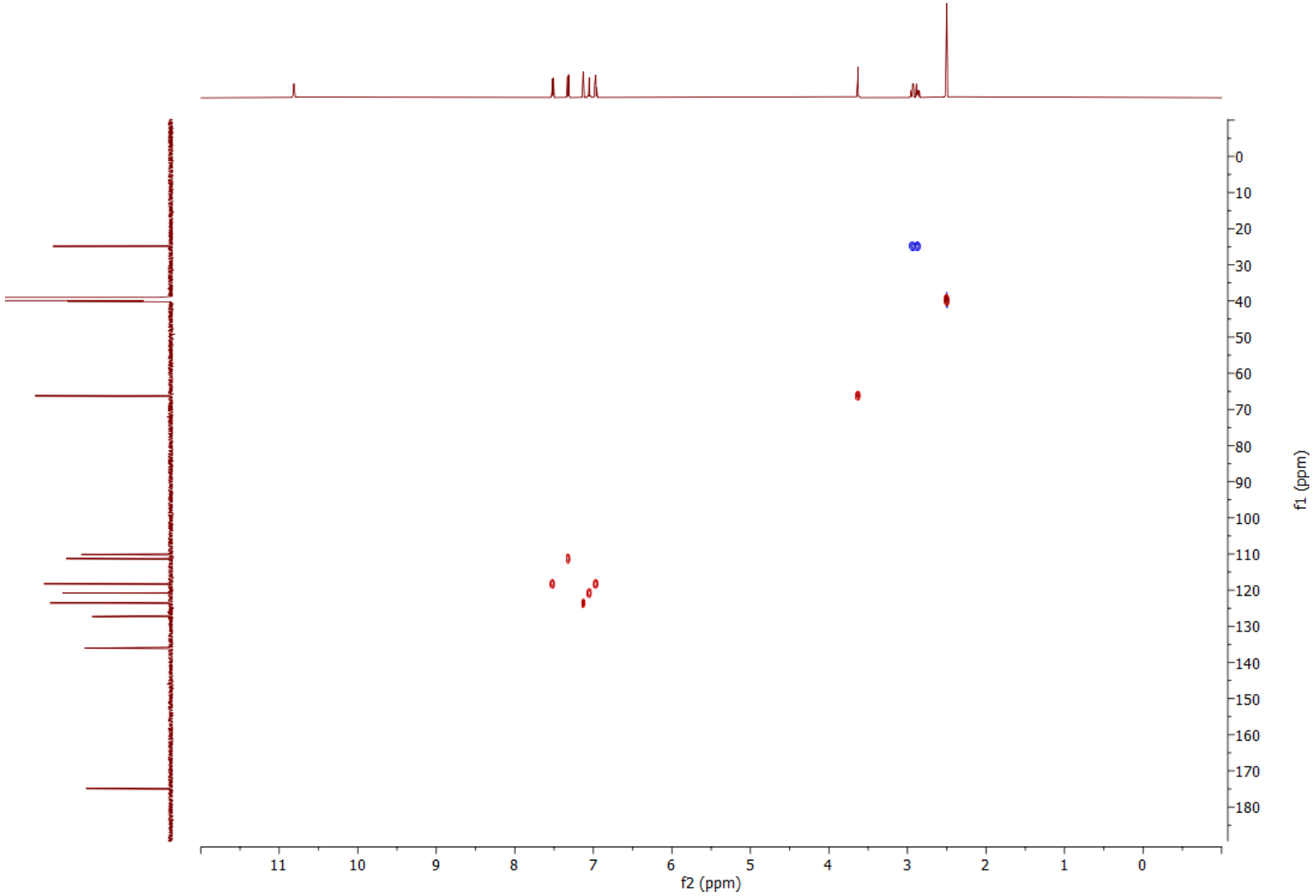


**Fig. S51. HSQC spectrum of *N*-hydroxy-DL-tryptophan (9) (298 K, DMSO-d$_6$, 600 MHz).**

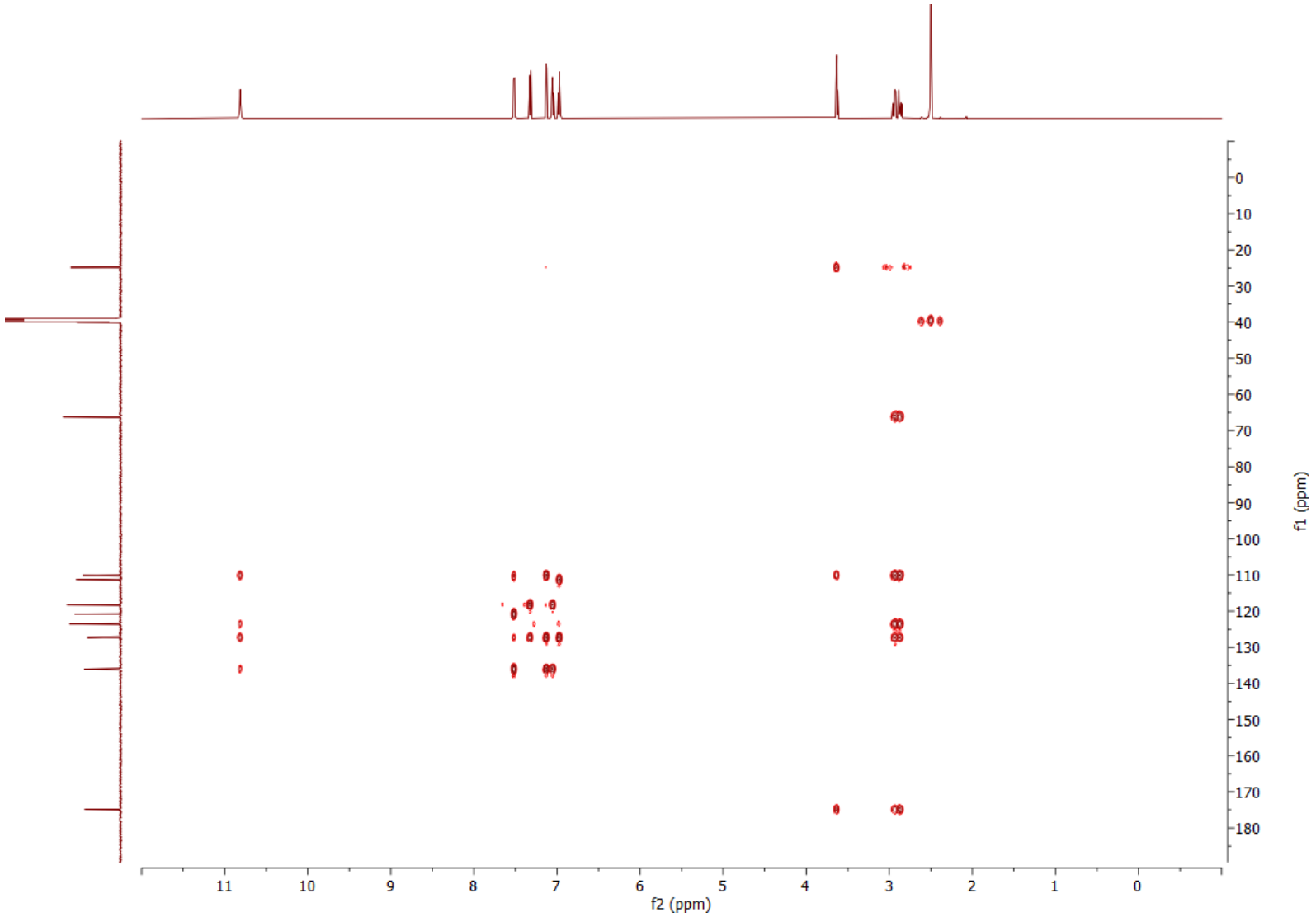


**Fig. S52. HMBC spectrum of *N*-hydroxy-DL-tryptophan (9) (298 K, DMSO-d$_6$, 600 MHz).**

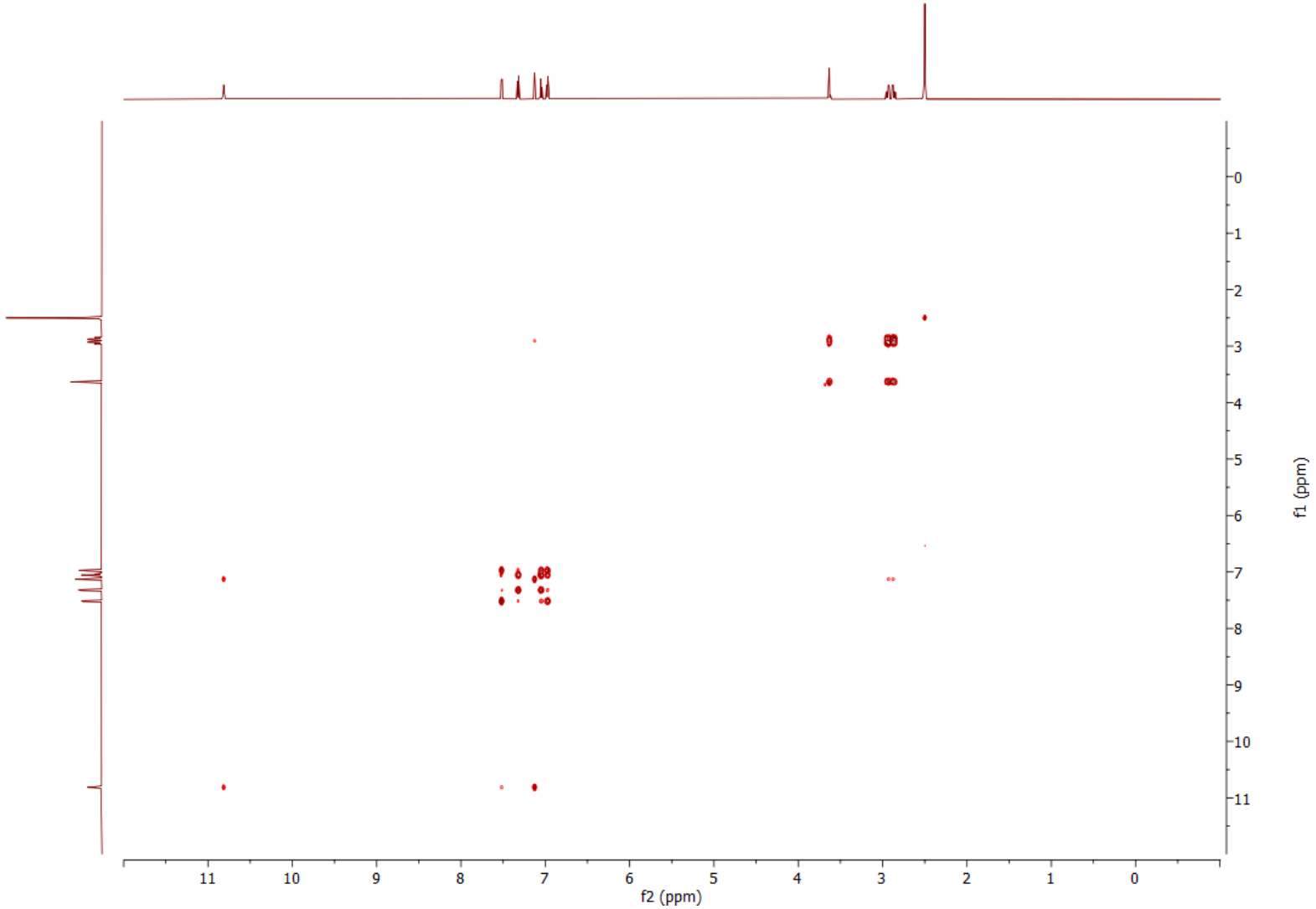


**Fig. S53. COSY spectrum of *N*-hydroxy-DL-tryptophan (9) (298 K, DMSO-d$_6$, 600 MHz).**

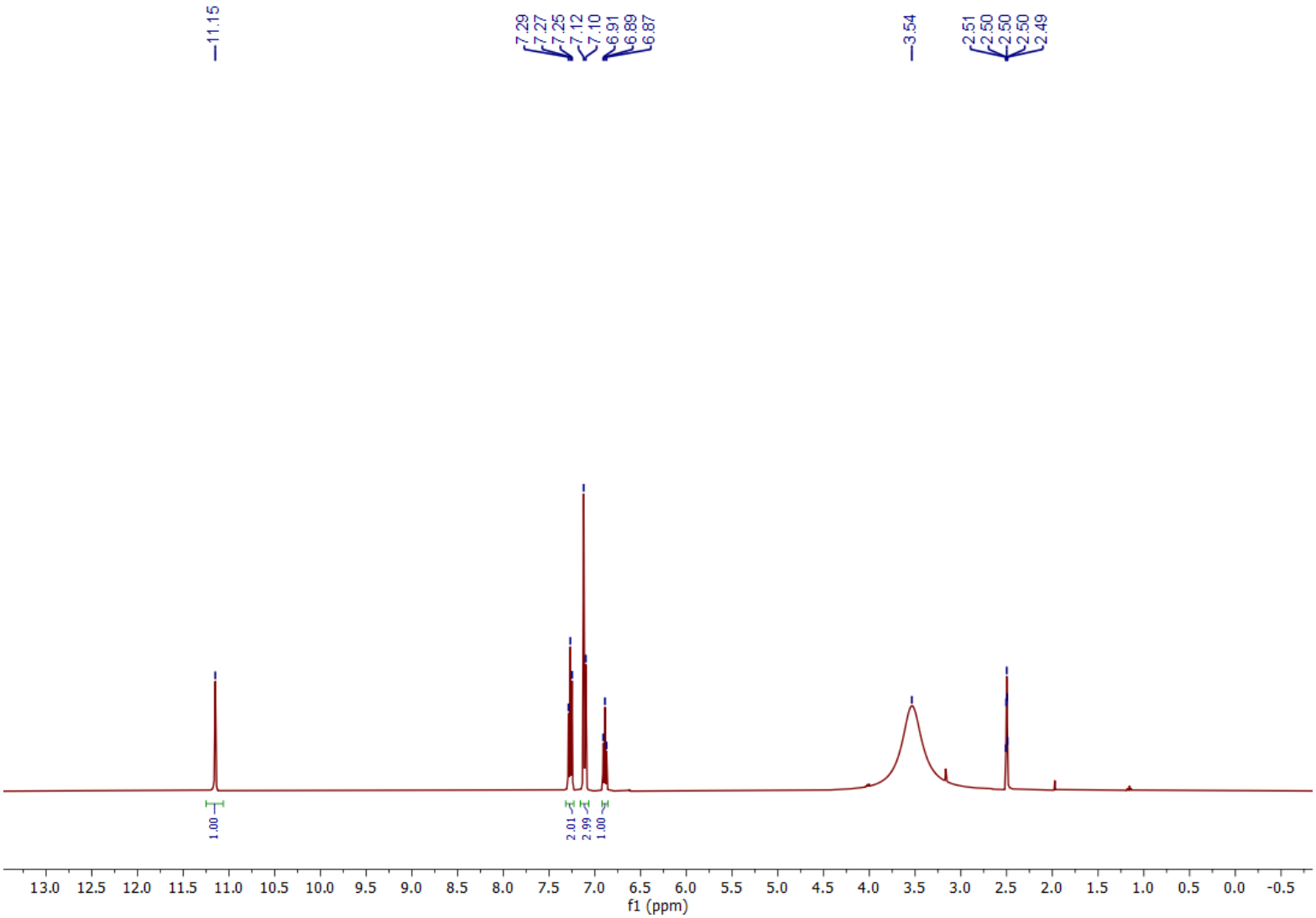


**Fig. S54. $^{1}$H spectrum of 2-(2-phenylhydrazinylidene)acetic acid (GA-phenylhydrazone) (7) (298 K, DMSO-d$_6$, 400 MHz).**

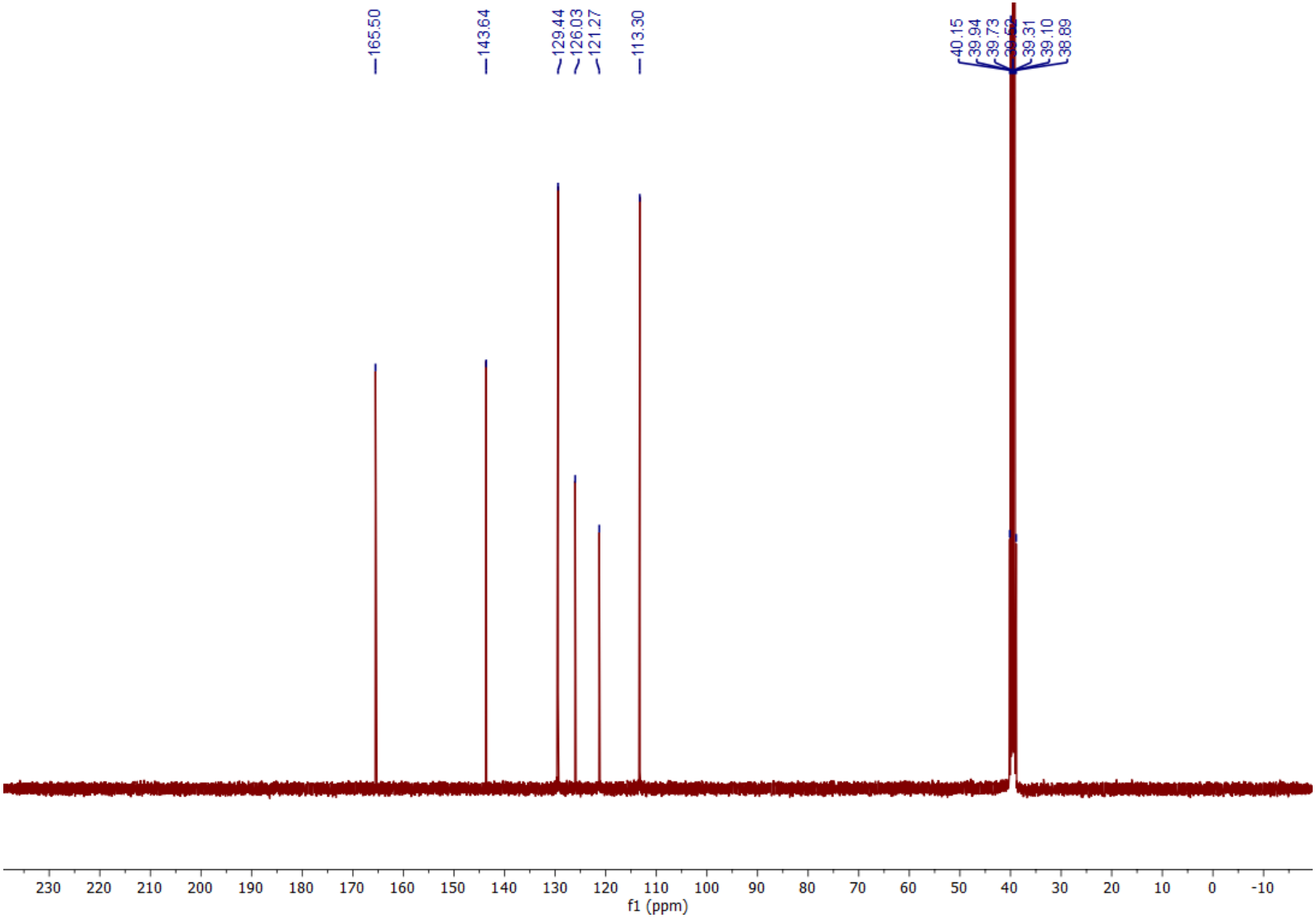


**Fig. S55. $^{13}$C spectrum of 2-(2-phenylhydrazinylidene)acetic acid (GA-phenylhydrazone) (7) (298 K, DMSO-d$_6$, 101 MHz).**

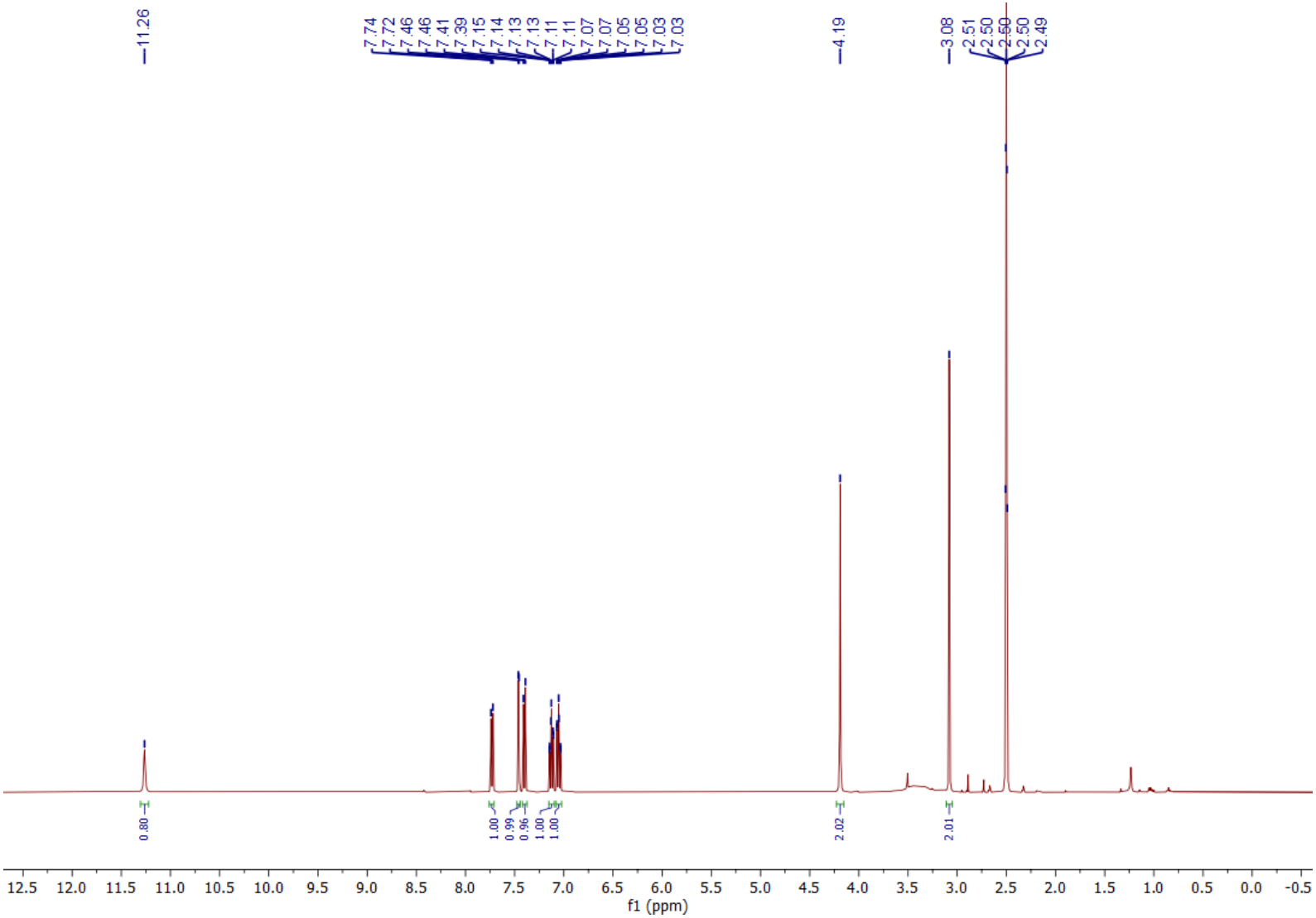


**Fig. S56. $^{1}$H spectrum of *N*-[(indol-3-yl) methyl]glycine (8) (298 K, DMSO-d$_6$, 400 MHz).**

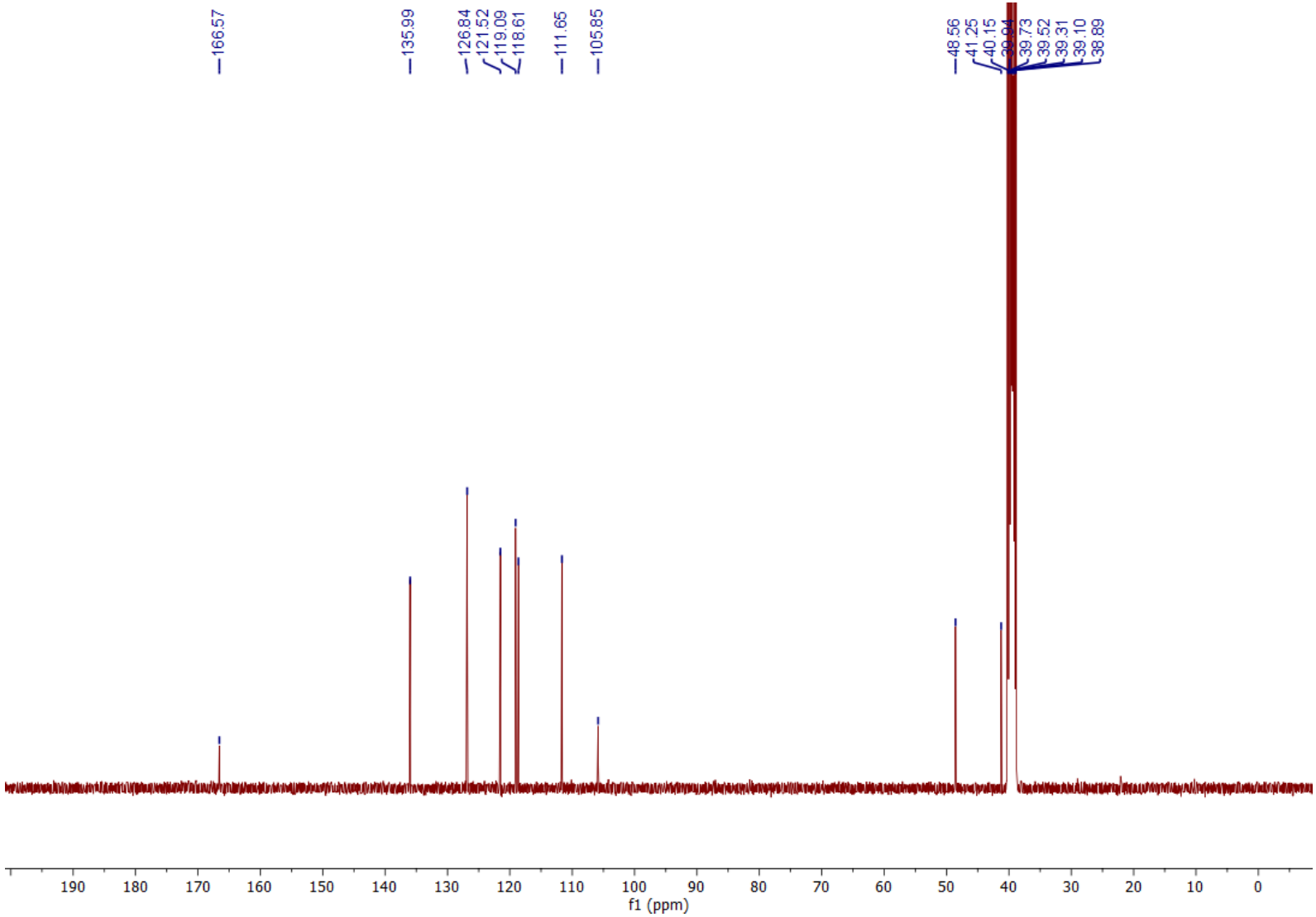


**Fig. S57. $^{13}$C spectrum of *N*-[(indol-3-yl) methyl]glycine (8) (298 K, DMSO-d$_6$, 101 MHz).**

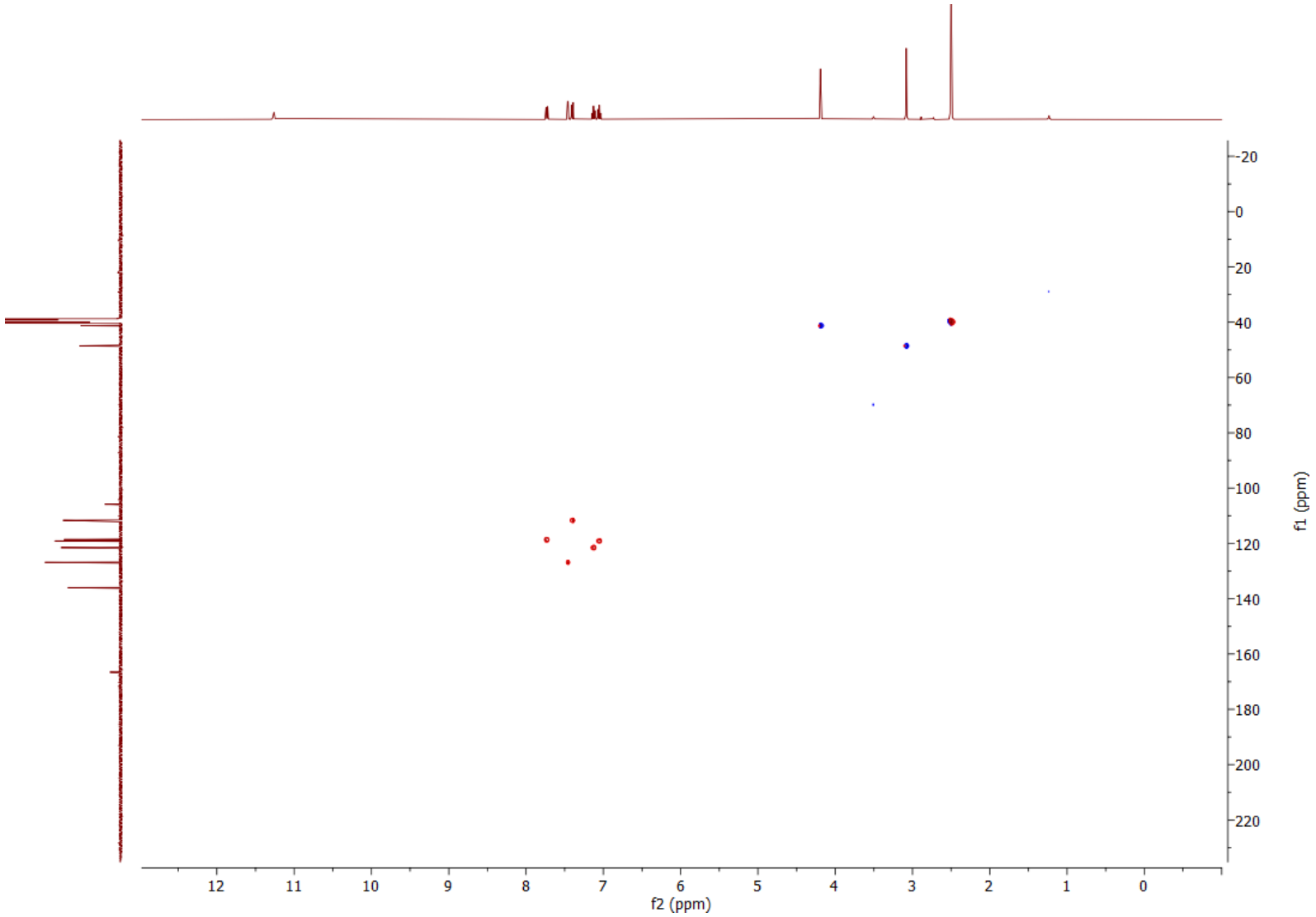


**Fig. S58. HSQC spectrum of *N*-[(indol-3-yl) methyl]glycine (8) (298 K, DMSO-$d_6$, 400 MHz).**

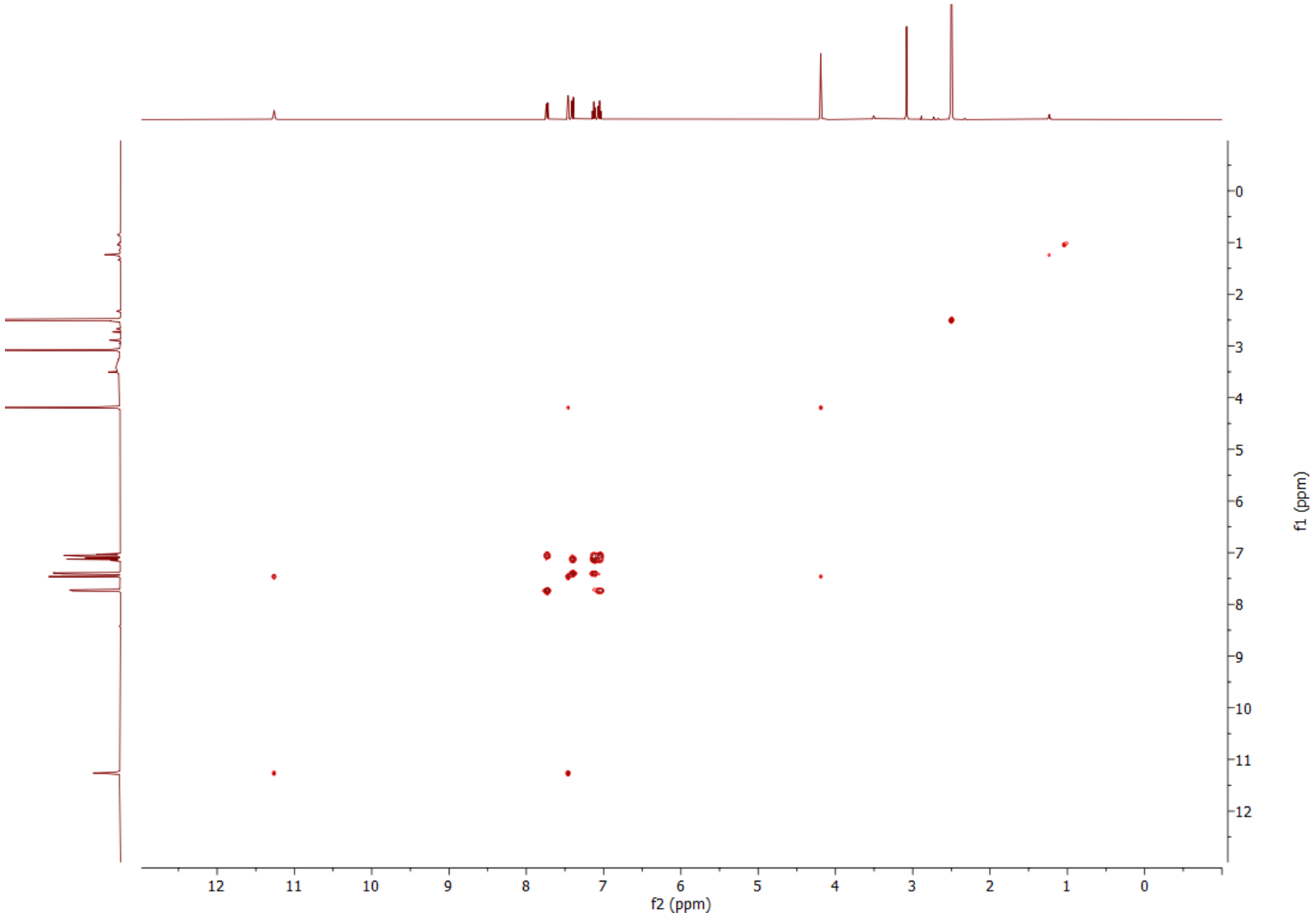


**Fig. S59. HMBC spectrum of *N*-[(indol-3-yl) methyl]glycine (8) (298 K, DMSO-$d_6$, 400 MHz).**

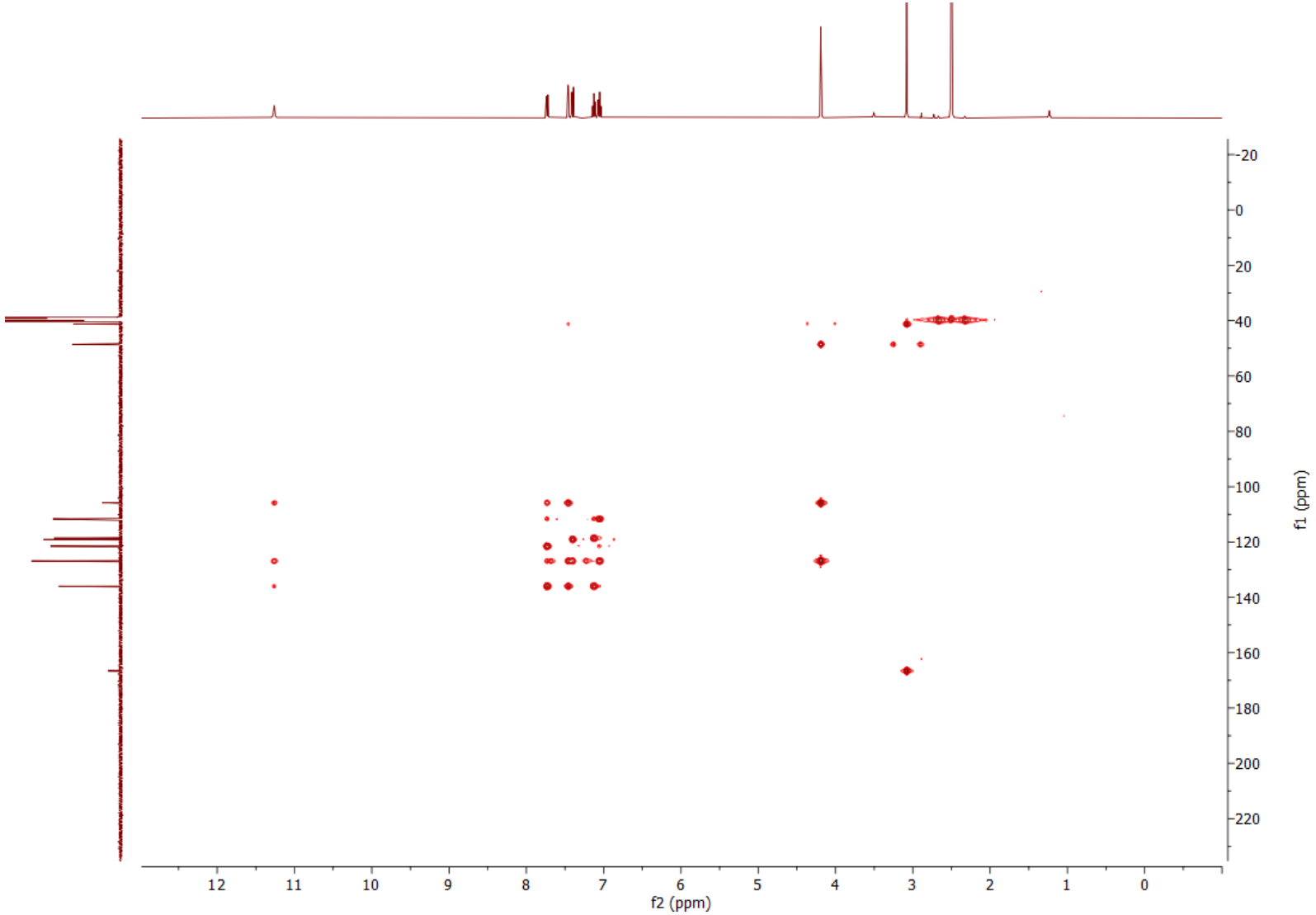


**Fig. S60. COSY spectrum of *N*-[(indol-3-yl) methyl]glycine (8) (298 K, DMSO-$d_6$, 400 MHz).**

**Table S1. Non-silent point mutations in *AMIS* genes in barley varieties ZDM_01467, B1K-04-12, and HOR3081.**

BLAST performed on GrainGenes (https://wheat.pw.usda.gov/GG3/)

| Accession (mutation) | Sequence |
|---|---|
| **HOR10350 (wildtype)** | ATGGAGCTGTTCCATGTTTGCATTGCACTCCTTGCGGTGTTACTCCTGTGCCGCAAGATGGTGTAC<br>ATGGGAAGAGGTGCCATGCGGTGGCCGCCGGGCCCCCGTCCATGGCCCATAGTCGGCAACCTCCTC<br>GACCTCCGCGGGGGCAATCTCCACCACAAGCTCGCGAGCCTGGCGCATGACCATGGCCCCGTGATG<br>ACGCTCAAGCTCGGCACGGTGAGCACCGTGTTTGTGTCCTCCCGGGACGCGGCATGGGAGGCGTTC<br>ACCAAGCACGACCGGCGCATTGCTGCACGCACCATACCGGACACTAGGCGTGCTGTTTCACATGCT<br>GACCGCTCCATGGTGTGGCTACCAAGCTCAGACCCATTGTGGAAGACGCTGCGTGGCATCGCTGCC<br>ACGCATGTCTTCTCGCCGCGCAGCCTTGCGGCCGCGCAGGGTACACGGGAGCGCGCTGTGCAAAAC<br>ATGCTAAATGATTTCCGCCGACAAGCTGGGCAGGAGGTGCACATCGGCCATGTCCTGTACCACGGC<br>ATGTTCGACCTTCTCACCAACACGCTCTTCTCCCTCGACAGCCAGGACAGGTTGAGGGACCTTCTG<br>GAAGACATTGTGGCACTTCTCGCCGAGCCCAATGTCTCGGACTTCTACCCGTTACTTCGGGTGATG<br>GACCTGCAGGGCCTGCGCCGCTGGACGGCCAAACACATGAACCGTGTGTTTCATGTCCTCGATAAG<br>ATCATTGACACCCGGCTGGGAGATGGACAGGCCGGTAGGCATCAGGACGTCCTGGATGCGCTGCTA<br>GCACTGATGACCACCGGTAAGCTGAGCCGGCAGGACGTGAAGGCCATGTTGTTTGACATCCTTGCA<br>GCAGGTACAGAGACAACCAAGATCACGGTGGAGTGGGCGATGGCGGAGCTGTTGCGGAACCCGGGC<br>GTGATGGCTGCGGTGTGCGCCGAGATGAAGGCCGCCCTCGCGCAGGAACAAGAGAGGATGATCACA<br>GAGGCAGACGTGGCAAAGCTGCCATACCTGCAGGCCGCGGTAAAGGAGTCGATGCGGCTACACCCC<br>GTGGCACCGCTACTGCTGCCGCACATGGTCGTAGAGGAGGGCGTGGAGATAGGCGGCTATGACGTG<br>CCTATGGGCGCCACCATCATCTTCAACTCGTGGTCCATCATGCGCGACCCTGAAGCATGGGAGAGG<br>CCCGATGAATTTGTGCCAGAGCGGTTTTTGGGGAAGACAGAGCATGGCATGTGGGGGAAGGACGTC<br>AAGTTCATCCCGCTGGGCACCGGCCGGAGGCTGTGCCCTGCATTGCCCATGGTGGAGCTCGTCGTG<br>CCCTTCATGGTGGCATCCATGTTGCATGCCTTTGAGTGGAGGCTACCCCAGGGCATGTCACCTGAC<br>CAGGTGGATGTGACCGAGAGGTATACAAGCAATGATATCCTCGTTATGGATGTGCCTCTCAAGGTT<br>GTTCCGATACCCGTTGTTGCCATCTAG |
| **ZDM_01467 (S211W)** | ATGGAGCTGTTCCATGTTTGCATTGCACTCCTTGCGGTGTTACTCCTGTGCCGCAAGATGGTGTAC<br>ATGGGAAGAGGTGCCATGCGGTGGCCGCCGGGCCCCCGTCCATGGCCCATAGTCGGCAACCTCCTC<br>GACCTCCGCGGGGGCAATCTCCACCACAAGCTCGCGAGCCTGGCGCATGACCATGGCCCCGTGATG<br>ACGCTCAAGCTCGGCACGGTGAGCACCGTGTTTGTGTCCTCCCGGGACGCGGCATGGGAGGCGTTC<br>ACCAAGCACGACCGGCGCATTGCTGCACGCACCATACCGGACACTAGGCGTGCTGTTTCACATGCT<br>GACCGCTCCATGGTGTGGCTACCAAGCTCAGACCCATTGTGGAAGACGCTGCGTGGCATCGCTGCC<br>ACGCATGTCTTCTCGCCGCGCAGCCTTGCGGCCGCGCAGGGTACACGGGAGCGCGCTGTGCAAAAC<br>ATGCTAAATGATTTCCGCCGACAAGCTGGGCAGGAGGTGCACATCGGCCATGTCCTGTACCACGGC<br>ATGTTCGACCTTCTCACCAACACGCTCTTCTCCCTCGACAGCCAGGACAGGTTGAGGGACCTTCTG<br>GAAGACATTGTGGCACTTCTCGCCGAGCCCAATGTCTGGGACTTCTACCCGTTACTTCGGGTGATG<br>GACCTGCAGGGCCTGCGCCGCTGGACGGCCAAACACATGAACCGTGTGTTTCATGTCCTCGATAAG<br>ATCATTGACACCCGGCTGGGAGATGGACAGGCCGGTAGGCATCAGGACGTCCTGGATGCGCTGCTA<br>GCACTGATGACCACCGGTAAGCTGAGCCGGCAGGACGTGAAGGCCATGTTGTTTGACATCCTTGCA<br>GCAGGTACAGAGACAACCAAGATCACGGTGGAGTGGGCGATGGCGGAGCTGTTGCGGAACCCGGGC<br>GTGATGGCTGCGGTGTGCGCCGAGATGAAGGCCGCCCTCGCGCAGGAACAAGAGAGGATGATCACA<br>GAGGCAGACGTGGCAAAGCTGCCATACCTGCAGGCCGCGGTAAAGGAGTCGATGCGGCTACACCCC<br>GTGGCACCGCTACTGCTGCCGCACATGGTCGTAGAGGAGGGCGTGGAGATAGGCGGCTATGACGTG<br>CCTATGGGCGCCACCATCATCTTCAACTCGTGGTCCATCATGCGCGACCCTGAAGCATGGGAGAGG<br>CCCGATGAATTTGTGCCAGAGCGGTTTTTGGGGAAGACAGAGCATGGCATGTGGGGGAAGGACGTC<br>AAGTTCATCCCGCTGGGCACCGGCCGGAGGCTGTGCCCTGCATTGCCCATGGTGGAGCTCGTCGTG<br>CCCTTCATGGTGGCATCCATGTTGCATGCCTTTGAGTGGAGGCTACCCCAGGGCATGTCACCTGAC<br>CAGGTGGATGTGACCGAGAGGTATACAAGCAATGATATCCTCGTTATGGATGTGCCTCTCAAGGTT<br>GTTCCGATACCCGTTGTTGCCATCTAG |
| **B1K-04-12 (M300I)** | ATGGAGCTGTTCCATGTTTGCATTGCACTCCTTGCGGTGTTACTCCTGTGCCGCAAGATGGTGTAC<br>ATGGGAAGAGGTGCCATGCGGTGGCCGCCGGGCCCCCGTCCATGGCCCATAGTCGGCAACCTCCTC<br>GACCTCCGCGGGGGCAATCTCCACCACAAGCTCGCGAGCCTGGCGCATGACCATGGCCCCGTGATG<br>ACGCTCAAGCTCGGCACGGTGAGCACCGTGTTTGTGTCCTCCCGGGACGCGGCATGGGAGGCGTTC |

| | |
|---|---|
| | ACCAAGCACGACCGGCGCATTGCTGCACGCACCATACCGGACACTAGGCGTGCTGTTTCACATGCT<br>GACCGCTCCATGGTGTGGCTACCAAGCTCAGACCCATTGTGGAAGACGCTGCGTGGCATCGCTGCC<br>ACGCATGTCTTCTCGCCGCGCAGCCTTGCGGCCGCGCAGGGTACACGGGAGCGCGCTGTGCAAAAC<br>ATGCTAAATGATTTCCGCCGACAAGCTGGGCAGGAGGTGCACATCGGCCATGTCCTGTACCACGGC<br>ATGTTCGACCTTCTCACCAACACGCTCTTCTCCCTCGACAGCCAGGACAGGTTGAGGGACCTTCTG<br>GAAGACATTGTGGCACTTCTCGCCGAGCCCAATGTCTCGGACTTCTACCCGTTACTTCGGGTGATG<br>GACCTGCAGGGCCTGCGCCGCTGGACGGCCAAACACATGAACCGTGTGTTTCATGTCCTCGATAAG<br>ATCATTGACACCCGGCTGGGAGATGGACAGGCCGGTAGGCATCAGGACGTCCTGGATGCGCTGCTA<br>GCACTGATGACCACCGGTAAGCTGAGCCGGCAGGACGTGAAGGCCATGTTGTTTGACATCCTTGCA<br>GCAGGTACAGAGACAACCAAGATCACGGTGGAGTGGGCGATAGCGGAGCTGTTGCGGAACCCGGGC<br>GTGATGGCTGCGGTGTGCGCCGAGATGAAGGCCGCCCTCGCGCAGGAACAAGAGAGGATGATCACA<br>GAGGCAGACGTGGCAAAGCTGCCATACCTGCAGGCCGCGGTAAAGGAGTCGATGCGGCTACACCCC<br>GTGGCACCGCTACTGCTGCCGCACATGGTCGTAGAGGAGGGCGTGGAGATAGGCGGCTATGACGTG<br>CCTATGGGCGCCACCATCATCTTCAACTCGTGGTCCATCATGCGCGACCCTGAAGCATGGGAGAGG<br>CCCGATGAATTTGTGCCAGAGCGGTTTTTGGGGAAGACAGAGCATGGCATGTGGGGGAAGGACGTC<br>AAGTTCATCCCGCTGGGCACCGGCCGGAGGCTGTGCCCTGCATTGCCCATGGTGGAGCTCGTCGTG<br>CCCTTCATGGTGGCATCCATGTTGCATGCCTTTGAGTGGAGGCTACCCCAGGGCATGTCACCTGAC<br>CAGGTGGATGTGACCGAGAGGTATACAAGCAATGATATCCTCGTTATGGATGTGCCTCTCAAGGTT<br>GTTCCGATACCCGTTGTTGCCATCTAG |
| **HOR3081 (M459I)** | ATGGAGCTGTTCCATGTTTGCATTGCACTCCTTGCGGTGTTACTCCTGTGCCGCAAGATGGTGTAC<br>ATGGGAAGAGGTGCCATGCGGTGGCCGCCGGGCCCCCGTCCATGGCCCATAGTCGGCAACCTCCTC<br>GACCTCCGCGGGGGCAATCTCCACCACAAGCTCGCGAGCCTGGCGCATGACCATGGCCCCGTGATG<br>ACGCTCAAGCTCGGCACGGTGAGCACCGTGTTTGTGTCCTCCCGGGACGCGGCATGGGAGGCGTTC<br>ACCAAGCACGACCGGCGCATTGCTGCACGCACCATACCGGACACTAGGCGTGCTGTTTCACATGCT<br>GACCGCTCCATGGTGTGGCTACCAAGCTCAGACCCATTGTGGAAGACGCTGCGTGGCATCGCTGCC<br>ACGCATGTCTTCTCGCCGCGCAGCCTTGCGGCCGCGCAGGGTACACGGGAGCGCGCTGTGCAAAAC<br>ATGCTAAATGATTTCCGCCGACAAGCTGGGCAGGAGGTGCACATCGGCCATGTCCTGTACCACGGC<br>ATGTTCGACCTTCTCACCAACACGCTCTTCTCCCTCGACAGCCAGGACAGGTTGAGGGACCTTCTG<br>GAAGACATTGTGGCACTTCTCGCCGAGCCCAATGTCTCGGACTTCTACCCGTTACTTCGGGTGATG<br>GACCTGCAGGGCCTGCGCCGCTGGACGGCCAAACACATGAACCGTGTGTTTCATGTCCTCGATAAG<br>ATCATTGACACCCGGCTGGGAGATGGACAGGCCGGTAGGCATCAGGACGTCCTGGATGCGCTGCTA<br>GCACTGATGACCACCGGTAAGCTGAGCCGGCAGGACGTGAAGGCCATGTTGTTTGACATCCTTGCA<br>GCAGGTACAGAGACAACCAAGATCACGGTGGAGTGGGCGATGGCGGAGCTGTTGCGGAACCCGGGC<br>GTGATGGCTGCGGTGTGCGCCGAGATGAAGGCCGCCCTCGCGCAGGAACAAGAGAGGATGATCACA<br>GAGGCAGACGTGGCAAAGCTGCCATACCTGCAGGCCGCGGTAAAGGAGTCGATGCGGCTACACCCC<br>GTGGCACCGCTACTGCTGCCGCACATGGTCGTAGAGGAGGGCGTGGAGATAGGCGGCTATGACGTG<br>CCTATGGGCGCCACCATCATCTTCAACTCGTGGTCCATCATGCGCGACCCTGAAGCATGGGAGAGG<br>CCCGATGAATTTGTGCCAGAGCGGTTTTTGGGGAAGACAGAGCATGGCATGTGGGGGAAGGACGTC<br>AAGTTCATCCCGCTGGGCACCGGCCGGAGGCTGTGCCCTGCATTGCCCATGGTGGAGCTCGTCGTG<br>CCCTTCATGGTGGCATCCATGTTGCATGCCTTTGAGTGGAGGCTACCCCAGGGCATCTCACCTGAC<br>CAGGTGGATGTGACCGAGAGGTATACAAGCAATGATATCCTCGTTATGGATGTGCCTCTCAAGGTT<br>GTTCCGATACCCGTTGTTGCCATCTAG |

**Table S2. Comparison of NMR data for AMI (3) produced in *N. benthamiana* and from synthesis.**

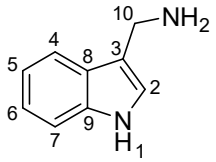


AMI (**3**)

| | $^{1}$H ppm (m, Hz) [a] | | $^{13}$C ppm [b] | |
|---|---|---|---|---|
| **Atom** | ***HvAMIS*** [c] | **Synthetic AMI** | ***HvAMIS*** [c] | **Synthetic AMI** |
| 1 | 10.80 (s, 1H) | 10.84 (s, 1H) | - | - |
| 2 | 7.19 (s, 1H) | 7.20 (s, 1H) | 122.3 | 122.3 |
| 3 | - | - | 117.4 | 117.4 |
| 4 | 7.58 (d, *J* = 7.8 Hz, 1H) | 7.59 (d, *J* = 7.8 Hz, 1H) | 118.7 | 118.7 |
| 5 | 7.00 – 6.92 (m, 1H) | 7.00 – 6.93 (m, 1H) | 118.1 | 118.2 |
| 6 | 7.10 – 7.02 (m, 1H) | 7.11 – 7.03 (m, 1H) | 120.9 | 120.9 |
| 7 | 7.33 (d, *J* = 8.1 Hz, 1H) | 7.34 (d, *J* = 8.1 Hz, 1H) | 111.3 | 111.3 |
| 8 | - | - | 126.4 | 126.5 |
| 9 | - | - | 136.4 | 136.5 |
| 10 | 3.87 (s, 2H) | 3.88 (s, 2H) | 37.2 | 37.2 |

[a] Obtained at 298 K, DMSO-$d_6$, 400 MHz.

[b] Obtained at 298 K, DMSO-$d_6$, 101 MHz.

[c] Isolated AMI from *N. benthamiana* leaves after transient expression of *HvAMIS*.

**Table S3. Comparison of NMR data for gramine (1) produced in *Nicotiana benthamiana*, commercially available gramine and literature data (*60*).**

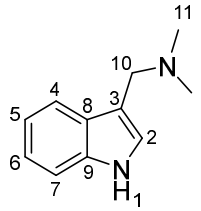


Gramine (**1**)

| | $^{1}$H ppm (m, Hz) [a] | | | $^{13}$C ppm [b] | | |
|---|---|---|---|---|---|---|
| **Atom** | ***HvAMIS* + *HvNMT*** [c] | **Gramine** [d] | **Literature** (*60*) | ***HvAMIS* + *HvNMT*** [c] | **Gramine** [d] | **Literature** (*60*) |
| 1 | 10.89 (s, 1H) | 10.88 (s, 1H) | 10.86 (s, 1H) | - | - | - |
| 2 | 7.20 (d, *J* = 2.3 Hz, 1H) | 7.19 (d, *J* = 2.3 Hz, 1H) | 7.18 (d, *J* = 2.2 Hz, 1H) | 124.4 | 124.3 | 124.4 |
| 3 | - | - | - | 111.6 | 111.7 | 111.8 |
| 4 | 7.59 (d, *J* = 7.9 Hz, 1H) | 7.59 (d, *J* = 8.0 Hz, 1H) | 7.58 (d, *J* = 8.0 Hz, 1H) | 119.1 | 119.1 | 119.2 |
| 5 | 7.00 – 6.92 (m, 1H) | 7.00 – 6.93 (m, 1H) | 6.95 (dd, *J* = 8.1, 7.0, 1.1 Hz, 1H) [e] | 118.3 | 118.3 | 118.4 |
| 6 | 7.09 – 7.02 (m, 1H) | 7.09 – 7.03 (m, 1H) | 7.05 (dd, *J* = 8.2, 7.0 Hz, 1H) | 120.9 | 120.9 | 121.0 |
| 7 | 7.34 (d, *J* = 8.1 Hz, 1H) | 7.34 (d, *J* = 8.1 Hz, 1H) | 7.36 – 7.29 (m, 1H) | 111.3 | 111.3 | 111.2 |
| 8 | - | - | - | 127.5 | 127.5 | 127.7 |
| 9 | - | - | - | 136.3 | 136.3 | 136.5 |
| 10 | 3.52 (s, 2H) | 3.52 (s, 2H) | 3.51 (s, 2H) | 54.4 | 54.4 | 54.6 |
| 11 | 2.14 (s, 6H) | 2.14 (s, 6H) | 2.13 (s, 6H) | 44.9 | 44.9 | 45.0 |

[a] Obtained at 298 K, DMSO-$d_6$, 400 MHz.

[b] Obtained at 298 K, DMSO-$d_6$, 101 MHz.

[c] Isolated gramine from *N. benthamiana* leaves after transient expression of *HvAMIS* + *HvNMT*.

[d] Commercially available gramine purified using the same column chromatography method as in [c].

[e] As reported in ref. (*60*).

**Table S4. Sequences of primers for transformation and sequencing of *Arabidopsis thaliana* and barley.**

**Sequences in red indicate start/stop codons.**

| Primer name | Primer sequence | Purpose |
|---|---|---|
| ***Arabidopsis thaliana*** | | |
| Left Border FWD | TGGTGTAAACAAATTGACGCTTAG | Sequencing |
| Bar FWD 1 | GATCTGGATCGTTTCGCATGTC | |
| HvNMT FWD Rc | GAAAGGTGCTGAAATCTTGTCCAT | |
| Bar FWD 2 | GGGATTCTGGCAGCTTGATTTC | |
| HvNMT REV | TCACTTGGTGAACTCAAGAGCATA | |
| HvNMT FWD | ATGGACAAGATTTCAGCACCTTTC | |
| NMT4379 FWD | ATCTGCCTCATGTTATCGCCCA | |
| HvNMT REV Rc FWD | TATGCTCTTGAGTTCACCAAGTGA | |
| Start35SPromoter FWD | CTAGAATTCGAGCTCGGAGGTC | |
| HvP450 FWD | ATGGAGTTGTTCCATGTTTGTATTGC | |
| RightBorder REV | TGGCACATACAAATGGACGAA | |
| HvP450 FWD 2 | GCTTTCTCGGCAAGACGTGAAGG | |
| ***H. vulgare* cv. Golden Promise transgenesis** | | |
| HvP450_BamHI_FWD | ATATATGGATCCCCCGGGATGGAGTTGTTC CATGTTTGTATTGC | Cloning HvP450 (AMIS) codon optimized ORF into UbiFull-AB-M vector |
| HvP450_MluI_REV | GCGCACGCGTTCAGATGGCAACAACAGGTATC | |
| HvNMT_XmaI FWD | ATATACCCGGGATGGACAAGATTTCAGCACCTT | Cloning HvNMT codon optimized ORF into UbiFull-AB-M vector |
| HvNMT_MluI REV | CACAACGCGTTCACTTGGTGAACTCAAGAGC | |
| HvP450 genomic FWD | ATGGAGCTGTTCCATGTTTGC | Primers for isolating native HvP450 (AMIS) ORF from Barley cDNA |
| HvP450 genomic REV | CTAGATGGCAACAACGGGTATC | |
| Ubi Promoter FWD | AGCCCTGCCTTCATACGC | Sequencing of HvP450 (AMIS) or HvNMT in between Ubi promoter and Nos terminator of p6i-d35S |
| Nos Terminator REV | TTAAATGTATAATTGCGGGACTCTAATCATA | |
| ***H. vulgare* cv. Tafeno knockout** | | |
| IK70 fwd | GCTCACATGTTCTTTCCTGCG | For colony screening and sequencing of pIK48 plasmid assembly |
| IK71 rev | CACCTGACGTCTAAGAAACC | |
| HvP450 genomic FWD | ATGGAGCTGTTCCATGTTTGC | Sequencing |
| HvP450 genomic REV | CTAGATGGCAACAACGGGTATC | |

**Table S5. Sequences of primers for cloning into *Nicotiana benthamiana* transient expression vectors in this study.**

**The start and stop codons are marked in red. BsaI restriction sites for Golden Gate cloning are marked in green, and the cutting site is indicated with a slash.**

| Primer name | Primer sequence | Purpose |
|---|---|---|
| rLC193_HvAMIS_F | CACCACAGGTCTCG/AAAAATGGAGCTGTTCCATGTTTGC | Cloning *HvAMIS* into pHREAC |
| rLC194_HvAMIS_R | CACCACAGGTCTCG/AGCGCTAGATGGCAACAACGGGTA | |
| rLC191_HvNMT_F | CACCACAGGTCTCG/AAAAATGGACAAGATTTCAGCACCT | Cloning *HvNMT* into pHREAC |
| rLC192_HvNMT_R | CACCACAGGTCTCG/AGCGCTACTTGGTGAACTCAAGAGCG | |
| rLC42_pHREAC_SF | CTGTCACTTTATTGAGAAGATAGTGG | Sequencing (-385 bp to multiple cloning site on pHREAC) |
| rLC59_pHREAC_SR | CCTTGCTGAAGGGACGACCTG | Sequencing (+187 bp to multiple cloning site on pHREAC) |
| AB20_HvAMIS(Δ2-23)_F | CACCACAGGTCTCG/AAAAATGGGAAGAGGTGC | Cloning of *tAMIS* into pHREAC |
| AB27_tAMIS_R | CACCACAGGTCTCG/AGCGTTATTTTTCAAATTGAGGATGTGACCAACCGGCGCCGACAGCATAATCTGGAACATCGTATGGATAACCCCCGGGGATGGCAACAACGG | Cloning of *tAMIS* into pHREAC |

**Table S6. Sequences of primers for yeast genomic integration *via* EasyClone-MarkerFree system.**

**Uracil-containing overhangs for USER cloning are underlined.**

| Primer name | Primer sequence | Purpose |
|---|---|---|
| BB1 *Cr*CPR_fw | **AGTGCAGGU**ATGGATTCTAGCTCGGAGAAGTTG | Amplification of *CPR* gene from *Catharanthus roseus* cDNA with USER-overhangs |
| BB1 *Cr*CPR _rv | **CGTGCGAU**TCACCAGACATCTCGGAGATACCTT | |
| BB4 *Cr*Cyb5_fw | **ATCTGTCAU**ATGGCGTCGGATCAGAAATTGC | Amplification of *CYB5* gene from *Catharanthus roseus* cDNA with USER-overhangs |
| BB4 *Cr*Cyb5_rv | **CACGCGAU**TTACTTCTCCTTAGTATAGTGTCGGAC | |
| BB2_pADH2_fw | **ACCTGCACU**TGTGTATTACGATATAGTTAATAGTTG | Amplification of *ADH2* promoter region from *S. cerevisiae* with USER-overhangs for double gene construct |
| BB2_pADH2_rv | **AGTAGCTAU**TATCTAAAAATTGCCTTATGATCCG | |
| BB3_pPCK1_fw | **ATGACAGAU**GTTGTTATTTTATTATGGAATAATTA | Amplification of *PCK1* promoter region from *S. cerevisiae* with USER-overhangs for double gene construct |
| BB3_pPCK1_rv | **ATAGCTACU**ATAGGAAAAAACCGAGCTTC | |
| BB2/2 pADH2_rv | **CACGCGAU**TATCTAAAAATTGCCTTATGATCCGTCTCTCCGGTT | Amplification of *ADH2* promoter region from *S. cerevisiae* with USER-overhangs for single gene construct |
| BB1 *Hv*_P450_fw | **AGTGCAGGU**ATGGAGCTGTTCCATGTTTGC | Amplification of *HvAMIS* gene with USER-overhangs |
| BB1 *Hv*_P450_rv | **CGTGCGAU**CTAGATGGCAACAACGGGTATCG | |
| BB1 *Hv*_NMT_fw | **AGTGCAGGU**ATGGACAAGATTTCAGCACCTTTC | Amplification of *HvNMT* gene with USER-overhangs |
| BB1 *Hv*_NMT_rv | **CGTGCGAU**CTACTTGGTGAACTCAAGAGCG | |
| INFU *Hv*_P450_fw | GGTAGAAGTCCCAGACATTGGGCTCGGC | Mutagenesis of *HvAMIS* gene to construct $HvAMIS^{S211W}$ |
| INFU *Hv*_P450_rv | CAATGTCTGGGACTTCTACCCGTTACTTCGG | |
| pADH2_1/cPCR_ADH2 | GTTTTTATCACTTCTTGTTTCTTC | Sequencing and cPCR |
| pADH2_2 | ACATTAGAATGGTGATTAGAAAGG | Sequencing |
| *Cr*Cyb5_1/cPCR_pPCK1 | CAGCTTAAACAATAATTATATTTGTT | Sequencing and cPCR |
| pPCK1_1 | TCTTTCCCTTGTATAACTTAAAAT | Sequencing |
| *Cr*CPR_1 | ATGATTATGCGGCTGATGATG | Sequencing |
| *Cr*CPR_2 | GAAGCAAATGGCCATGCC | Sequencing |
| *Cr*CPR_3 | ACTAGTTGCAAATCAGAGAAGC | Sequencing |
| *Cr*CPR_4 | CTGCAGTTTTCTTTTTTGGATGC | Sequencing |
| *Hv*_P450_1 | AGGACACAAACACGGTGCTCAC | Sequencing |
| *Hv*_P450_2 | AACCGTGTGTTTCATGTCCTCGATA | Sequencing |
| *Hv*_NMT_1 | GGCTTGTGGACGTCGGTGGTG | Sequencing |
| *Hv*_NMT_2 | AGGAGAGGTACCTGAGGATACGGTC | Sequencing |

**Table S7. List of yeast strains (Saccharomyces cerevisiae) used in this study.**

| Name | Genotype | Reference |
|---|---|---|
| ST7574 | MATa; HIS3; TRP1; LEU2; TRP1; URA3; MAL2-8c SUC2 + pCfB2312 (2µ cas9 KanMX) | Euroscarf |
| BSY1 | ST7574, X-2::$P_{ADH2}$-*CrCPR*-$T_{ADH1}$, $P_{PCK1}$-*CrCYB5*-$T_{CYC1}$ | This study |
| BSY23 | BSY1, X-4::$P_{ADH2}$-*HvAMIS*-$T_{ADH1}$ | This study |
| BSY24 | BSY1, XI-3::$P_{ADH2}$-*HvNMT*-$T_{ADH1}$ | This study |
| BSY25 | BSY1, X-4::$P_{ADH2}$-*HvAMIS*-$T_{ADH1}$, XI-3::$P_{ADH2}$-*HvNMT*-$T_{ADH1}$ | This study |
| BSY114 | ST7574, X-4::$P_{ADH2}$-*HvAMIS*-$T_{ADH1}$ | This study |
| BSY115 | BSY1, X-4::$P_{ADH2}$-*HvAMIS*$^{S211W}$-$T_{ADH1}$ | This study |

**Table S8. Nucleotide sequences of genes amplified from *Catharanthus roseus* and *Hordeum vulgare* cDNA.**

**Non-silent differences of *CrCPR* from the GenBank reference are marked in red (V234G, D338E).**

| Name (accession number) | Amplified sequence |
|---|---|
| *C. roseus CPR* (X69791.1) | ATGGATTCTAGCTCGGAGAAGTTGTCGCCGTTCGAATTGATGAGCGCGATCTTGAAGG<br>GAGCTAAATTAGATGGGTCTAACTCTTCAGATTCTGGCGTAGCTGTGTCGCCGGCAGT<br>TATGGCTATGTTGTTGGAGAATAAGGAGTTAGTGATGATTTTGACTACTTCAGTGGCG<br>GTTTTGATCGGTTGTGTCGTAGTTTTGATATGGCGGCGATCTTCCGGATCGGGTAAAA<br>AAGTCGTGGAGCCTCCGAAGCTCATAGTGCCTAAATCTGTTGTAGAACCGGAGGAAAT<br>TGATGAAGGGAAGAAGAAATTTACCATATTTTTTGGAACACAAACTGGAACAGCTGAA<br>GGCTTCGCTAAGGCTCTAGCTGAGGAAGCCAAAGCTCGATATGAAAAGGCAGTTATCA<br>AAGTGATTGATATAGATGATTATGCGGCTGATGATGAAGAATACGAGGAGAAATTCAG<br>AAAAGAGACCTTGGCATTTTTCATCTTGGCCACGTATGGAGATGGTGAGCCAACCGAC<br>AATGCTGCAAGGTTCTACAAATGGTTTGTAGAGGGAAATGATAGAGGGGACTGGCTAA<br>AGAATCTGCAATATGGAGTTTTTGGCCTTGGTAACAGACAATATGAGCATTTCAACAA<br>GATTGCTAAAGTGGTGGATGAGAAAGTTGCTGAACAGGGTGGTAAGCGGATTGTTCCA<br>TTGGGTCTGGGAGACGATGACCAGTGCATTGAAGATGACTTTGCTGCATGGCGTGAGA<br>ATGTATGGCCTGAGTTGGATAACTTGCTCCGGGATGAGGATGATACAACTGTTTCTAC<br>AACCTACACTGCTGCTATTCCAGAATATCGTGTTGTGTTCCCTGACAAATCAGATTCA<br>CTTATTTCAGAAGCAAATGGCCATGCCAATGGTTATGCTAATGGCAACACCGTATATG<br>ATGCCCAGCATCCTTGCAGATCTAATGTTGCAGTGAGGAAGGAGCTTCATACTCCAGC<br>ATCTGATCGTTCTTGCACCCATTTGGAGTTTGACATTGCTGGCACTGGCCTTTCATAT<br>GGAACTGGAGATCATGTTGGAGTGTACTGTGATAATCTATCTGAAACCGTGGAGGAGG<br>CTGAGAGATTACTGAATTTACCCCCAGAAACTTATTTCTCGCTTCATGCTGATAAAGA<br>GGATGGAACCCCACTTGCTGGGAGCTCATTGCCTCCTCCTTTCCCACCTTGTACTCTA<br>AGAACCGCCCTCACTCGTTATGCAGATCTCTTAAATACTCCTAAGAAGTCTGCTTTGT<br>TAGCTCTAGCAGCTTATGCATCTGATCCAAATGAGGCCGATCGTCTAAAATATCTTGC<br>TTCTCCAGCCGGAAAGGATGAATATGCTCAGTCACTAGTTGCAAATCAGAGAAGCCTC<br>CTCGAGGTCATGGCTGAATTTCCATCAGCAAAGCCTCCTCTTGGAGTATTCTTTGCAG<br>CAATTGCTCCACGCCTCCAACCCAGATTCTATTCTATATCGTCTTCTCCAAGGATGGC<br>ACCATCTAGAATTCATGTCACTTGTGCACTTGTTTATGAAAAAACACCTGGAGGACGA<br>ATTCACAAGGGTGTGTGTTCGACATGGATGAAGAATGCCATTCCATTGGAGGAAAGCC<br>GTGACTGCAGCTGGGCTCCTATCTTTGTCAGGCAGTCTAACTTCAAACTCCCTGCCGA<br>TCCTAAAGTGCCTGTTATAATGATCGGCCCTGGTACTGGACTAGCTCCCTTCAGAGGA<br>TTCCTTCAGGAAAGATTAGCTCTGAAGGAAGAAGGAGCTGAACTTGGTACTGCAGTTT<br>TCTTTTTTGGATGCAGGAACCGCAAAATGGATTACATCTATGAAGATGAGCTAAACCA<br>TTTCCTTGAAATTGGTGCACTTTCCGAGCTACTTGTTGCTTTCTCACGTGAGGGACCC<br>ACTAAGCAGTATGTGCAACACAAGATGGCAGAAAAGGCTTCTGATATTTGGAGGATGA<br>TTTCTGATGGAGCATATGTTTACGTCTGCGGTGATGCCAAAGGCATGGCCAGGGATGT<br>CCACAGAACTCTCCACACCATTGCTCAAGAGCAGGGATCGATGGATAGCACACAGGCT<br>GAGGGTTTTGTGAAGAATCTGCAAATGACCGGAAGGTATCTCCGAGATGTCTGGTGA |
| *C. roseus CYB5* (KP411010.1) | identical to GenBank sequence |
| *H. vulgare NMT* (U54767.1) | identical to GenBank sequence |

**Table S9. Nucleotide sequence of gene encoding truncated and tagged AMIS (tAMIS).**

**For the construct design see Fig. S10A.**

**The part encoding tAMIS (lacking amino acids 2-23) is shown in bold, HA tag is highlighted in red and StrepII tag in blue.**

| Sequence |
|---|
| **ATGGGAAGAGGTGCCATGCGGTGGCCGCCGGGCCCCCGTCCATGGCCCATAGTCGGCAACCTCCTCGACCTCCGCGGG**<br>**GGCAATCTCCACCACAAGCTCGCGAGCCTGGCGCATGACCATGGCCCCGTGATGACGCTCAAGCTCGGCACGGTGAGC**<br>**ACCGTGTTTGTGTCCTCCCGGGACGCGGCATGGGAGGCGTTCACCAAGCACGACCGGCGCATTGCTGCACGCACCATA**<br>**CCGGACACTAGGCGTGCTGTTTCACATGCTGACCGCTCCATGGTGTGGCTACCAAGCTCAGACCCATTGTGGAAGACG**<br>**CTGCGTGGCATCGCTGCCACGCATGTCTTCTCGCCGCGCAGCCTTGCGGCCGCGCAGGGTACACGGGAGCGCGCTGTG**<br>**CAAAACATGCTAAATGATTTCCGCCGACAAGCTGGGCAGGAGGTGCACATCGGCCATGTCCTGTACCACGGCATGTTC**<br>**GACCTTCTCACCAACACGCTCTTCTCCCTCGACAGCCAGGACAGGTTGAGGGACCTTCTGGAAGACATTGTGGCACTT**<br>**CTCGCCGAGCCCAATGTCTCGGACTTCTACCCGTTACTTCGGGTGATGGACCTGCAGGGCCTGCGCCGCTGGACGGCC**<br>**AAACACATGAACCGTGTGTTTCATGTCCTCGATAAGATCATTGACACCCGGCTGGGAGATGGACAGGCCGGTAGGCAT**<br>**CAGGACGTCCTGGATGCGCTGCTAGCACTGATGACCACCGGTAAGCTGAGCCGGCAGGACGTGAAGGCCATGTTGTTT**<br>**GACATCCTTGCAGCAGGTACAGAGACAACCAAGATCACGGTGGAGTGGGCGATGGCGGAGCTGTTGCGGAACCCGGGC**<br>**GTGATGGCTGCGGTGTGCGCCGAGATGAAGGCCGCCCTCGCGCAGGAACAAGAGAGGATGATCACAGAGGCAGACGTG**<br>**GCAAAGCTGCCATACCTGCAGGCCGCGGTAAAGGAGTCGATGCGGCTACACCCCGTGGCACCGCTACTGCTGCCGCAC**<br>**ATGGTCGTAGAGGAGGGCGTGGAGATAGGCGGCTATGACGTGCCTATGGGCGCCACCATCATCTTCAACTCGTGGTCC**<br>**ATCATGCGCGACCCTGAAGCATGGGAGAGGCCCGATGAATTTGTGCCAGAGCGGTTTTTGGGGAAGACAGAGCATGGC**<br>**ATGTGGGGGAAGGACGTCAAGTTCATCCCGCTGGGCACCGGCCGGAGGCTGTGCCCTGCATTGCCCATGGTGGAGCTC**<br>**GTCGTGCCCTTCATGGTGGCATCCATGTTGCATGCCTTTGAGTGGAGGCTACCCCAGGGCATGTCACCTGACCAGGTG**<br>**GATGTGACCGAGAGGTATACAAGCAATGATATCCTCGTTATGGATGTGCCTCTCAAGGTTGTTCCGATACCCGTTGTT**<br>**GCCATC**CCCGGGGGTTATCCATACGATGTTCCAGATTATGCTGTCGGCGCCGGTTGGTCACATCCTCAATTTGAAAAA<br>TAA |

**Table S10. Accession numbers of characterized CYP76s used for phylogenetic analysis.**

| Protein name | Species | Accession number |
|---|---|---|
| CYP76A26 | *Catharanthus roseus* | KF302066 |
| CYP76AD1 | *Beta vulgaris* | HQ656023 |
| CYP76AD6 | *Beta vulgaris* | KT962274 |
| CYP76AH1 | *Salvia miltiorrhiza* | S4UX02 |
| CYP76AH22 | *Rosmarinus officinalis* | KP091843 |
| CYP76AH23 | *Rosmarinus officinalis* | KP091844 |
| CYP76AH24 | *Salvia pomifera* | A0A0S1TP26 |
| CYP76AH3 | *Salvia miltiorrhiza* | KR140168 |
| CYP76AK1 | *Salvia miltiorrhiza* | KR140169 |
| CYP76AK2 | *Salvia miltiorrhiza* | KP337688 |
| CYP76AK6 | *Salvia pomifera* | A0A0S1TPC7 |
| CYP76AK8 | *Rosmarinus officinalis* | A0A1D8QMG4 |
| CYP76B6 | *Catharanthus roseus* | Q8VWZ7 |
| CYP76B74 | *Arnebia euchroma* | MH077962 |
| CYP76BK1 | *Vitex agnus-castus* | MG696754 |
| CYP76C1 | *Arabidopsis thaliana* | NP_850439 |
| CYP76C4 | *Arabidopsis thaliana* | OAP09091 |
| CYP76F37v1 | *Santalum album* | KC533717 |
| CYP76F38v1 | *Santalum album* | KC533715 |
| CYP76F39v1 | *Santalum album* | KC533716 |
| CYP76F40 | *Santalum album* | KC698968 |
| CYP76F41 | *Santalum album* | KC698969 |
| CYP76F42 | *Santalum album* | KC698965 |
| CYP76J1 | *Petunia hybrida* | AB265193 |
| CYP76L11 | *Oryza sativa* | XP_015610661 |
| CYP76M14 | *Oryza sativa* | XP_015628496 |
| CYP76M17 | *Oryza sativa* | NP_001408569 |
| CYP76M5 | *Oryza sativa* | AK059010 |
| CYP76M6 | *Oryza sativa* | AK101003 |
| CYP76M7 | *Oryza sativa* | AK105913 |
| CYP76M8 | *Oryza sativa* | AK069701 |

**References and Notes**


1. M. Vicari, D. R. Bazely, Do grasses fight back? The case for antiherbivore defences. *Trends Ecol. Evol.* **8**, 137–141 (1993). doi:10.1016/0169-5347(93)90026-L Medline

2. J. V. Lovett, A. H. C. Hoult, "Allelopathy and self-defense in barley" in *Allelopathy*, vol. 582 of ACS Symposium Series, Inderjit, K. M. M. Dakshani, F. A. Einhelllig, Eds. (American Chemical Society, 1994), pp. 170–183.

3. L. J. Corcuera, Effects of indole alkaloids from gramineae on aphids. *Phytochemistry* **23**, 539–541 (1984). doi:10.1016/S0031-9422(00)80376-3

4. A. Lu, T. Wang, H. Hui, X. Wei, W. Cui, C. Zhou, H. Li, Z. Wang, J. Guo, D. Ma, Q. Wang, Natural products for drug discovery: Discovery of gramines as novel agents against a plant virus. *J. Agric. Food Chem.* **67**, 2148–2156 (2019). doi:10.1021/acs.jafc.8b06859 Medline

5. K. S. Brown Jr., J. R. Trigo, "The ecological activity of alkaloids" in vol. 47 of *The Alkaloids: Chemistry and Pharmacology*, G. A. Cordell, Ed. (Academic Press, 1995), pp. 227–354.

6. A. D. Hanson, P. L. Traynor, K. M. Ditz, D. A. Reicosky, Gramine in barley forage - Effects of genotype and environment. *Crop Sci.* **21**, 726–730 (1981). doi:10.2135/cropsci1981.0011183X002100050024x

7. E. Leete, L. Marion, The biogenesis of alkaloids: Ix. further investigations on the formation of gramine from tryptophan. *Can. J. Chem.* **31**, 1195–1202 (1953). doi:10.1139/v53-154

8. B. G. Gower, E. Leete, Biosynthesis of gramine: The immediate precursors of the alkaloid. *J. Am. Chem. Soc.* **85**, 3683–3685 (1963). doi:10.1021/ja00905a034

9. K. A. E. Larsson, I. Zetterlund, G. Delp, L. M. V. Jonsson, *N*-Methyltransferase involved in gramine biosynthesis in barley: Cloning and characterization. *Phytochemistry* **67**, 2002–2008 (2006). doi:10.1016/j.phytochem.2006.06.036 Medline

10. E. Ishikawa, S. Kanai, M. Sue, Detection of a novel intramolecular rearrangement during gramine biosynthesis in barley using stable isotope-labeled tryptophan. *Biochem. Biophys. Rep.* **34**, 101439 (2023). doi:10.1016/j.bbrep.2023.101439 Medline

11. D. O'Donovan, E. Leete, Biosynthesis of gramine: Feeding experiments with tryptophan-β-[$H^3$,$C^{14}$]. *J. Am. Chem. Soc.* **85**, 461–463 (1963). doi:10.1021/ja00887a021

12. E. Wenkert, Biosynthesis of indole alkaloids. The Aspidosperma and Iboga bases. *J. Am. Chem. Soc.* **84**, 98–102 (1962). doi:10.1021/ja00860a023

13. M. Jayakodi, S. Padmarasu, G. Haberer, V. S. Bonthala, H. Gundlach, C. Monat, T. Lux, N. Kamal, D. Lang, A. Himmelbach, J. Ens, X.-Q. Zhang, T. T. Angessa, G. Zhou, C. Tan, C. Hill, P. Wang, M. Schreiber, L. B. Boston, C. Plott, J. Jenkins, Y. Guo, A. Fiebig, H. Budak, D. Xu, J. Zhang, C. Wang, J. Grimwood, J. Schmutz, G. Guo, G. Zhang, K. Mochida, T. Hirayama, K. Sato, K. J. Chalmers, P. Langridge, R. Waugh, C. J. Pozniak, U. Scholz, K. F. X. Mayer, M. Spannagl, C. Li, M. Mascher, N. Stein, The barley pan-genome reveals the hidden legacy of mutation breeding. *Nature* **588**, 284–289 (2020). doi:10.1038/s41586-020-2947-8 Medline

14. T. J. Leland, R. Grumet, A. D. Hanson, Biochemical, immunological and genetic characterization of natural gramine-free variants of *Hordeum vulgare* L. *Plant Sci.* **42**, 77–82 (1985). doi:10.1016/0168-9452(85)90145-1

15. S. Leite Dias, A. Garibay-Hernández, F. L. Brendel, B. Gabriel Chavez, E. Brückner, H.-P. Mock, J. Franke, J. C. D'Auria, A new fluorescence detection method for tryptophan- and tyrosine-derived allelopathic compounds in barley and lupin. *Plants* **12**, 1930 (2023). doi:10.3390/plants12101930 Medline

16. B. Liu, M. Zhao, How transposable elements are recognized and epigenetically silenced in plants? *Curr. Opin. Plant Biol.* **75**, 102428 (2023). doi:10.1016/j.pbi.2023.102428 Medline

17. L. Chuang, J. Franke, "Rapid combinatorial coexpression of biosynthetic genes by transient expression in the plant host *Nicotiana benthamiana*" in *Engineering Natural Product Biosynthesis: Methods and Protocols*, vol. 2489 of Methods in Molecular Biology, E. Skellam, Ed. (Springer, 2022), pp. 395–420.

18. S. Brown, M. Clastre, V. Courdavault, S. E. O'Connor, De novo production of the plant-derived alkaloid strictosidine in yeast. *Proc. Natl. Acad. Sci. U.S.A.* **112**, 3205–3210 (2015). doi:10.1073/pnas.1423555112 Medline

19. I. V. O. Hoffie, "Entwicklung des modularen CasCADE-Vektorsystems und dessen Verwendung zur gezielten Mutagenese der Stp13-Orthologe von Weizen und Gerste für die Etablierung dauerhafter Resistenz gegen Rost- und Mehltaupilze," thesis, Institutionelles Repositorium der Leibniz Universität Hannover (2022).

20. M. Lange, M. Mályusz, Fast method for the simultaneous determination of 2-oxo acids in biological fluids by high-performance liquid chromatography. *J. Chromatogr. B Biomed. Appl.* **662**, 97–102 (1994). doi:10.1016/0378-4347(94)00383-1 Medline

21. B. R. Lichman, The scaffold-forming steps of plant alkaloid biosynthesis. *Nat. Prod. Rep.* **38**, 103–129 (2021). doi:10.1039/D0NP00031K Medline

22. G. Polturak, Z. Liu, A. Osbourn, New and emerging concepts in the evolution and function of plant biosynthetic gene clusters. *Curr. Opin. Green Sustain. Chem.* **33**, 100568 (2022). doi:10.1016/j.cogsc.2021.100568

23. S. J. Smit, B. R. Lichman, Plant biosynthetic gene clusters in the context of metabolic evolution. *Nat. Prod. Rep.* **39**, 1465–1482 (2022). doi:10.1039/D2NP00005A Medline

24. J. Colinas, S. C. Schmidler, G. Bohrer, B. Iordanov, P. N. Benfey, Intergenic and genic sequence lengths have opposite relationships with respect to gene expression. *PLOS ONE* **3**, e3670 (2008). doi:10.1371/journal.pone.0003670 Medline

25. R. M. Clark, T. N. Wagler, P. Quijada, J. Doebley, A distant upstream enhancer at the maize domestication gene *tb1* has pleiotropic effects on plant and inflorescent architecture. *Nat. Genet.* **38**, 594–597 (2006). doi:10.1038/ng1784 Medline

26. U. Bathe, A. Tissier, Cytochrome P450 enzymes: A driving force of plant diterpene diversity. *Phytochemistry* **161**, 149–162 (2019). doi:10.1016/j.phytochem.2018.12.003 Medline

27. N. Kitaoka, J. Zhang, R. K. Oyagbenro, B. Brown, Y. Wu, B. Yang, Z. Li, R. J. Peters, Interdependent evolution of biosynthetic gene clusters for momilactone production in rice. *Plant Cell* **33**, 290–305 (2021). doi:10.1093/plcell/koaa023 Medline

28. G. Polturak, D. Breitel, N. Grossman, A. Sarrion-Perdigones, E. Weithorn, M. Pliner, D. Orzaez, A. Granell, I. Rogachev, A. Aharoni, Elucidation of the first committed step in betalain biosynthesis enables the heterologous engineering of betalain pigments in plants. *New Phytol.* **210**, 269–283 (2016). doi:10.1111/nph.13796 Medline

29. C. C. Hansen, D. R. Nelson, B. L. Møller, D. Werck-Reichhart, Plant cytochrome P450 plasticity and evolution. *Mol. Plant* **14**, 1244–1265 (2021). doi:10.1016/j.molp.2021.06.028 Medline

30. K. Malhotra, J. Franke, Cytochrome P450 monooxygenase-mediated tailoring of triterpenoids and steroids in plants. *Beilstein J. Org. Chem.* **18**, 1289–1310 (2022). doi:10.3762/bjoc.18.135 Medline

31. M. S. C. Pedras, E. E. Yaya, Dissecting metabolic puzzles through isotope feeding: A novel amino acid in the biosynthetic pathway of the cruciferous phytoalexins rapalexin A and isocyalexin A. *Org. Biomol. Chem.* **11**, 1149–1166 (2013). doi:10.1039/c2ob27076e Medline

32. A. P. Klein, E. S. Sattely, Biosynthesis of cabbage phytoalexins from indole glucosinolate. *Proc. Natl. Acad. Sci. U.S.A.* **114**, 1910–1915 (2017). doi:10.1073/pnas.1615625114 Medline

33. F. S. Hanschen, E. Lamy, M. Schreiner, S. Rohn, Reactivity and stability of glucosinolates and their breakdown products in foods. *Angew. Chem. Int. Ed.* **53**, 11430–11450 (2014). doi:10.1002/anie.201402639 Medline

34. F. Kudo, A. Miyanaga, T. Eguchi, Biosynthesis of natural products containing β-amino acids. *Nat. Prod. Rep.* **31**, 1056–1073 (2014). doi:10.1039/C4NP00007B Medline

35. J. B. Hedges, K. S. Ryan, Biosynthetic pathways to nonproteinogenic α-amino acids. *Chem. Rev.* **120**, 3161–3209 (2020). doi:10.1021/acs.chemrev.9b00408 Medline

36. Z. Wang, "Stieglitz rearrangement" in *Comprehensive Organic Name Reactions and Reagents*, Z. Wang, Ed. (Wiley, 2010), pp. 2673–2676.

37. W. Yamakoshi, M. Arisawa, K. Murai, Oxidative rearrangement of primary amines using $PhI(OAc)_2$ and $Cs_2CO_3$. *Org. Lett.* **21**, 3023–3027 (2019). doi:10.1021/acs.orglett.9b00559 Medline

38. J. Jirschitzka, D. J. Mattern, J. Gershenzon, J. C. D'Auria, Learning from nature: New approaches to the metabolic engineering of plant defense pathways. *Curr. Opin. Biotechnol.* **24**, 320–328 (2013). doi:10.1016/j.copbio.2012.10.014 Medline

39. J. Zhang, L. G. Hansen, O. Gudich, K. Viehrig, L. M. M. Lassen, L. Schrübbers, K. B. Adhikari, P. Rubaszka, E. Carrasquer-Alvarez, L. Chen, V. D'Ambrosio, B. Lehka, A. K. Haidar, S. Nallapareddy, K. Giannakou, M. Laloux, D. Arsovska, M. A. K. Jørgensen, L. J. G. Chan, M. Kristensen, H. B. Christensen, S. Sudarsan, E. A. Stander, E. Baidoo, C. J. Petzold, T. Wulff, S. E. O'Connor, V. Courdavault, M. K. Jensen, J. D. Keasling, A microbial supply chain for production of the anti-cancer drug vinblastine. *Nature* **609**, 341–347 (2022). doi:10.1038/s41586-022-05157-3 Medline

40. C. Engler, M. Youles, R. Gruetzner, T.-M. Ehnert, S. Werner, J. D. G. Jones, N. J. Patron, S. Marillonnet, A golden gate modular cloning toolbox for plants. *ACS Synth. Biol.* **3**, 839–843 (2014). doi:10.1021/sb4001504 Medline

41. D. Weigel, J. Glazebrook, Transformation of *Agrobacterium* using the freeze-thaw method. *CSH Protoc.* **2006**, pdb.prot4666 (2006). doi:10.1101/pdb.prot4666 Medline

42. T. Komari, Y. Hiei, Y. Saito, N. Murai, T. Kumashiro, Vectors carrying two separate T-DNAs for co-transformation of higher plants mediated by *Agrobacterium tumefaciens* and segregation of transformants free from selection markers. *Plant J.* **10**, 165–174 (1996). doi:10.1046/j.1365-313X.1996.10010165.x Medline

43. C. Marthe, J. Kumlehn, G. Hensel, "Barley (*Hordeum vulgare* L.) transformation using immature embryos" in *Agrobacterium Protocols: Volume 1*, vol. 1223 of Methods in Molecular Biology, K. Wang, Ed. (Springer, 2015), pp. 71–83.

44. M. A. Pallotta, R. D. Graham, P. Langridge, D. H. B. Sparrow, S. J. Barker, RFLP mapping of manganese efficiency in barley. *Theor. Appl. Genet.* **101**, 1100–1108 (2000). doi:10.1007/s001220051585

45. B. Poocharoen, J. F. Barbour, L. M. Libbey, R. A. Scanlan, Precursors of *N*-nitrosodimethylamine in malted barley. 1. Determination of hordenine and gramine. *J. Agric. Food Chem.* **40**, 2216–2221 (1992). doi:10.1021/jf00023a033

46. M. M. Jessop-Fabre, T. Jakočiūnas, V. Stovicek, Z. Dai, M. K. Jensen, J. D. Keasling, I. Borodina, EasyClone-MarkerFree: A vector toolkit for marker-less integration of genes into Saccharomyces cerevisiae via CRISPR-Cas9. *Biotechnol. J.* **11**, 1110–1117 (2016). doi:10.1002/biot.201600147 Medline

47. H. H. Nour-Eldin, F. Geu-Flores, B. A. Halkier, "USER cloning and USER fusion: The ideal cloning techniques for small and big laboratories" in *Plant Secondary Metabolism Engineering: Methods and Applications*, vol. 643 of Methods in Molecular Biology, A. G. Fett-Neto, Ed. (Humana Press, 2010), pp. 185–200.

48. R. D. Gietz, R. H. Schiestl, High-efficiency yeast transformation using the LiAc/SS carrier DNA/PEG method. *Nat. Protoc.* **2**, 31–34 (2007). doi:10.1038/nprot.2007.13 Medline

49. I. Barr, F. Guo, Pyridine hemochromagen assay for determining the concentration of heme in purified protein solutions. *Bio Protoc.* **5**, e1594 (2015). doi:10.21769/BioProtoc.1594 Medline

50. E. A. Berry, B. L. Trumpower, Simultaneous determination of hemes *a*, *b*, and *c* from pyridine hemochrome spectra. *Anal. Biochem.* **161**, 1–15 (1987). doi:10.1016/0003-2697(87)90643-9 Medline

51. S. Guha, S. Gadde, N. Kumar, D. S. Black, S. Sen, Orthogonal Syntheses of γ-carbolinone and spiro[pyrrolidinone-3,3′]indole derivatives in one pot through reaction telescoping. *J. Org. Chem.* **86**, 5234–5244 (2021). doi:10.1021/acs.joc.1c00141 Medline

52. J. Ma, J. Luo, K. Jiang, G. Zhang, S. Liu, B. Yin, Access to polycyclic thienoindolines via formal [2+2+1] cyclization of alkynyl indoles with $S_8$ and $K_2S$. *Org. Lett.* **23**, 8033–8038 (2021). doi:10.1021/acs.orglett.1c03035 Medline

53. H. C. J. Ottenheijm, R. Plate, J. H. Noordik, J. D. M. Herscheid, *N*-Hydroxytryptophan in the synthesis of natural products containing oxidized dioxopiperazines. An approach to the neoechinulin and sporidesmin series. *J. Org. Chem.* **47**, 2147–2154 (1982). doi:10.1021/jo00132a032

54. R. Plate, R. J. F. Nivard, H. C. J. Ottenheijm, Conversion of *N*-hydroxytryptophans into α,β-dehydrotryptophan. An approach to the neoechinulin series. *J. Chem. Soc. Perkin Trans. 1* **1**, 2473–2480 (1987). doi:10.1039/P19870002473

55. D. Matsui, Y. Hirata, A. Iwakawa, Y. Toyotake, M. Wakayama, Y. Asano, Combination of enzymatic oxidation of amino acid and native chemical ligation with hydroxylamine for amide formation toward a one-pot process. *Chem. Lett.* **50**, 1632–1634 (2021). doi:10.1246/cl.210286

56. X.-L. Deng, J. Xie, Y.-Q. Li, D.-K. Yuan, X.-P. Hu, L. Zhang, Q.-M. Wang, M. Chi, X.-L. Yang, Design, synthesis and biological activity of novel substituted pyrazole amide derivatives targeting EcR/USP receptor. *Chin. Chem. Lett.* **27**, 566–570 (2016). doi:10.1016/j.cclet.2016.02.009

57. M. Wiedemann, P. J. Altmann, L. Hintermann, Mannich *N*-indolylmethylation of amino acids. *Synthesis (Stuttg.)* **49**, 2257–2265 (2017). doi:10.1055/s-0036-1588934

58. S. Guindon, J.-F. Dufayard, V. Lefort, M. Anisimova, W. Hordijk, O. Gascuel, New algorithms and methods to estimate maximum-likelihood phylogenies: Assessing the performance of PhyML 3.0. *Syst. Biol.* **59**, 307–321 (2010). doi:10.1093/sysbio/syq010 Medline

59. R. C. Edgar, MUSCLE: Multiple sequence alignment with high accuracy and high throughput. *Nucleic Acids Res.* **32**, 1792–1797 (2004). doi:10.1093/nar/gkh340 Medline

60. T. Pillaiyar, E. Gorska, G. Schnakenburg, C. E. Müller, General synthesis of unsymmetrical 3,3′-(aza)diindolylmethane derivatives. *J. Org. Chem.* **83**, 9902–9913 (2018). doi:10.1021/acs.joc.8b01349 Medline